

---

# **Fatigue Assessment of Aluminium Welded Box-stiffener Joints in Ships**

*Doktor Ingeniør Thesis*

*by*

**Naiquan Ye**



**Department of Marine Technology  
Faculty of Engineering Science and Technology  
Norwegian University of Science and Technology**

**2007**

**Trondheim Norway**

---

---

TO MY DEAREST WIFE, SHANSHAN JIANG  
AND OUR CHILDREN  
KRISTIAN, FREDRIK AND ASTRID



---

## *Abstract*

One of the trends in ship building is the building of larger and faster ships. However, increasing demand for speed has forced the ship designers to search for alternative materials to reduce the weight of the ship without compromising strength. Aluminium alloys, once properly designed, can achieve this goal by reducing the weight of structural components by over 50% compared to those made of normal carbon steel. Another advantage of aluminium alloys is that its corrosion resistance. In a sea environment, steel has been found to corrode about 100 times faster than aluminium alloys under the same corrosive environment.

As the size of aluminium ship increases, fatigue has become one of the main design criteria. In order to effectively make use of the high strength/weight ratio of aluminium alloys, the cross section of the structural components as well as the joint design should be optimized to provide sufficient fatigue strength while still maintain acceptable fabrication cost. Extruded hollow stiffeners have been proven to be able to provide excellent light and stiff panels for aluminium ships.

Box stiffener is such a cross section profile investigated in the present study. The box stiffener is usually oriented longitudinally by interacting with a large number of web frames by fillet welds. These welded joints may be exposed to larger fatigue damage due to its significant stress variations experienced during the service of the ships. In addition, welding of these joints is quite costly since there are a large amount of them and it is difficult to apply automatic welding due to complex profile. Any simplification in the welding procedure would cause a significant benefit to the ship builders.

Three similar web frame/box stiffener connections are considered in these studies, by varying the opening shape on the web frame and accordingly the welding procedure. The objective is to achieve sufficient fatigue strength while still maintaining an economically efficient joint. The first connection (denoted as Alt-1) tries to make a relatively larger opening on the web frame for easy assembling and more space for welding. The second and third alternatives (denoted as Alt-2 and Alt-3) are identical in the opening on the web frame while differs on welding procedure only. Interrupted welding is performed for Alt-2 to save both the human resource and weld material while continuous welding is required for Alt-3 for a simple welding procedure. Alt-3 also provides a water tight solution due to the continuous welding.

It is found that the change of cutting shapes on the web frame as well as the corresponding weld procedure has great impact on both the static and fatigue properties of the joints. Extra welding around the web frame may cause a high stress concentration at the weld toe and therefore imply an unacceptable fatigue damage. However, a simple weld can be a good candidate to achieve sufficient fatigue strength.

Butt weld is usually used to join two pre-fabricated units to obtain sufficient overall strength of the joined single piece structure. However, difficulty may arise for such units when the box stiffeners are presented as the longitudinal stiffeners due to relatively large shrinkage and distortion introduced in the fabrication process including welding in the adjacent area. A special type of lap joint, denoted as box stiffener lap joint is designed to provide a joining solution for the box stiffeners. By enabling the

---

inside profile of the lapping plate to be identical to the outside profile of the box stiffener, the joining of two box stiffeners is just to weld the intersection lines between the lapping plate and box stiffener. Only the wide flanges of the box stiffener require a conventional weld. Cracking from the weld root should be avoided to ensure sufficient fatigue strength.

Good fatigue performance is observed for the box stiffener lap joint. The weld leg length is found to be a determining factor that affects both the fatigue strength and fatigue crack initiation site. Weld leg length between 6.0 and 7.5 mm is suggested to avoid high stress concentration at the weld toe. Moreover, this design reduces the likelihood of fatigue cracks to initiate from the most complex manual welding area.

Information about fatigue analysis of welded aluminium structures is quite limited in the open literature. This thesis deals with fatigue assessment methods of welded aluminium plate structures based on both numerical analysis and experimental tests. Various stress based fatigue assessment methods such as the nominal, structural and notch stress approaches have been applied to the investigated joints.

The nominal stress range approach can not provide a satisfactory prediction of the fatigue strength of novel welded joints because the local geometrical details including structural geometry and weld geometry are implicitly embedded in the nominal design SN curves. Laboratory tests would hence be needed to establish nominal stress approaches. More refined local approaches including the structural stress range approach and the notch stress range approach have been developed for a more accurate assessment of the fatigue strength. The main challenge for these local approaches is to find suitable stress calculation methods in the vicinity of the weld and thereby the uncertainties that determine the fatigue strength of the joint can be quantitatively reflected in a local stress concentration factor. Several of these methods are applied in the study of novel types of welded aluminium joints in this thesis. The choice of design SN curves must be consistent with the way by which the design stress range is calculated. Fatigue test data support the use of a structural stress design SN curve of fatigue class 40 for the fatigue assessment of aluminium fillet welded in-plane bracket connections when the structural stress has been derived from the extrapolation methods. It has been shown that a structural stress design SN curve of fatigue class 44 for the fatigue assessment of aluminium lap joints can be used.

Another important issue is to investigate the effect of the local weld geometry such as the weld toe angle, weld toe radius, and weld leg length on the value of the structural/notch stress and accordingly on fatigue behaviour. The weld parameters of the joints have been measured in the laboratory and the statistical measured values are used in the numerical finite element models (FEM).

Improving fatigue strength of critical joints is found to be necessary late in the design process or during the service time of a structure to extend the whole service life of the structure. The effect of weld toe grinding on the stress concentration at the weld toe is studied by finite element analysis (FEA). Fatigue tests show that the fatigue life in terms of number of cycles to failure is nearly doubled by simply grinding the weld toe of the joint. However, the standard deviations are not so much affected as the fatigue strength. The effect of weld parameters such as the grinding depth has been found to play a decisive role in fatigue life improvement.

---

## *Acknowledgements*

The thesis work has been carried out at the Department of Marine Technology, Norwegian University of Science and Technology (NTNU), under supervision of Professor Torgeir Moan.

It is the author's great pleasure to recognize the contributions of his advisor Professor Torgeir Moan who initiated and supervised this work. His invaluable guidance and outstanding knowledge of marine structures has truly been a great inspiration to the author. His numerous suggestions for the improvement of the manuscript and his patience and kindness have made this study an enjoyable and memorable experience. The author expresses his deepest gratitude to Professor Moan.

The gratitude of the author is also expressed to Dr. Bård Wathne Tveiten at the Department of Material Technology at SINTEF for his suggestions and contributions in developing fatigue assessment methods for welded joints.

The author is very grateful to the project "Aluminium in Ships" funded by Hydro Aluminium Maritime a.s. The author gratefully acknowledges the financial support and especially the support provided by Jon Erslund and Eirik Smedstad to this work. Appreciation is also extended to the Department of Marine Structures for part of the financial support.

I would also like to acknowledge all other friends in the Structural Laboratory at the Marine Technology Centre. The help of Roar Skjetne who designed the test rigs is appreciated. I would also like to thank Erik Fleischer for his guidance on using the acquisition equipments during the tests. Johan Terje Lines is also appreciated for his help in preparing the test specimens.

Special thanks are also directed to Mr. Bjørn Østbye for his help with the configuration of the computer system that made the numerical modelling an enjoyable experience.

Finally, I would like to say thanks to my dearest wife Shanshan Jiang and our lovely children Kristian (8), Fredrik (6) and Astrid (3) who have always been the constant support behind me during these unforgettable years. It is simply not possible to complete the work without being continuously encouraged by them and it has been always a great joy to embrace them with the greasy hands after working in the laboratory.





---

# *Contents*

<b>Abstract.....</b>	<b>i</b>
<b>Acknowledgements .....</b>	<b>iii</b>
<b>Contents .....</b>	<b>v</b>
<b>List of Figures.....</b>	<b>ix</b>
<b>List of Tables .....</b>	<b>x</b>
<b>Nomenclatures.....</b>	<b>xi</b>
<b>Abbreviations .....</b>	<b>xiii</b>
<b>1 Introduction .....</b>	<b>1</b>
1.1 History	1
1.2 Research objectives and thesis organization	2
1.3 Background and previous work	4
1.4 Thesis structure	6
<b>2 Fatigue of Aluminium Welded Joints .....</b>	<b>7</b>
2.1 Aluminium vs. steel in ship building	7
2.2 A short history of aluminium in ships	9
2.3 Design of welded joints	10
2.3.1 General.....	10
2.3.2 Designing web frame/box stiffener joints .....	11
2.4 Weld measurements and laboratory tests	13
2.4.1 Weld measurement .....	13
2.4.2 Test set-up.....	14
2.4.3 Instrumentation.....	15
2.5 Fatigue analysis of aluminium welded joints	16
2.5.1 General.....	16
2.5.2 Development of fatigue assessment methods.....	17
2.6 Stress-based fatigue assessment method	18

---

2.6.1	Introduction .....	18
2.6.2	Nominal stress range approach.....	20
2.6.3	Structural stress range approach.....	22
2.6.4	Evaluation of the structural stress calculation methods.....	36
2.6.5	CEM in determining the structural stress .....	39
2.6.6	Notch stress range approach.....	40
2.7	<i>Fatigue life improvement techniques</i> .....	44
2.7.1	Introduction .....	44
2.7.2	Post weld treatment techniques .....	44
2.7.3	Weld toe grinding for aluminium welded joints.....	45
<b>3</b>	<b>Results and Recommendations.....</b>	<b>49</b>
3.1	<i>General</i> .....	49
3.2	<i>Box stiffener/web frame connections</i> .....	50
3.2.1	Introduction .....	50
3.2.2	Joint description.....	50
3.2.3	Static behaviour .....	51
3.2.4	Fatigue behaviour .....	52
3.2.5	Design considerations.....	53
3.3	<i>Box stiffener lap joint</i> .....	53
3.3.1	Introduction .....	53
3.3.2	Static behaviour .....	54
3.3.3	Fatigue behaviour .....	54
3.3.4	Design considerations.....	56
3.4	<i>Cruciform joints</i> .....	56
3.4.1	Introduction .....	56
3.4.2	Static behaviour .....	56
3.4.3	Fatigue behaviour .....	56
3.5	<i>Recommendations for further work</i> .....	59
3.5.1	Joint design and optimization.....	59
3.5.2	Fatigue assessment methods.....	59
3.5.3	Fatigue design curves .....	60
3.5.4	Fatigue improvement techniques.....	60

---

<b>4</b>	<b>References.....</b>	<b>61</b>
<b>5</b>	<b>Appendix A: Published and to be published papers .....</b>	<b>67</b>
<b>6</b>	<b>Appendix B: Materials certificates .....</b>	<b>129</b>
<b>7</b>	<b>Appendix C: Measuring weld parameters .....</b>	<b>139</b>
<b>8</b>	<b>Appendix D: Photos in colour.....</b>	<b>143</b>



---

## *List of Figures*

Figure 1-1 Objectives and thesis organization .....	3
Figure 2-1 Load and stress components in an aluminium ship hull (adapted after Heggland et al. 2002) .....	8
Figure 2-2 Large aluminium ships built in recent years by Austal (left: Benchijigua Express, right: US navy's LCS - Littoral Combat Ship) .....	9
Figure 2-3 Example of joint types, Lap joint and T joint .....	10
Figure 2-4 Extruded hollow sections and web frame/box stiffener connections .....	10
Figure 2-5 Overview of the web frame/box stiffener connection .....	11
Figure 2-6 Joint difference for the web frame/box stiffener connection .....	11
Figure 2-7 Box stiffener lap joint and joining details .....	13
Figure 2-8 A simple illustration of the weld parameters for T-joint and lap joint .....	13
Figure 2-9 Test set up for four-point bending load condition .....	14
Figure 2-10 Details of the four-point bending test set up .....	15
Figure 2-11 Fatigue comparison between aluminium and steel .....	17
Figure 2-12 A typical bi-linear SN curve .....	19
Figure 2-13 A typical bi-linear SN curve .....	20
Figure 2-14 Stress distribution in front of a weld toe .....	24
Figure 2-15 Types of fatigue failure locations at the weld toe (Fricke 2002) .....	24
Figure 2-16 Asymptotic behaviour of stress in front of an idealized notch (weld toe) in a bi-logarithmic plane .....	29
Figure 2-17 Stress components at the weld toe in the thickness direction .....	31
Figure 2-18 Stress components on a cross section at a distance of $s$ to the weld toe ....	31
Figure 2-19 SN data expressed in terms of IIW (Hobbacher 1996) structural stress range definition (Maddox 2001) .....	34
Figure 2-20 SN data expressed in terms of the definition suggested by Tveiten and Moan (2000) and IIW (Hobbacher 1996) without thickness penalty factors .....	35
Figure 2-21 Small FPSO details analyzed by Hong and Dong (2004) .....	38
Figure 2-22 Stress near the weld toe .....	39
Figure 2-23 Basic SN curves for aluminium (DNV 1997) .....	43
Figure 2-24 Weld profile after toe grinding .....	45
Figure 2-25 Photograph of as-welded (to the left) and toe-ground specimens .....	46
Figure 3-1 Test data against design SN curves .....	49
Figure 3-2 Overview of the box-stiffener/web frame connections .....	51
Figure 7-1 Duplication of the weld profile .....	141
Figure 7-2 Magnified weld profile for measuring weld parameters .....	142
Figure 7-3 Measuring the weld parameter by transparent millimetre block paper .....	142
Figure 8-1 Overview of the web frame/box stiffener connection .....	145

---

Figure 8-2 Overall of the lap joint .....	145
Figure 8-3 Test set up for four-point bending load condition .....	146
Figure 8-4 Photograph of as-welded (to the left) and toe-ground specimens .....	147

### ***List of Tables***

Table 2-1 Comparison of structural stress calculation methods.....	36
Table 2-2 Parameters for standard SN curves (DNV 1997).....	42

---

## *Nomenclatures*

a	weld throat thickness, element length
b	element height
I	inertia moment of a cross section
K	notch stress concentration factor
$K_g$	structural stress concentration factor
$K_w$	stress concentration factor due to the weld
N	fatigue life expressed by number of cycles
$N_0$	characteristic fatigue life, normally two million cycles
m	slope of one parameter SN curve
$m_1$	slope of two parameter SN curve, constant amplitude
$m_2$	slope of two parameter SN curve, variable amplitude
M	bending moment
R	polar coordinate at the weld toe, radius
R	load/stress ratio
S	stress range
$S_0$	characteristic stress range at a fatigue life of two million cycles
t	thickness of the main stressed member of a joint
y	distance from the base line to neutral axis of a cross section
$\lambda$	distance to the fatigue cracking point
$\theta$	flank angle at the weld toe
$\rho$	weld toe radius
$\psi$	polar coordinate at the weld toe, angle
$\sigma_{\text{nominal}}$	nominal normal stress
$\sigma_{\text{structural}}$	structural normal stress
$\sigma_{\text{notch}}$	notch stress
$\tau$	shear stress at the weld root on the weld throat surface





---

## *Abbreviations*

AA	The Aluminium Association
BS	British Standard
DEn	Department of Energy, the United Kingdom
DNV	Det Norske Veritas
FEA	fatigue element analysis
FEM	fatigue element method
HSLC	high speed light craft
IIW	International Institute of Welding
SCF	stress concentration factor
SN curve	fatigue design curve



---

# ***1 Introduction***

---

In this chapter, the background to the research and the research objectives are briefly presented.

## **1.1 History**

The thesis work started in the fall of 1998 and the main work was completed in the end of year 2001. The initiation of the research topic was to propose and verify a cost-effective web frame/box stiffener welded joints for high speed light craft (HSLC) based on numerical as well as experimental investigations with regard to their fatigue performance. A novel joint solution, so called box stiffener lap joint, for joining two separate box stiffeners is proposed as well. This joint solution is necessary in the areas where transverse components such as web frames are not allowed. These alternative joints were grouped into two categories depending on whether a web frame is included or not.

The fatigue assessment methods based on local stresses such as the structural stress have been evolving during the research period. Therefore, various methods were applied to the present investigation as well.

The research results for the box stiffener connections were summarized in several research papers, each containing both the numerical results as well as the test data (Ye and Moan 2002b; 2007a).

After the completion of the test program for the box stiffener connections, the question about the fatigue life improvement by weld toe grinding emerged. Another series of testing was therefore carried out to compare the fatigue performance of the as-welded and toe-ground non-load carrying fillet welded cruciform joints. The results were presented in a separate paper (Ye and Moan 2007b).

These papers were published from 2002 to 2007 and therefore some of the most recent developments may not be reflected in early papers published.

## 1.2 Research objectives and thesis organization

Hollow extruded stiffeners have been widely adopted as a main stiffener type in the ship building practice of aluminium vessels because of its excellent weight/strength properties. A variety of web frame/box stiffener welded connections in a mid-sized aluminium ships may be envisaged. The primary objective of the present work is therefore to propose an economically efficient box stiffener /web frame connection that would guarantee sufficient fatigue strength while in the mean time maintain reasonable fabrication costs (Objective 1). Variations in the overall geometry as well as welding features are examined. A related topic on how to join two box separate stiffeners is also studied by proposing a box stiffener lap joint within the same objective.

Methods for fatigue assessment of such joints was explored based on various stress-based methods including the nominal, structural and notch stress methods. The ultimate goal is to assess their feasibility as practical methods to perform local stress calculation together with consistent selection of design SN curves for engineers in their quest for assessing fatigue performance of welded aluminium structures (Objective 2). Another aim is to examine the role of the weld parameters such as the weld toe angle, weld toe radius and weld leg length, etc. in the fatigue evaluating progress as well as their influence on the fatigue life of the welded joints (Objective 3). An additional aim is to evaluate the effect of weld toe grinding on fatigue life improvement (Objective 4).

The relations between different joint types and objectives are reflected in different papers as shown in Figure 1-1. Most parts of the work have been published in the following papers:

- **Paper 1** (Ye and Moan 2002a) was published in the International Journal of Fatigue. It presented the research work on the novel box-stiffener lap joint for joining two individual box-stiffeners. The effect of the weld parameters on both the static and fatigue behaviour of the box stiffener lap joint was studied. A selection of fatigue class 44 is suggested for such kind of lap joints.
- **Paper 2** (Ye and Moan 2007a) was also published in the International Journal of Fatigue. It examined the effect of cutting shape as well as correspondent welding procedure for box-stiffener/web frame connections by fillet weld. Influence of several weld parameters were investigated as well.
- **Paper 3** (Ye and Moan 2007b) has been accepted by Fatigue and Fracture of Engineering Materials and Structures. It investigated the benefit on fatigue improvement by toe grinding on non-load carrying fillet weld cruciform joints. Various fatigue assessment methods were compared. Grinding depth was found to be decisive for fatigue improving.
- **Paper 4** (Tveiten, Ye and Moan 2002) was presented in the Fatigue Congress 2002. It reviewed published SN data of welded aluminium structures together

with finite element analysis results in order to discuss the various effects that influence a consistent selection of design SN data.

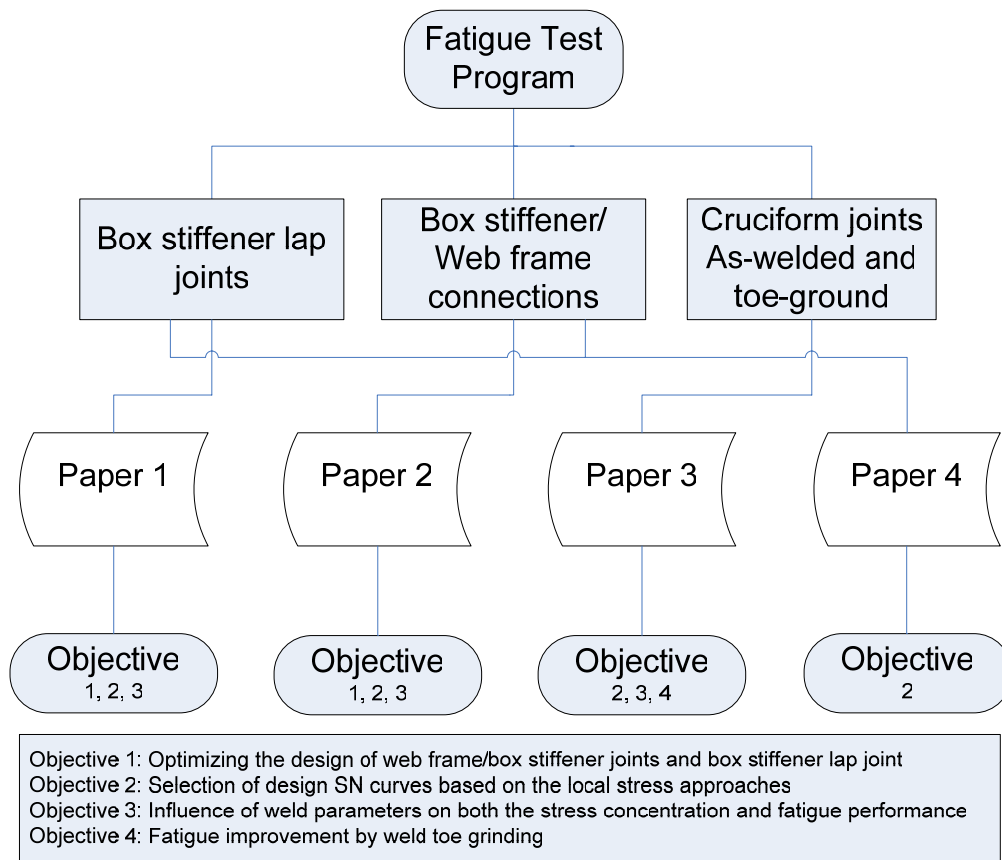


**Figure 1-1 Objectives and thesis organization**

The above mentioned papers are collected in the thesis as appendices. Several other conference papers have also been published for the investigated joints. They are not included as parts of the thesis because most of the contents of these papers were extracted from the journal papers 1 to 3 while without extensive discussion due to page limits. These papers are listed below:

- **Paper 5** (Ye, Moan and Tveiten 2001) was presented in PRADS2001. It presented the main results for the box-stiffener lap joint as published in Paper 1.
- **Paper 6** (Ye and Moan 2002b) was presented in Fatigue Congress 2002. It contained the main test data for the box-stiffener/web frame connections. Paper 2 is an extension version of this paper.
- **Paper 7** (Ye and Moan 2006) was presented in Fatigue Congress 2006. It summarized most often used local stress based fatigue assessment methods and proposes a general purpose structural stress calibration scheme. No significant benefit was obtained by applying such a method to the tested

joints in the thesis. Therefore, the author decided not to include this paper as part of the thesis. However, this paper proved that existing methods are good enough to serve as practical methods for fatigue assessment of aluminium welded joints.

- **Paper 8** (Ye and Moan 2007c) was presented in PRADS2007. Extensive discussions were contained in Paper 3.

### 1.3 Background and previous work

Weight control is a key issue in product construction when the designers try to make maximum benefit of the high strength/weight ratio of aluminium. The extrusion technology makes the choice of complex cross section profiles possible to meet the strength requirements. Extruded hollow cross section profiles have been proven to be an excellent building block for aluminium ships. Box stiffeners are such profiles which have been successfully used in aluminium ships. There are a great number web frame/box stiffener welded connections in a mid-sized ship and hence any simplification of such joint would be of great benefit to the ship builders. The main concern for these joints is to achieve sufficient fatigue strength because they are located relatively far from the neutral axis of the hull and will invariably experience a large number of cyclic loads during the service that may cause cracks to form and grow and in the worst case collapses the whole structure with numerous fatalities and significant property damage as for other similar structures (Bishop 1955; Petroski 1983).

The variety of web frame/box stiffener geometries and corresponding welding features are envisaged. On the condition that sufficient fatigue strength is provided, the design goal is to find an economically efficient solution by limiting the requirement of human resources or simplifying the assembly process. Joining two box stiffeners is an interesting topic because conventional butt weld may not be realistic for box type cross section profiles. A box stiffener lap joint provides a possible solution that may ease the assembling of two separate box stiffeners. Moreover, this lap joint should be preferably located at sections where the global longitudinal stresses are small.

Fatigue design provisions were not explicitly included in the design of aluminium structures (Fredriksen 1997) until the fatigue had become a critical design criterion in connection with the large catamarans such as the Stena HSS 1500 (Nordhammer 1998). Therefore, previous design rules that were primarily established for small-sized structural components seem to be inadequate to provide a sound basis for the fatigue design of aluminium structural components.

Fatigue assessment methods for aluminium structures are primarily based on the Wöhler curve or SN curve when the fatigue life is relatively long, for instance, the number of cyclic loads can be up to  $10^8$  in a design life of 20 years for a ship structure.

Current design codes and classifications can be divided into three categories according to the stress definition used in conjunction with SN curves. The nominal stress range approach is the most popular one in which the design stress does not explicitly reflect the stress raising factors due to neither the local joint geometry nor the weld geometry. This method provides a quick estimate of the fatigue strength of a given

joint. This method depends entirely on relevant experimental data to judge which SN curve is relevant. The nominal stress range approach is widely adopted by design codes and classifications such as the Aluminium Association (AA 1994), British Standard (BS 1991), ECCS (1992), IIW (Hobbacher 2003), and Eurocode 9 (1998).

A number of joint details are usually included in the design codes and classified into different “detail classes” depending on attachment type, fatigue cracking location, weld specification and load conditions. One “detail class” is often deduced by performing small-scale fatigue tests which involve some kind of scatter. The design SN curves are then obtained by the so-called “mean minus two standard deviations” method. This way of developing such an SN curve is appropriate in the steel industry because the geometry of the joints have been standardised over long period and enormous amount of test data provides a strong confidence in using the design SN curves.

This is not the case for aluminium, at least, for the following reasons. First, aluminium is a relatively young engineering construction material even though there has been an expansion in the use of aluminium because of its good mechanical properties such as its high strength/weight ratio. Second, the most important reason is that the section profile can be fabricated into any desired shape by extrusion techniques. A standard section profile database is therefore impractical because a structure designer may use a self-designed complex section profile for a special purpose. In addition, as indicated in the previous part, fatigue of aluminium has not been implemented in the design codes and classification until recently.

Local stress based approaches, such as the structural (or hot-spot) and notch stress range approaches are, therefore, useful in the fatigue assessment of the aluminium structures. A common feature of these local approaches is that the effect of the local joint geometry (that is called the structural geometry in this study) as well as the weld geometry is taken into account by the reference stress and not in SN data themselves. In the nominal stress range approach, these effects are implicitly embedded in the design SN curves.

Fatigue assessment methods based on the local stresses greatly simplify the “detail classes” appeared in the nominal stress range approach (Eurocode 9 1998; DNV 1997). However, how to calculate the local stresses becomes another challenge for these methods. A universal and practical method for all types of joints is hard to obtain. On one hand, the existing methods are usually joint dependent, such as the extrapolation methods (Niemi 1995; Niemi et al. 2006; Hobbacher 1996). On the other hand, some joint-independent methods such as the method proposed by Tveiten and Moan (2000) and another one proposed by Xiao and Yamada (2004) require very fine mesh size in the finite element analysis (time consuming), thus limiting its practical application.

Geometrical parameters of the weld play decisive roles in determining the fatigue life of a welded joint (Engesvik and Moan 1983). The modelling of the weld in the finite element analysis influences the local stress calculations. A modelling principle was summarised by Tveiten et al (2002). These parameters including the weld toe angle, weld toe radius, weld throat thickness and weld leg length scatter randomly while hard to account for in the finite element model. The influence of these parameters on the local stress concentration factors is not explicitly reflected in current design codes and classifications.

Selection of proper fatigue design curve by means of structural stress for welded aluminium structures is equal important to the developing of the calculation method of the stress. Existing design guidelines do not clearly comment on the choice of design curves together with consistent use of certain type of local stress calculation methods.

Fatigue improvement by weld toe grinding has been observed for the steel structure by a factor of approximate 2.0 in terms of number of cycles at a given stress range level (Haagensen and Maddox 2004). Improvement has also been reported by Haagensen and Maddox (2004). In aluminium, however, no consistent benefit factor has been claimed (Tveiten 1999).

## **1.4 Thesis structure**

Chapter 2 gives the state-of-the-art of relevant fields of this thesis and explains the reasons for proposing the research topics. Chapter 3 is a summary of the results and findings for each topic and give recommendations relating to corresponding topics.

Papers 1 to 4 are collected in appendix A and Appendix B includes the material certificates and welding inspection documents. Appendix C describes the measuring details of the weld parameters. Some coloured photos are reprinted in Appendix D.



## **2      *Fatigue of Aluminium Welded Joints***

---

This chapter describes the design of appropriate welded joints for aluminium ships which have sufficient fatigue life while still being cost-effective. The focus is on welded joints of box stiffened panels. Various fatigue assessment methods together with corresponding design SN curves are reviewed. A general structural stress definition is proposed for the selected welded joints. Methods for improving the fatigue performance of as-welded and toe-ground non-load carrying fillet weld cruciform joints are also reviewed. Finally, the specimens and the set-up for the experimental investigation of the fatigue strength are described.

### **2.1    Aluminium vs. steel in ship building**

The ship building industry has been using steel as a main construction material for more than one and half century and the trend will still continue in a foreseeable future. The size of ship has never ceased to increase to satisfy the new requirements for larger and larger ships. For example, the “unsinkable” Titanic built in 1910 weighs only about 46,000 tons while the most recently launched cruise ship “Freedom of the seas” built in 2007 has a record weight of 160,000 tons that weighs nearly three and a half times of its predecessor. Increasing demands for larger ships have forced the designers to search for substituting materials to reduce the weight of the ship without sacrificing strength. Among many available materials, aluminium and its alloys has become one of the main candidates that can provide competitive strength compared to normal strength steel. A properly designed structural component made of aluminium alloy can reduce the weight by more than 50% compared to that made of normal strength steel.

High strength steels with yield strength beyond 350 MPa are not replaceable in ship building applications where high strength is critical. Even though any aluminium alloys do not have such high yield strength as the high strength steels, there are many aluminium alloys which do have nearly identical/higher minimum yield strength compared to normal strength structural steel, for instance, the most popular A36 steel

which has yield strength of 250 MPa while the 5000 family aluminium alloy has average yield strength of 275 MPa and has been mainly developed as marine alloys.

Aluminium has a density of only 2720 kg/m<sup>3</sup> which is approximately one-third as much as steel (7850 kg/m<sup>3</sup>). Its elastic modulus (70 GPa) is also nearly one-third of steel (200 GPa). The combination of these properties makes aluminium an appealing construction material especially in the components carrying significant bending load, particularly in skinned/plate structures such as ships. Significant bending loads have to be carried by the main structures in these products as the one showing in Figure 2-1 where the load conditions for an aluminium catamaran hull was illustrated (Heggelund et al. 2002).

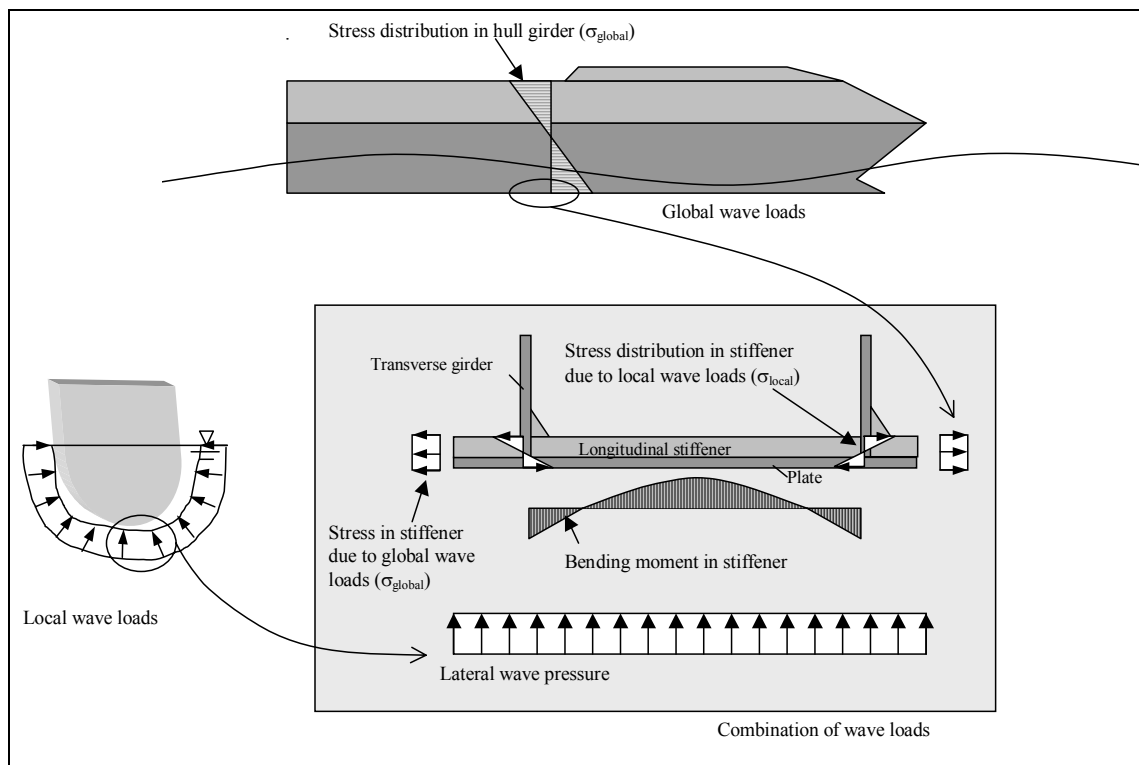


**Figure 2-1 Load and stress components in an aluminium ship hull (adapted after Heggelund et al. 2002)**

Aluminium structure with the same weight as steel has also better resistance to compressive load such as to buckling. Another great advantage of using aluminium in ship building is its unrivalled resistance to sea water corrosion with a corrosion rate of only 1% as much as steel. Aluminium alloys have been commonly used for marine structures where weight and high speed are important such as for high speed ferries and military ships. For example, the guided missile destroyer, Scott, uses aluminium as the construction material for superstructure while aluminium is used for whole body of the patrol combatant missile hydrofoil, Gemini, according to Naval Vessel Register (NVR). Dramatic advances in technology have allowed the use of aluminium for building

larger-sized ships. A recent record with overall length more than 126 meters has been successfully set up by Austal in building both high speed express and combat ships as shown in Figure 2-2. These vessels can travel at a high speed of more than 40 knots for much faster passenger/car transportation and navy deployment (Austal 2007).



**Figure 2-2 Large aluminium ships built in recent years by Austal (left: Benchijigua Express, right: US navy's LCS - Littoral Combat Ship)**

Energy efficiency is becoming more and more important. In these connections aluminium is advantageous due to its significant energy savings in recycling.

## **2.2 A short history of aluminium in ships**

Using aluminium as a main construction material in ship building industry can be traced back to 1930's. The size of the ship during that age was in a length range of 60 m and ever since it had been confined to small sized ships until 1960s.

A combination of steel and aluminium has been another choice for ship building industry to mainly reduce weight of the superstructures, as mentioned in the previous section. An increasing interest in using aluminium as a main construction material has emerged in the recent decades, particularly in the ferry and cruise ship industry, where speed and comfort are main concerns. Military requirement for ultra-high speed vessels plays another important role of pushing aluminium in the eyesight of the ship designers and builders.

A 74 m long catamaran "Hoverspeed Great Britain" was built at the end of 1980s which made a record fast trip during its trans-Atlantic voyage from Australia to the UK in 1990 (AA 1997). The record was exceeded by the building of the Stena HSS1500 with a length of 126.6 m (Storey 1997). The hull design of aluminium ships has also significantly evolved from mono-hull to catamaran (as for Stena series), trimaran (as for LCS). Application of aluminium in new concepts such as quadrimarans or pentamarans is also being investigated.

## 2.3 Design of welded joints

### 2.3.1 General

A joint is conventionally defined as a manner by which structural parts meet each other. Examples are lap joint and T-joint as shown in Figure 2-3. The structural parts can be made into one functional component by weld such as butt and fillet weld and accordingly addressed as a welded joint. The strength of the welded joint depends both on the material and the weld. Butt welded joints have a potential for higher performance than joints with fillet welds but are more costly to make. Therefore, butt welds are applied in the areas where higher strength is desired while fillet welds are used in less important parts.

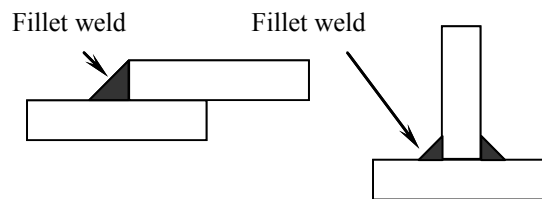


**Figure 2-3 Example of joint types, Lap joint and T joint**

The basic components in shipbuilding are rolled plates and hollow section extruded profiles (Figure 2-4). Box stiffener is such a hollow section that can provide excellent strength/weight properties as demonstrated in practice by the design of the Stena HSS.

The box stiffeners are integrated in the hull by a large number of joints with the web frames by fillet welds, as shown in Figure 2-4. The fatigue strength of such joints is becoming decisive when the size the vessels are becoming large. In addition, welding of these joints requires a huge amount of human labour and therefore any simplification of the welding may bring significant benefit to the builders. However, any simplification should not be at a price of sacrificing the overall strength of the welded joints.

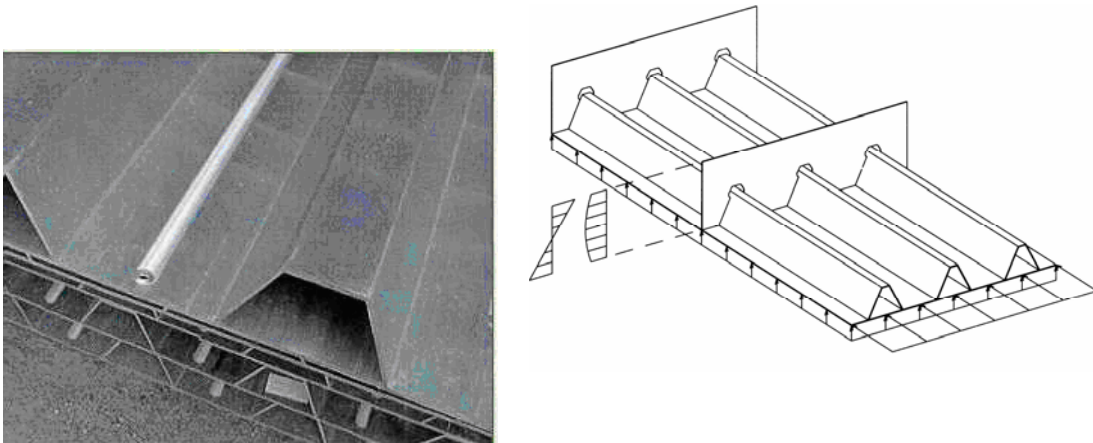


**Figure 2-4 Extruded hollow sections and web frame/box stiffener connections**

### 2.3.2 Designing web frame/box stiffener joints

Three similar web frame/box stiffener connections for the panels in Figure 2-4 were proposed and analysed in this study. The overall structure is identical while only small modifications for each individual connection as illustrated in Figure 2-5 and Figure 2-6.

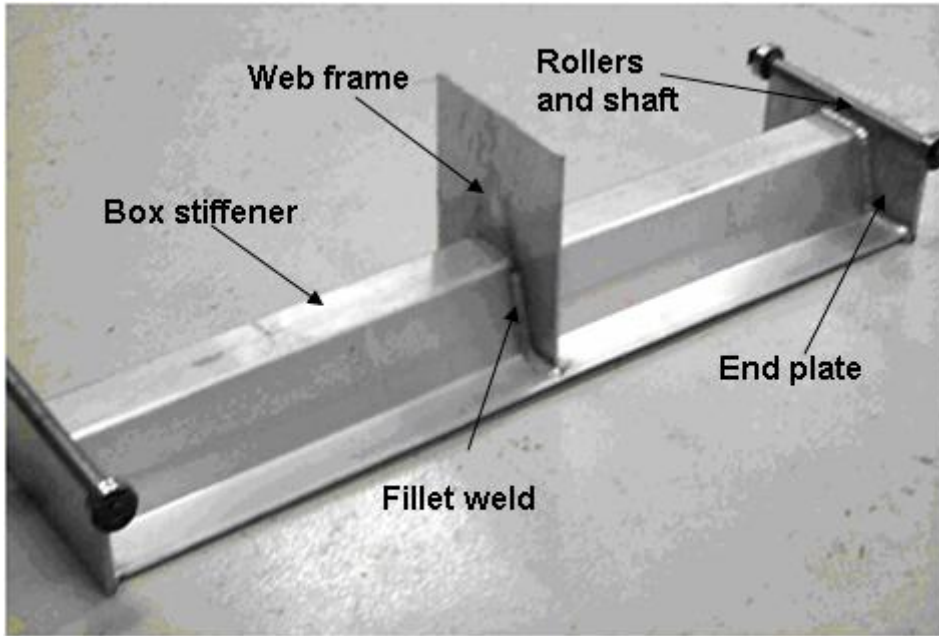


Figure 2-5 Overview of the web frame/box stiffener connection

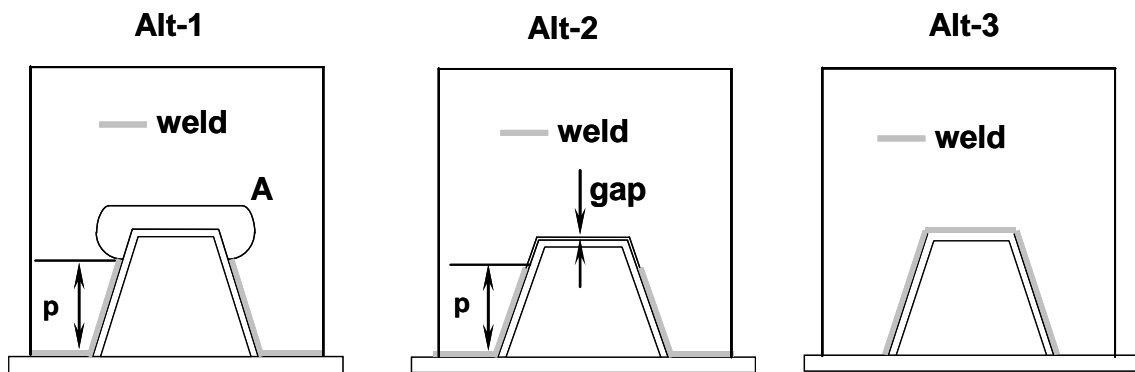
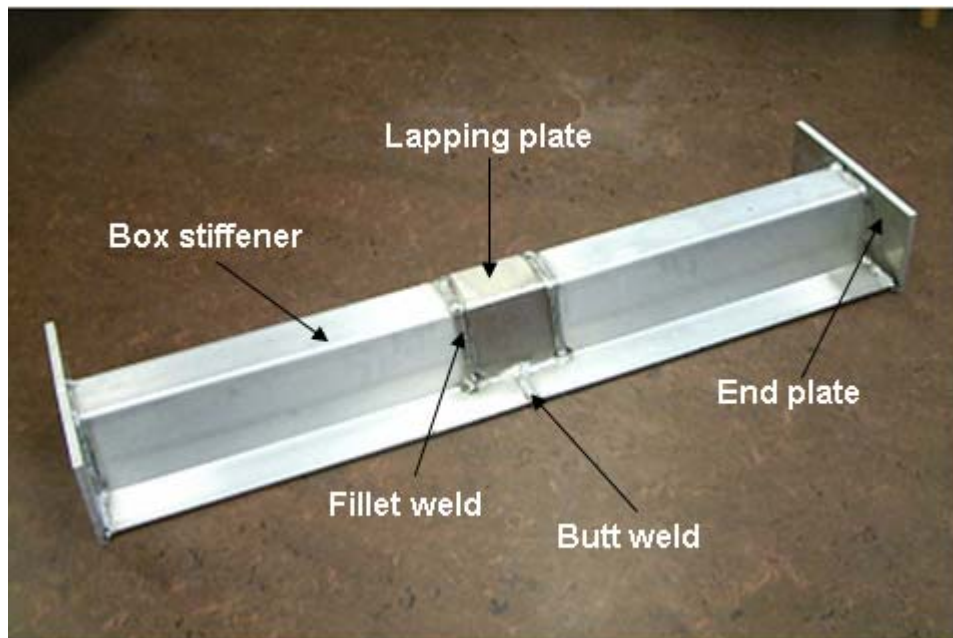


Figure 2-6 Joint difference for the web frame/box stiffener connection

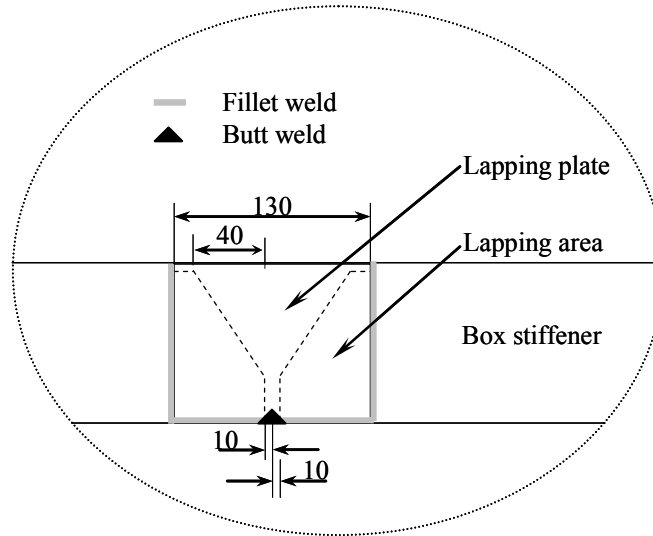
A large opening at A on the web frame is made for Alt-1. Welding is performed along the intersection lines of the two parts (gray line in Figure 2-6). Ensuring easy assembling of the two parts and providing free access for the welding to be carried out around the web frame are the main intention for using a large opening. Alt-2 differs from Alt-1 in both the cutting shape and weld feature. The opening on the web frame is

tailor cut to fit to the profile of the stiffener with a small gap of approximately 1 mm. Welding across the web frame is not possible due to the small gap. Therefore the welding is simply terminated at some distance (denoted as  $p$  in Figure 2-6) from the bottom flange of the box stiffener. No difference on the opening on the web frame is made compared to Alt-2. However, welding is performed without termination around the box stiffener for Alt-3. Hence, a continuous weld around the cross section of the box stiffener is formed. The last solution also provides a water tight connection which makes it different from the other two connections.

Welding on aluminium profiles may cause larger shrinkage and distortion of the cross section than for steel structures. This fact makes it difficult to join two pre-fabricated units where a number of parallel box stiffeners must meet each other, by means of for instance butt weld. In order to effectively join such profiles, a novel box stiffener lap joint is proposed, as shown in Figure 2-7. The wide flange (bottom) of the box stiffeners is joined by conventional butt welds while the hollow sections are joined by such a special lap joint. The covering plate (lap plate) is so designed that its inside profile is identical to the outside profile of the box stiffener. By applying fillet welds around the joining lines between the lap plate and box stiffeners, the two sections will then be formed into one piece. There are no special requirements for the cutting shape on the joining end of each box stiffener as long as the lapping area is sufficient to transfer the load acted on the joint. The lapping length increases from the top flange to the bottom flange as shown in Figure 2-7, until the bottom flanges meet with a small gap where butt weld will be performed. This design will enable larger contacting area and therefore increase the rigidity of the joint, particularly under bending loads.



(a) Overall of the lap joint



(b) Geometry details of the lapping area

**Figure 2-7 Box stiffener lap joint and joining details**

## 2.4 Weld measurements and laboratory tests

### 2.4.1 Weld measurement

Weld parameters such as the weld toe angle ( $\theta$ ), weld toe radius ( $\rho$ ), weld throat thickness ( $a$ ) and weld leg length ( $\lambda$ ) as shown in Figure 2-8. Welds both for typical T-joints and lap joints are illustrated. These parameters play an important role in determining the fatigue behaviour of the welded joints (Engesvik and Moan 1983).

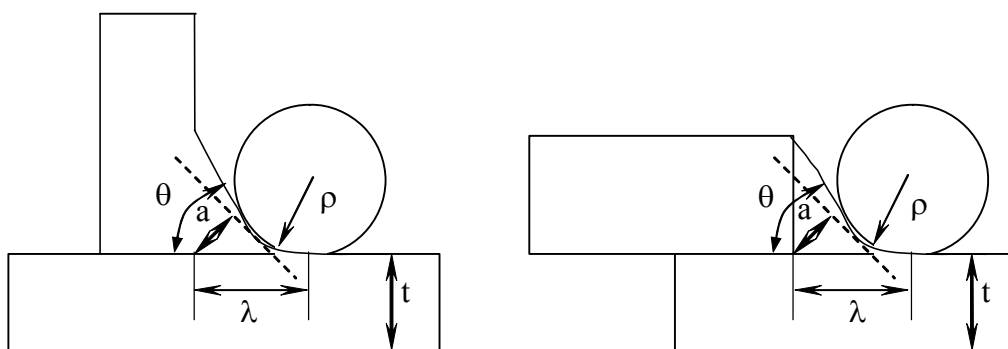


**Figure 2-8 A simple illustration of the weld parameters for T-joint and lap joint**

### 2.4.2 Test set-up

The test specimens are tested under a four-point bending load condition as shown in Figure 2-9.

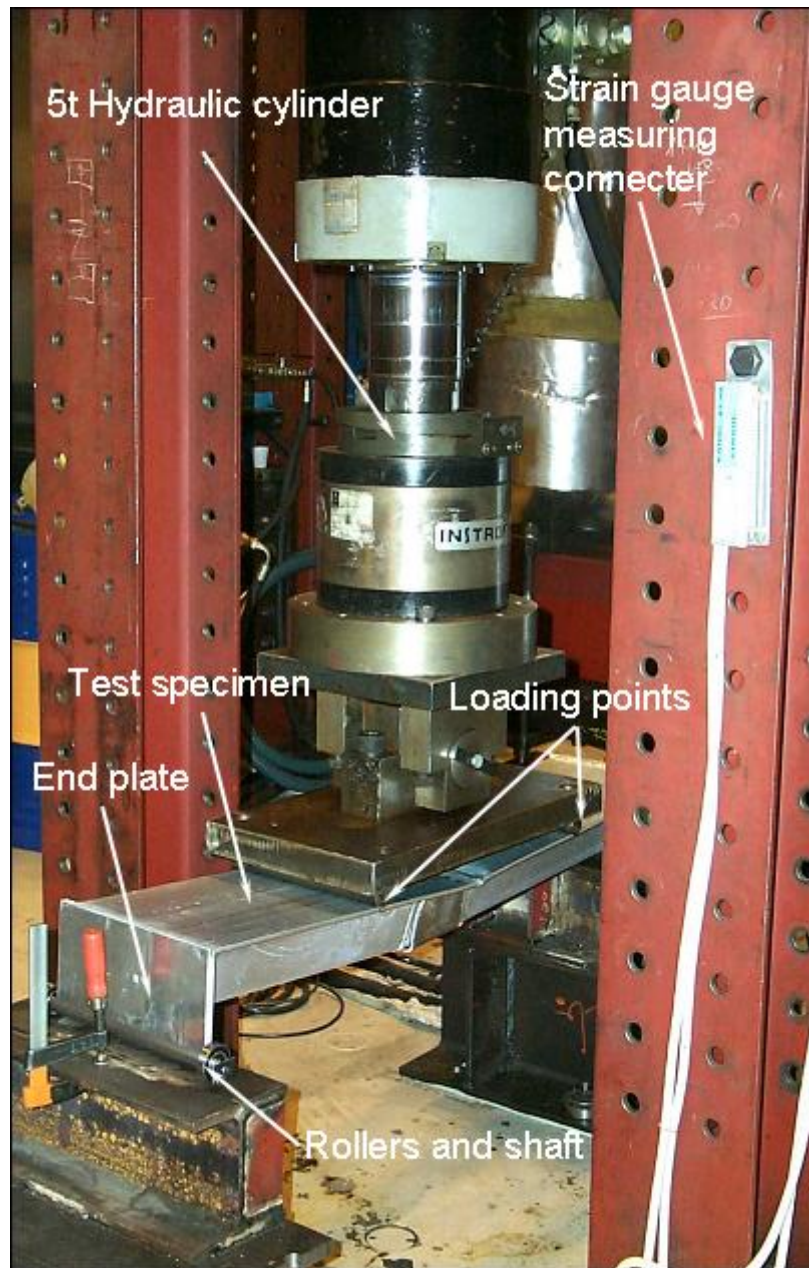
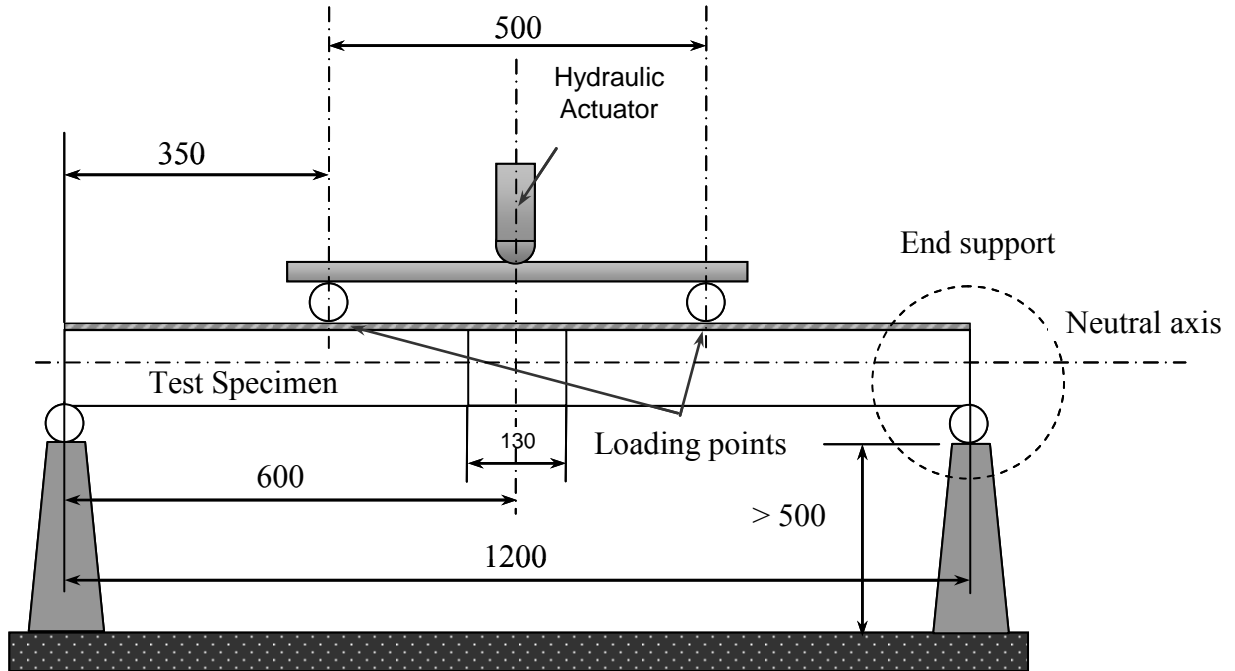


**Figure 2-9 Test set up for four-point bending load condition**

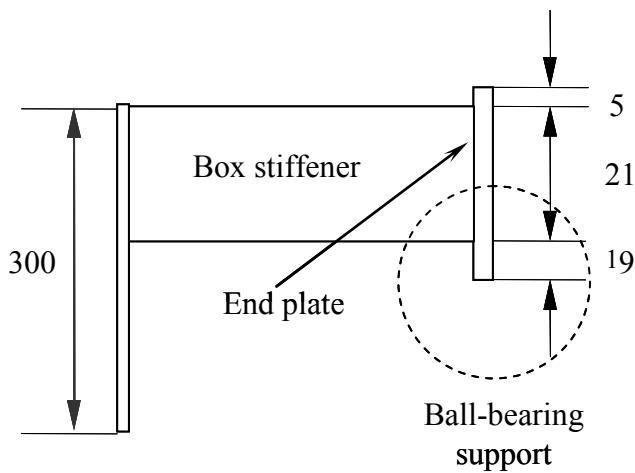
Figure 2-10(a) schematically shows the dimensions of the test set-up together with the details of the end supporting, Figure 2-10(b). A slot is machined along the shaft as shown in Figure 2-10 (c) so that the end plate can be fitted into the shaft. Two roller



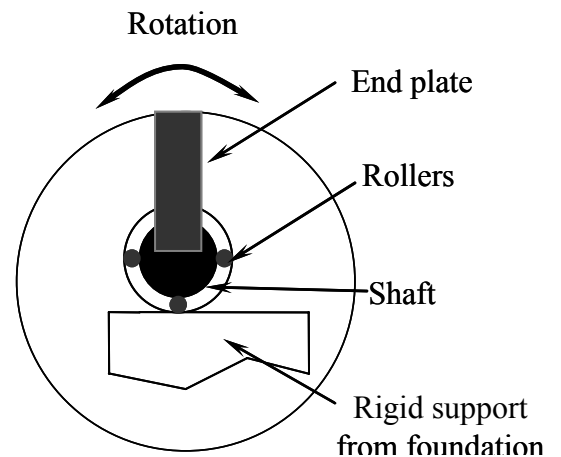
bearings are then fixed at each end of the shaft to ensure the end plate can slightly rotate about the neutral axis when the specimen deforms. Longitudinal movement of the specimen is well restricted by the friction between the loading points (actually two lines with the same width of the specimen flange)



(a) Four point bending test set-up



(b) Details of the end support



(c) Ball-bearing support details

**Figure 2-10 Details of the four-point bending test set up**

### 2.4.3 Instrumentation

In order to eliminate the compressive residual stress introduced by welding procedure, a load ratio of 0.44 is applied to ensure that the main stress component (axial stress along the box stiffener) at the critical fatigue location remains as tensile stress.

## 2.5 Fatigue analysis of aluminium welded joints

### 2.5.1 General

Fatigue is defined as “Failure under a repeated or otherwise varying load, which never reaches a level sufficient to cause failure in a single application”. Fatigue of metals has been studied for more than one and half century since Wilhelm Albert first observed and reported the phenomenon of metal fatigue in 1838 (Schütz 1996). Schütz (1996) also cited the most important conclusion in Wöhler’s final report in 1870 about the phenomenon of fatigue, “Material can be induced to fail by many repetitions of stresses, all of which are lower than the static strength. The stress amplitudes are decisive for the destruction of the cohesion of the material.” The most famous SN diagram in which the nominal stress is plotted versus the number of cycles to failure for fatigue analysis was a “creation” of August Wöhler and each curve is still referred to as a Wöhler curve.

“Between 50-90 per cent of all structural failures occur through a fatigue mechanism“, reported by Fuchs and Stephens (1980). The percentage may vary with the types of structure and service environment, but incorporating fatigue into design of engineering structures is of great importance.

Almost all structures are experiencing some kind of varying load. However, fatigue failures are more likely to happen in ship and offshore structures because they are exposed to sea waves (and winds) that impose a great number of fluctuating loads on the ship during its service lifetime. The number of load may amount to  $10^8$  within a design life of 20 years. In addition to these loading factors, vibration caused by machinery, propeller, etc. is another source of varying load. These repeated loads can cause fatigue damage or failure at a stress level usually well below the design allowable of material.

Fatigue is more important for aluminium than steel structures because the fatigue resistance of the aluminium is quite limited compare to steel as illustrated in Figure 2-11 (USS 2007). The importance of fatigue increases when high strength materials are applied in welded structures because the fatigue strength does not increase with the static material strength

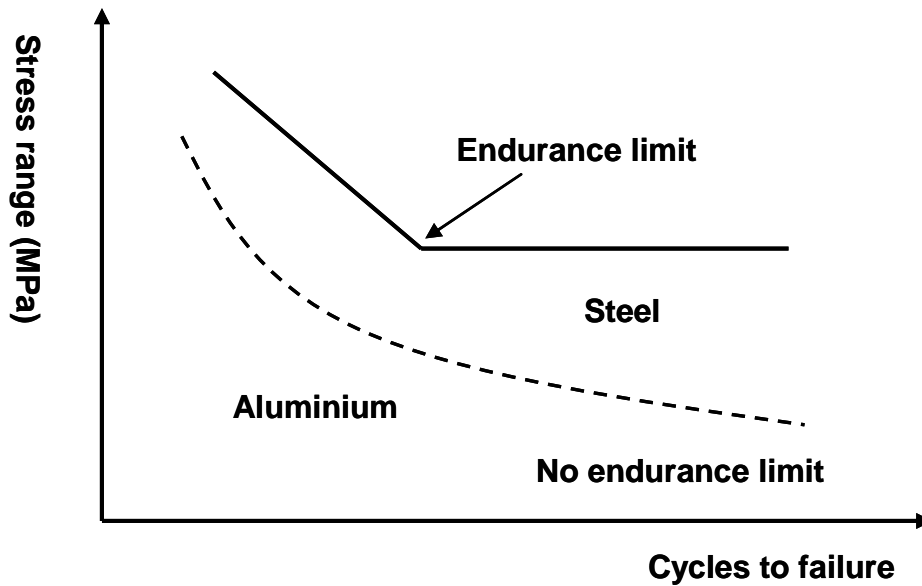


Figure 2-11 Fatigue comparison between aluminium and steel

### 2.5.2 Development of fatigue assessment methods

Three main fatigue assessment methods have been developed to predict fatigue life. These methods include strain-life, stress-life and fracture mechanics depending on whether the focus is on crack initiation, total fatigue life or crack growth. The strain-life method is based on the stress-strain history at the fatigue critical location and mainly developed for low-cycle fatigue involving large cycles with significant amounts of plastic deformation. This method combines material behaviour and local strains in the critical regions for life fatigue life prediction based on the initiation of a crack. Therefore, this method is often considered as “initiation” estimates. Details and applications of the method are well documented in the 1980s (Fuchs and Stephens 1980).

Stress-life method have been established as a standard fatigue design method for almost 100 years and was used in an attempt to understand and quantify metal fatigue. This method assumes that the stress-strain behaviour is elastic for the whole structure including the locations where fatigue failures initiate. Therefore, this approach can be used when the applied stress is within the elastic range of the material and the corresponding fatigue life is long.

In practice, the nominal loads acting on most engineering structures and components normally cause stresses in elastic range and plastic strain zone can be neglected. The stress-life and strain-life are then essentially equivalent.

Most fabricated engineering components, particularly welded components, contain initial defects such as weld porosity, inclusions, scratches (Fisher 1984), etc. In principle, there is no crack initiation phase in these components. Fracture mechanics then provides a methodology to relate the crack growth to fatigue life estimation. This method utilizes linear elastic fracture mechanics and cycle-by-cycle modelling of crack closure. A stress intensity factor  $K$  is introduced in this method to relate the local

stresses and strains to the applied stresses and strains by equation  $da/dN = C(\Delta K)^m$ ,  $K = \sigma\sqrt{\pi a}$ . The fatigue crack growth rate can be related to the stress intensity factor. Thereby, cycles to failure may be calculated. The accuracy of the fracture mechanics method depends strongly on the initial crack size and is not significantly sensitive to the size of the final crack.

The strain-life, stress-life and the fracture mechanics methods have their own advantages and disadvantages. Even though the strain-life and fracture mechanics methods may give better insight into the mechanism of fatigue, the stress-life method based on SN data is applied in fatigue design of ships and other structures. This is because they are simple to apply and data have been accumulated for almost any variations in surface finish, load configuration, environment, and so on.

## 2.6 Stress-based fatigue assessment method

### 2.6.1 Introduction

Fatigue strength data are commonly presented in the form of Wöhler or SN curves, in which a stress parameter generically indicated with S, say the stress range  $\Delta\sigma$  or  $\sigma_{\max}$ , is plotted as function of cycle number N. Equation (2-1) gives this relationship:

$$N = N_0 \left( \frac{\Delta\sigma}{\Delta\sigma_0} \right)^{-m} \quad (2-1)$$

$N_0$  and  $\Delta\sigma_0$  are the coordinates of a given point of the curve. Basquin (1910) proposed a log-log relationship for SN curves using Wöhler's test data in 1910. In the plane  $\log\Delta\sigma$ - $\log N$ , Equation (2-1) corresponds to the equation of a line of slope  $-m$ . Hence,

$$\log N = \log K - m \log \Delta\sigma \quad (2-2)$$

in which  $A$  is a constant depending on the joint features and load parameters.

The SN curves are usually presented in a log-log plane as shown in Figure 2-12.

Four behavioural zones with slope being 0,  $m_1$ ,  $m_2$  and 0 are used for the typical SN curve in Figure 2-12. The zones with zero slope coincide with the static strength and fatigue limit, respectively. No crack propagation is observed with the fluctuating stress being below fatigue limit and fatigue collapse does not occur for constant varying loadings imposed on steel or titanium structures. However, such a limit is not detected in aluminium structural components and in variable amplitude loading cycles for steel structures. Instead, a reduction in the slope of the SN curve ( $m_2$ ) is observed.

When engineering structures and components are exposed to an alternating load, the stress (strain) range, the mean stress, sequences of the stress peaks, surface finish and treatment etc. at the fatigue critical location influence the fatigue life. An important consideration for welded structures is that the residual weld-induced stresses at tensile yield level will be present at the potential crack sites. For this reason, it is commonly assumed that the whole stress range is effective in the crack propagation. From a fracture mechanics point of view it is the crack opening stresses that propagate a crack.

Compressive stresses are, hence, not fully effective in the fatigue process. However, the cyclic stress range  $\Delta\sigma$  has been concluded to be the most important parameter for determining fatigue life since detected by Wöhler in 1870 (Schütz 1996). Therefore, the stress (strain) range has been taken as the only critical parameter that governs the fatigue strength as a whole (Gurney 1992). Influence of the factors such as the mean stress can be related to a correction factor, e.g. the mean stress correction relationship given by Goodman (1899) and Morrow (1968). These correction factors are available in most of the fatigue design manuals (Rice 1988).

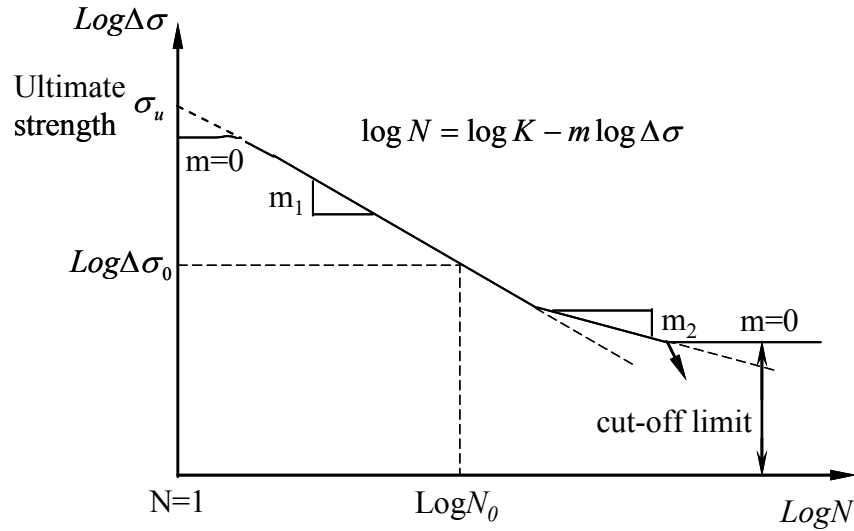


**Figure 2-12 A typical bi-linear SN curve**

Fatigue analysis based on the stress-life method can be summarized as the following steps:

1. to determine and estimate the cyclic load
2. to determine the fatigue critical sites and to estimate stresses
3. to select analysis and design method
4. to select appropriate SN curves

Verification by fatigue test may be helpful to increase the confidence in design.

On the bases of what kind of stress used in the SN curves, fatigue assessment methods are categorized by Fricke (2003) as the nominal, structural (also called “hot-spot”) and notch stress range approaches. Corresponding stress concentration factor calculation methods are then developed and fatigue test database are established for the application of each method. Figure 2-13 schematically illustrates how these factors are associated with different design SN curves. Related topics will be discussed in this study based on different kind of joints.

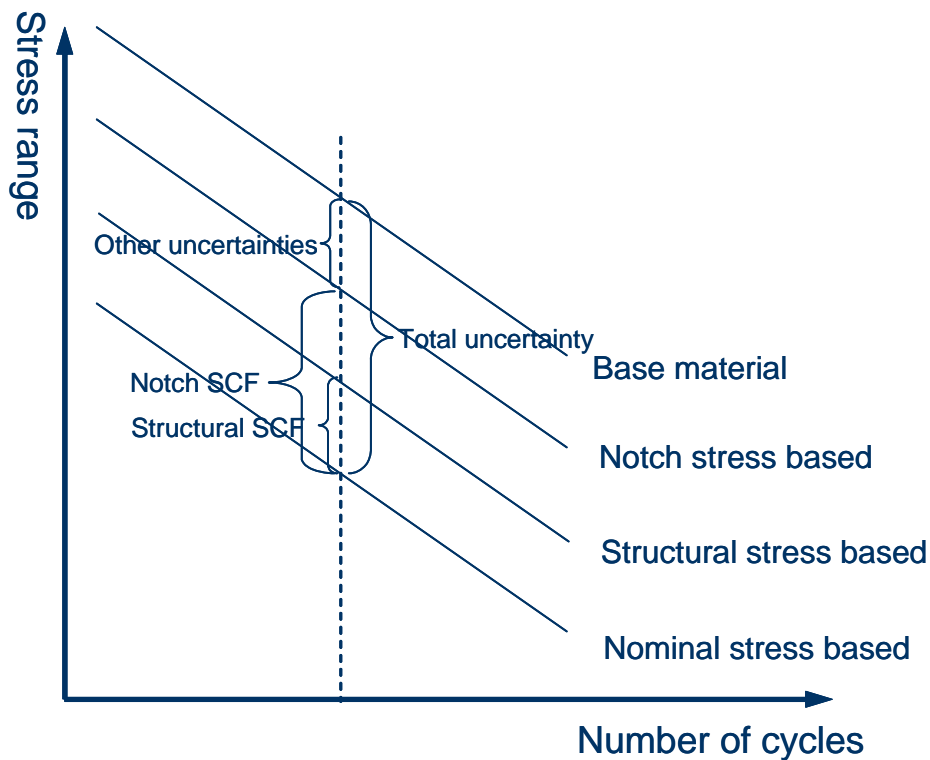


Figure 2-13 A typical bi-linear SN curve

## 2.6.2 Nominal stress range approach

### ***Definition of the nominal stress***

The nominal stress can be described as the stress at a nominal cross-section. The nominal cross-section refers to the cross-section where no stress concentration occurs. Simple structural mechanics can be applied to determine the nominal stress.

A typical nominal cross-section is a beam cross-section since the local discontinuities are neglected. The calculation of the nominal stress becomes easy by means of elastic beam theory or coarse mesh finite element analysis. Consider the stiffener in the bottom of the large catamaran in Figure 2-1. The nominal stress in this stiffener consists of two contributions, namely

- The axial stress due to the global bending of the catamaran
- The bending stress due to lateral pressure

While the former stress for some types of ships can be determined by beam theory, the global longitudinal stresses in (large) catamarans need to be determined by a finite element analysis. This is because of the significant number of window cut-outs in the super structure (Heggelund and Moan 1999).

The local bending stress is defined according to the bending beam theory taking account of possible brackets which provide some stiffness require particular caution. Simplified formulae have been established to reduce the problem to determine the bending moment (and stresses) in a beam with fixed ends and effective span width and also effective width, as used in a design guideline issued by DNV (Ref)

### ***Factors affecting the nominal stress***

As described above, the nominal stress refers to the stresses at the critical cross-section originating directly from the external forces or moments. The local features are omitted. However, some macro-geometric features, as well as fields in the vicinity of the concentrated loads and reaction forces should be considered in determining the nominal stress (Niemi 1995). These features usually cause the membrane stress redistributed over the whole cross-section and thereby imply a magnifying factor on the nominal stress that should not be ignored in practice. The macro-geometric features include large openings, curved beam, shear lag, flange curling, discontinuity stresses in a shell, bending due to lap joint eccentricity, etc. Analytical solutions for these macro-geometric features are obtainable in the literature, for example, “effective flange width” is used to capture the stress magnifying effects due to the shear lag and flange curling. In addition, offset and angular misalignments that are called macro-geometric discontinuities should also be attended in practice (Maddox 1985 and 2001).

Generally, the nominal stress exists only when there is a nominal cross-section. In complex structures, a “visible” cross-section may become hard to detect, local stress analysis should be adopted and fatigue analysis based on local stress/strain should be applied, instead.

### ***Nominal stress design SN curves***

Once the nominal stress at the fatigue-prone location is determined, appropriate design SN curve should be selected in order to compare the fatigue strength of the component.

Fatigue design codes and ship rules usually provide a number of “detail classes” depending on the joint type, weld parameter and load conditions, etc. A “detail class” is also called the characteristic fatigue strength of a specific joint type that refers to a characteristic fatigue life of  $2 \times 10^6$  cycles. For instance, a “detail class 45” means the structural component has a fatigue life of  $2 \times 10^6$  cycles when the nominal stress is equal to 45 MPa.

It should be pointed out that a design SN curve is deduced on the basis of experimental data, by carrying out fatigue tests at different levels of stress on a number of nominally identical specimens representing the detail under consideration. Therefore, the “detail class” is a point with fatigue life of  $2 \times 10^6$  cycles at a statistically regressed fatigue strength curve that often refers to a 97.7 per cent survival probability curve by considering the median fatigue strength curve minus two standard deviations.

The accuracy by using a nominal design SN curve in predicting of the fatigue life of an engineering structural component depends mainly on its similarities to the selected “detail class” in the design codes. The similarities usually include the local geometrical features, weld specifications, and load conditions, etc. Uncertainties may arise in case of

any mismatching. Therefore, fatigue tests should be carried out if a well-matched “detail class” is not available in the design codes and classifications.

One should also remember that the specimens used for developing the design SN curves are often small-sized specimens. The features found in the real scale structures such as the high residual stress in the welded joints, large thickness, corrosive environment, etc. are not reflected in the design SN curves. These features should therefore be treated individually to get a satisfactory result. For instance, the high residual stress can be simulated by assuming a high stress ratio, and a penalty factor is assigned to account for the thickness effect.

It is seen that fatigue assessment based on the nominal stress range approach has the advantages of simple theoretical description, ease of use and high confidence. However, since the calculation of the nominal stress neglects all the local geometrical and weld features that are known as the most important fatigue-determining factors and are implicitly embedded in the design SN curves, high accuracy is hard to achieve and large uncertainties may arise in predicting the fatigue strength of a novel type of structural component.

In spite of the fact that the stress-life method by using the nominal stress as the design stress is well-documented and widely used in practice particularly for steel structures, there is a limited number of standard “detail classes” in the design codes and classifications that is not sufficient to cover all the engineering structural components and joints. Situation becomes more serious in dealing with the fatigue strength of aluminium structures because there is almost no limitation in producing any shape of cross-section profiles by the technique of extrusion. It is therefore economically impractical to deduce a great number of “detail classes”. On the contrary, taking the local geometrical and weld features into the calculation of the stress in the fatigue-prone locations may provide solutions for fatigue analysis.

Development in computer capacity and advances in finite element method have enabled a local stress analysis procedure to include the effect of the local geometrical and weld features. The fatigue assessment methods based on a structural and notch stresses have thereafter been developed in recent years.

### **2.6.3 Structural stress range approach**

#### ***Introduction***

Fatigue assessment based on the nominal stress makes use of a “detail class” database established based on small-scaled fatigue tests. The difference of joint features is classified into in a given “detail class” and the number of “detail class” can be large. By introducing the structural stress, the number of “detail class” is greatly reduced while the effect due to the weld geometry is still implicitly embedded in the structural design SN. Thickness effect should also be treated individually, e.g. by a penalty thickness factor.

The concept of using the structural stress in the fatigue assessment can be dated back to 1960s according to Radaj and Sonsino (1998). Fatigue strength was related to the local stress at a definite small distance from the weld toe, e.g. 2.0-2.5 mm considering



the centre of strain gauge. The local stress that describes the structural behaviour could be either measured by strain gauge or calculated by engineering formulae or finite element analysis. The structural stress is a fictitious stress at the weld toe and its value can be calculated based on surface extrapolation or by linearization of the through thickness stress distribution (Radaj 1990). The structural stress concept was first successfully applied to welded tubular joints where rather high stresses may occur locally due to the significant bending stresses occurring in this shell structure. Procedures for application of the structural stress range approach to tubular joints are available in some design guidelines such as the ECCS recommendation (1985), Eurocode 3 (1992), and DEn (1990).

The use of the structural stress for fatigue strength assessment is of great significance since it avoids the limitations of the nominal stress by taking the structural geometry explicitly into consideration. Actually the structural stress analysis is always required because notch stresses and stress intensity factors are based on the structural stress (Radaj 1996).

The structural stress was originally termed as the “hot-spot” stress because of the temperature at the crack initiation sites is increased by cyclic plastic deformation prior to the crack initiation. The structural stress appears more frequently and acceptable when this approach was later extended to other welded joints than tubular joints. The name “structural stress” was officially accepted as the standard terminology by the International Institute of Welding in (Hobbacher 2001). In order to have a clear and consistent description, the name “structural stress” is used in this study and there is no essential difference compared to the “hot-spot” stress unless explicitly stated.

### **Definition of the structural stress**

The stress concentrations at a fatigue-prone location originate from either the local geometrical features such as discontinuities e.g. attachments or weld. Both these features are not reflected in the calculation of the nominal stress. The structural stress accounts for the stress raising effects due to the local geometrical features (structural geometry). Figure 2-14 is a typical picture of the stress distribution approaching a fatigue-prone location (weld toe).

The stress distribution adjacent to the weld toe is characterised according to the distance from the discontinuity. The nominal stress refers to the region where the gross geometry dominates and the elastic beam theory is applicable. However, when it comes closer to the discontinuity, stress rising occurs. The stress distribution is not only determined by the gross geometry, but also depends on the local geometrical discontinuity, resulting in the stress concentration within a zone called structural geometry affected zone. In order to describe the stress rising effect due to the structural geometry, a structural stress concentration factor is introduced:

$$\sigma_{structural} = K_g \cdot \sigma_{nominal} \quad (2-3)$$

in which  $\sigma_{structural}$  and  $\sigma_{nominal}$  represent the structural and nominal stresses, and  $K_g$  is termed as the structural (hot-spot) stress concentration factor.

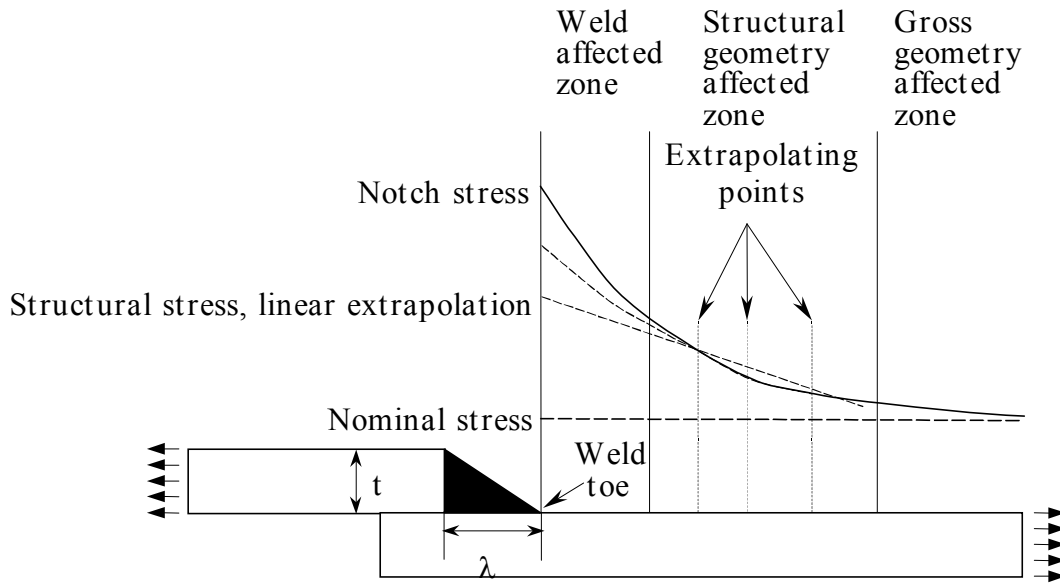


**Figure 2-14 Stress distribution in front of a weld toe**

In the nominal stress-life method, different structural geometries often relate to different “detail classes” and therefore different SN curves are established. However, the difference of the structural geometry is explicitly quantified by the structural stress concentration factor. In principle, a great number of “detail classes” required by the nominal stress range approach is not demanded by the structural stress range approach. On the contrary, the effects of the “detail classes” have been reflected explicitly by the factor  $K_g$ , therefore, an idealized design SN curve based on the base material ( $K_g = 1$ ) seems to be sufficient for fatigue strength assessment.

The use of structural stress as a design stress for weld joints is only suitable for weld toe fatigue failures. Fricke (2002) illustrated three types of possible weld toe failure locations as shown in Figure 2-15. Different failure sites may require different evaluation methods, as also indicated by Niemi (2001).

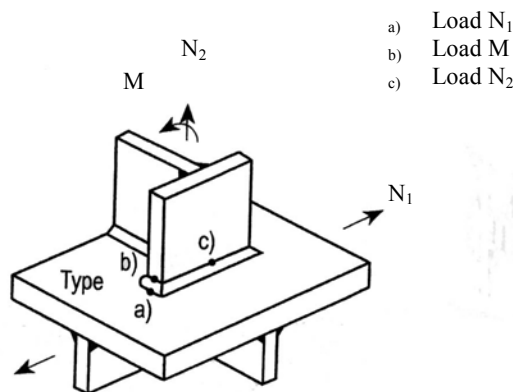


**Figure 2-15 Types of fatigue failure locations at the weld toe (Fricke 2002)**

Type “a” refers to the weld toe on the plate surface of an ending attachment, however, “b” is around the plate edge of an ending attachment. Type “c” refers to the weld toe lines along the weld of an attached plate both on the surfaces of stressed plate and the attached plate.

### ***Factors affecting the structural stress concentration factor $K_g$***

For a given joint with geometrical discontinuity as illustrated by Figure 2-14, the stress increases towards the discontinuity. Besides the effect of the specific joint, it is evident to imagine that the distance to the discontinuity plays the most significant role in determining the stress concentration due to the structural geometry. It was believed that the structural geometry has an influence zone (structural geometry affected zone in Figure 2-14) and a distance of  $0.4t$  to  $0.5t$  ( $t$  is assumed to be the thickness of the component member through which the cracks initiate and propagate) was taken as the starting point of this zone. The zone affected by the structural geometry terminates when the stress coincides with the nominal stress. Since the thickness of the main-stressed member is directly correlated to the zone affected by the structural geometry, it is therefore another critical factor in the calibration of the  $K_g$ , secondary only to the influence of the joint geometry itself. Actually, some design specifications even specify different design structural SN curves according to the thickness of the main-stressed structural member (Eurocode 9 1998)

The geometrical discontinuities are frequently accompanied by some kind of joining material such as the weld or adhesive. The stiffness of the local area is thereby changed and the influence on the  $K_g$  should also be investigated. The effect of weld parameters were studied by comparing different calculation methods and it was found that this feature influence should not be neglected (Ye and Moan 2002a, 2007a).

The structural stress refers to the stress at the fatigue-prone site that is usually a weld toe for a welded joint. The stress within the “weld affected zone” (Figure 2-14) is dominated by the presence of the weld (notch), that causes any direct calculation of the structural stress impractical. The influence of the weld should therefore be excluded from the calculation. The common principle for calculating the structural stress concentration factor is that the calculation is performed with the “structural geometry affected zone”. Extrapolation methods are the most popular way to determining the structural stress based on a finite element model with much more coarse mesh than required to account for the weld affected stress.

Some other solutions such as using an fixed point stress value, analytical tool to define the “structural geometry affected zone”, equilibrium formulae, have also been proposed and will be reviewed below.

Strain gauge measurements and finite element methods are the main tools for the determining the structural stress concentration factor. In the latter case, element type and mesh density adjacent to the weld toe affects the value of the concentration factor.

### **Extrapolation methods**

Stresses at two or more points located within the “structural geometry affected zone” are extrapolated to the weld toe to estimate the structural stress concentration factor. The location of the points selected for extrapolation is the key issue determining the magnitude of the concentration factor. Various methods have been proposed to determine the structural stress concentration factor. Extrapolation methods in which a linear (two extrapolating points) or non-linear (three or more points) mathematical model is established have been widely used to evaluate the structural stress. The location of these points then becomes a main issue concerning with the extrapolation methods. For steel structures such as tubular joints, numerous methods have been well established and are currently used (Radenkovic 1981). A full review of the extrapolation methods for tubular joints was summarized by van Wingerde, Pacher and Wardenier (1995). Extended applications to other welded joints can be found in the publication of Huther and Henry (1992), Huther et al. (1992; 1996), Yagi et al. (1991) and Machida et al. (1992). But Berge et al. (1994) reported that these methods may fail to provide a reasonable result for plated structures. A generalized structural stress approach for plate structures was applied to complex welded joints by Fricke and Petershagen (1992). Niemi (1995) presented recommendations for the determination of structural stress for fatigue analysis of welded components. A design guide was released recently (Niemi et al. 2006).

In the following some of the extrapolation methods are briefly reviewed.

#### *Method 1: Linear extrapolation over 0.5t and 1.5t*

Stress values at  $0.5t$  and  $1.5t$  ( $t$  is the thickness of the component through which the fatigue cracks initiate and propagates) away from the weld toe were used for extrapolation early in 1980s (Matoba et al. 1983). The structural stress concentration factor  $K_g$  at the weld toe can then be expressed as:

$$K_g = \frac{1.5\sigma_{0.5t} - 0.5\sigma_{1.5t}}{\sigma_{nominal}} \quad (2-4)$$

in which  $\sigma_{nominal}$ ,  $\sigma_{0.5t}$  and  $\sigma_{1.5t}$  refer to the nominal stress, stresses at  $0.5t$  and  $1.5t$  from the weld toe, respectively.

This method used by DNV in its design recommendations to calculate the structural stress concentration factor for both tubular and non-tubular welded joints (DNV 1993; 2000). Guidance on the finite element analysis is also given by the recommendations, and generally, both 20-node solid and 8-node shell elements can provide a reasonable answer provided that the mesh size is in the order of the thickness, for example, half of thickness of the main-stressed member when 20-node solid element is used.

#### *Method 2: Linear extrapolation over 0.4t and 1.0t*

This method was first proposed by Niemi (1994) to estimate the structural stress concentration factor in the vicinity of edge gussets welded to a stressed member such as stiffener. The factor  $K_g$  by means of this method is:

$$K_g = \frac{1.67\sigma_{0.4t} - 0.67\sigma_{1.0t}}{\sigma_{nominal}} \quad (2-5)$$

in which  $\sigma_{nominal}$ ,  $\sigma_{0.4t}$  and  $\sigma_{1.0t}$  refer to the nominal stress, stresses at  $0.4t$  and  $1.0t$  from the weld toe, respectively.

The IIW integrated this method into a design guidance for fatigue assessment (Hobbacher 1996; Niemi 2001). The first element should be no more than  $0.4t$  and the second no more than  $0.6t$  wide in the loading direction. 4-node shell and 8-node solid element can alternatively be used (Niemi 2001).

Niemi's (1994, 1995) investigation on gusset attachments laid a milestone for the development of extrapolation methods. More joint details have been investigated by this method and a more refined method was prepared as designer's guide by IIW (Niemi 2001).

### *Method 3: Non-linear extrapolation methods*

The structural stress concentration factors obtained by the linear extrapolation methods 1 and 2 may become non-conservative particularly when steep stress gradient towards the weld toe is found. Additional points with the "structural stress affected zone" are needed to reflect the real influence of the steep stress gradient on the structural stress at the weld toe. A non-linear extrapolation method was proposed by Niemi (1994):

$$K_g = \frac{2.52\sigma_{0.4t} - 2.24\sigma_{0.9t} + 0.72\sigma_{1.4t}}{\sigma_{nominal}} \quad (2-6)$$

in which  $\sigma_{nominal}$ ,  $\sigma_{0.4t}$ ,  $\sigma_{0.9t}$  and  $\sigma_{1.4t}$  refer to the nominal stress, stresses at  $0.4t$ ,  $0.9t$  and  $1.4t$  from the weld toe, respectively.

$$K_g = \frac{1.875\sigma_{0.5t} - 1.25\sigma_{1.5t} + 0.375\sigma_{2.5t}}{\sigma_{nominal}} \quad (2-7)$$

This method should be used in conjunction with fine mesh. When a coarse mesh is used an alternative method can be applied (Petershagen et al. 1991), in which the stresses at  $0.5t$ ,  $1.5t$  and  $2.5t$  were selected as the extrapolation points.

Methods 1, 2 and 3 are usually used for type "a" and "c" weld toe failures (Figure 2-15) because the thickness of the main-stressed member is directly correlated to the stresses at the extrapolation points. However, the stress approaching "b" is not apparently dependent on the plate thickness. Therefore, the extrapolation methods given above are no longer valid. Stresses at fixed distances of 5 mm and 15 mm are recommended by Fricke (2002) for extrapolation.

The weld failure sites in this study are either at "a" or "c" while failure at "b" is not in the scope of this study. Nevertheless, a quadratic extrapolation method (Niemi 1994; 2001) or a fixed-value method (Fricke and Bogdan 2001) can alternatively be used to address this issue.

### **Analytical solution to define “weld and structural geometry affected zone”**

A common feature for all the methods discussed above is that the influence of the local notch on the structural stress is limited within a local zone in front of the weld toe. The purpose of the fixed point evaluation or the extrapolation methods is to eliminate the effect of the local notch. Therefore, only the effect of the structural geometry can be reflected in the procedure of the structural stress calculation. This local zone is believed to be between  $0.4t$  and  $0.5t$ . In other words, the stress within this zone will be dominated by the local notch, however, the stress will be mainly controlled by the structural geometry beyond the zone until it reaches the zone where the structural stress coincides with the nominal stress. The common disadvantage of all these extrapolation methods is that they are generally developed on the basis of systematic finite element analysis and strain gauge measurements of particular welded joint details. Therefore, any attempt to apply these methods to other welded joints than the investigated ones may cause unexpected biases.

In addition, the existing methods have a direct relation to the thickness of the main-stressed structural components. Difficulties may arise when there is no apparent thickness in the stressed member such as a bulb stiffener. A structural stress evaluation method that is irrelevant to joint details is then becoming necessary.

After carefully investigating the stress gradient in front of the weld toe by sufficiently fine mesh size, Tveiten and Moan (2000) proposed an analytical solution that is capable of calibrating the influence zone of the structural geometry, thus developing a general method to calculate the structural stress concentration factor. The weld is ideally treated as a singularity in their proposal. The asymptotic stress gradient in front of the weld can be simulated by the following equation according to Williams (1952):

$$\sigma(r) = C_1 f(\theta) r^{\beta(\alpha)} + o(\theta) \quad (2-8)$$

where  $r$  and  $\theta$  are polar coordinates,  $C_1$  is a constant,  $f(\theta)$  is a dimensionless function of  $\theta$ , and  $o(\theta)$  are higher order terms of the stress field solution. It should be noted that the weld is modelled by an idealized notch by Williams, and hence, represents the maximum zone of influence of the singularity.

Infinite stress will appear when  $r$  approaches zero, therefore, the leading term in Equation (2-8) will become dominant over other expanded terms in the series if  $r$  is sufficiently small. Under this assumption, the stress varies proportional to the distance from the singularity powered to  $\beta(\alpha)$ . Considering to plotting the stress against the distance in front of the weld toe in a bi-logarithmic plane, a linear property will appear adjacent to the singularity. The log-linear relationship between the stress and distance provides a possibility of distinguishing zones influenced whether by the notch or the structural geometry. Three zones have been defined in Figure 2.3. The weld (singularity) affected zone can therefore be analytically located by plot the stress adjacent to the weld toe in a bi-logarithmic plane. The structural geometry affected zone is then located between the weld affected zone and the point where the structural stress coincides with the nominal stress. Figure 2.5 schematically shows this concept.

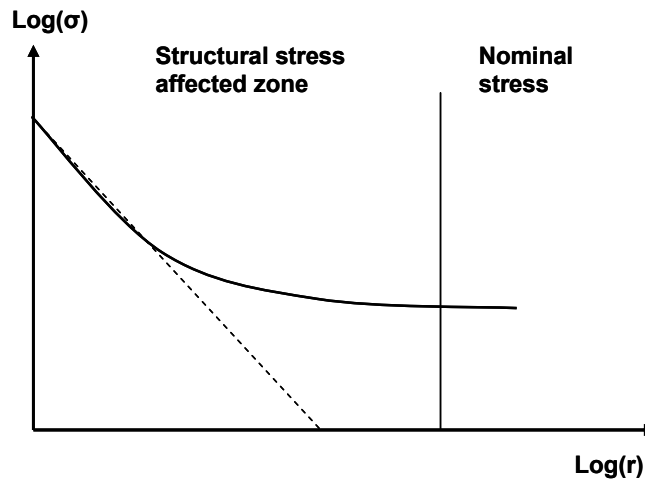


**Figure 2-16 Asymptotic behaviour of stress in front of an idealized notch (weld toe) in a bi-logarithmic plane**

After separating the “structural stress affected zone” from the “weld affected zone” and the nominal stress zone, a polynomial can be fit within this zone and the structural stress at the weld toe can thereafter be obtained by extrapolating the polynomial to the weld toe. Therefore, this method is strictly an extrapolation method as well. The polynomial order is dependent on the accuracy requirements. However, a second order polynomial would be sufficient for most cases.

Compared to the other extrapolation methods, Tveiten and Moan’s (2000) methods laid a ground for the interpretation of other extrapolation methods by analytically defining a structural geometry affected zone. That is to say, any extrapolation performed within the “structural geometry affected zone” defined by Tveiten and Moan (2000) would result in satisfactory stress value, however the extrapolation points should be so arranged that the stress gradient due to the structural geometry is reflected properly without over- or under-estimating the structural stress. Any extrapolation method with the extrapolation points at the leading part of the zone would result in relatively high structural stress concentration factor, and the rear part with lower value. For instance, the leading point  $0.4t$  in method 2 usually gives higher structural stress concentration factors compared to method 1 with the leading point at  $0.5t$ .

As stated above, most of the extrapolation methods can be applied only when the joint configurations match well with the assumed one. Any mismatch may bring unexpected factors. Tveiten and Moan (2000) did not introduce any restrictions with respect to joint specification. Therefore, their method is independent of any structural dimension to determine the region influenced solely by the structural geometry. Besides, the thickness effect is implicitly integrated in the determination of the “structural geometry affected zone”.

However, as Tveiten and Moan (2000) pointed out, a rather detailed finite element analysis is required to ensure that the local singularity at the weld notch is properly accounted for. This would obviously limit the application of this universal method.

**Remarks on extrapolation methods**

Structural stress determination methods have been rapidly developed since the last decade of the 20<sup>th</sup> century. It is found, however, whether the fixed point methods or extrapolation methods only use the surface stresses in the interested area where fatigue failure may arise. Fracture mechanics says that the total fatigue life comprises two phases that are crack initiation phase and the propagation phase. Once the crack forms, it propagates along the weld line and through the thickness and the latter direction for most cases is the most detrimental direction. Therefore, the involvement of the surface stresses in the structural stress calculation can only reflect the stress status on the surface where the crack initiates but it is inadequate to have a full view of the status of the stress after initiation has taken place particularly in the weld joints where the initiation phase is usually neglected and only the propagation period is considered as the fatigue life of the detail. Therefore, it would be more accurate to consider the actual stresses through the thickness in the structural stress calculation.

**Through thickness solution based on equilibrium formulae**

The limitation of linear finite element method is that it is incapable of evaluating the structural stress at the weld toe because the stress components become very large (and infinity in case of sharp relevant corners) when the mesh decreases. In order to calculate a meaningful stress by a relatively coarse mesh size at the weld toe, various methods such as the extrapolation methods discussed above have been proposed to capture the effect of the structural geometry. But the cracks at the weld toe may propagate tri-dimensionally, however, as a design criteria, the through thickness direction is taken as the most detrimental direction. Therefore, any stress calculation at the weld toe should take the tri-dimensional stress status into account.

In the methods discussed above, the relevant stress at the weld toe is normal to the weld toe line on the surface of the stressed member. It may vary over the thickness. Therefore, it becomes more reasonable to treat the normal stress as a function of the distance  $y$  in the thickness direction. The shear stress is treated in the same way. It is reasonable to express the normal and shear stress by a summation of a polynomial of order  $n+1$ ,

$$\sigma_{xx}(y) = \sum_{k=0}^n c_k y^k, \quad k = 0, 1, \dots, n \tag{2-9}$$

$$\tau_{xy}(y) = \sum_{k=0}^n d_k y^k, \quad k = 0, 1, \dots, n \tag{2-10}$$

where  $c_k$  and  $d_k$  are coefficients depending on the stress distribution along the thickness direction. The above equations are only applicable when no other shear components (e.g. in  $yz$  or  $zx$  plane) exist as shown in Figure 2-17 which illustrates a 2-dimensional stress status at the weld toe section in the thickness direction.



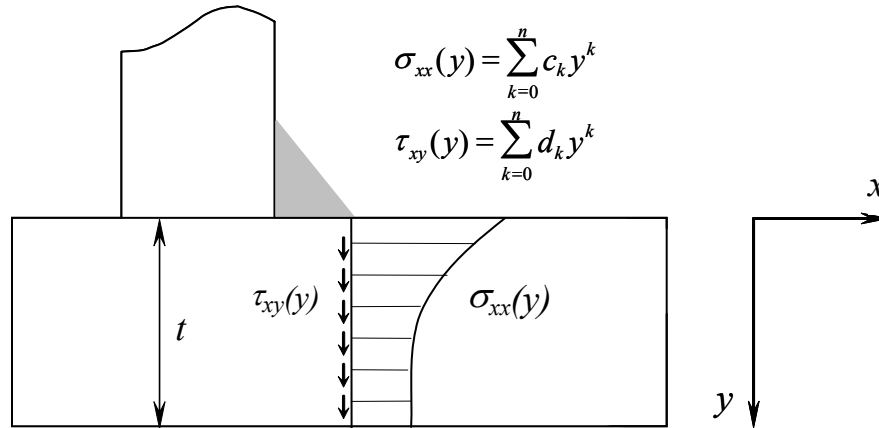


**Figure 2-17** Stress components at the weld toe in the thickness direction

By this definition, the traditional extrapolation methods become a special case where  $y$  is equal to zero.  $(n+1)$  variables are found in each equation that requires the same amount of conditions to quantify the coefficients.

The structural stress is defined as a linearly distributed stress through the thickness of the stressed member, thus being described by the above equations by setting  $k=1$ . In this case, the formulae can be solved by imposing equilibrium conditions referring to another section at a distance “ $s$ ” to the weld toe as shown in Figure 2-18.

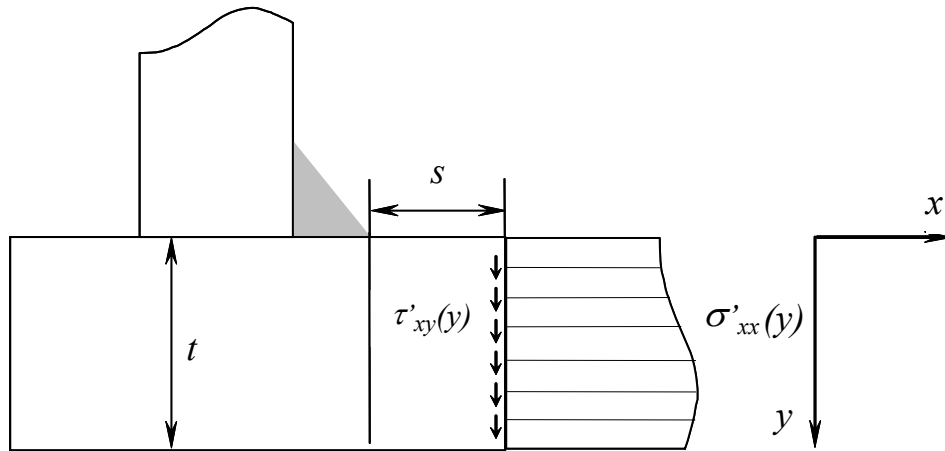


**Figure 2-18** Stress components on a cross section at a distance of  $s$  to the weld toe

The structural stress can therefore be expressed by the following equations:

$$\sigma_{xx}(y) = c_0 + c_1 y \quad (2-11)$$

$$\int_0^t \sigma_{xx}(y) dy = \int_0^t \sigma'_{xx}(y) dy \quad (2-12)$$

$$\int_0^t \sigma_{xx}(y) \cdot y dy = \int_0^t \sigma'_{xx}(y) \cdot y dy + s \int_0^t \tau'_{xy}(y) dy \quad (2-13)$$

in which  $s$  is the distance from the weld toe,  $\sigma'_{xx}(y)$  and  $\tau'_{xy}(y)$  represent the normal and shear stresses at the cross-section corresponding to  $s$ , respectively, as shown in Figure 2-18. As stated previously, these equations are only applicable on the absence of other shear components. The influence of such components was demonstrated by Poutiainen et al. (2004).

Equation (2-12) indicates the equilibrium of forces acting on the two cross-sections, and Equation (2-13) represents a moment equilibrium referring to the weld toe. Equation (2-11) describes the linear structural stress in the thickness direction. The coefficients  $c_0$  and  $c_1$  can be derived from equations (2-12) and (2-13).

Dong et al. (2001) and Dong (2003) defined the coefficient  $c_0$  in equation (2-11) as the structural stress and decomposed it into membrane and bending stresses and claimed that the magnitude of the structural stress according to this definition is mesh insensitive. However, a comparison study by Doerk et al. (2002), Poutiainen et al. (2004), Fricke and Kahl (2005) showed that the mesh-insensitive property was found mainly in two-dimensional problems such as a plate fillet welded lap joint. Even in this case, the “mesh-insensitive” property was also found by means of certain extrapolation methods e.g. method 2. Larger scatter than the extrapolation methods were reported in dealing with some other joints such as the one-sided doubling plate, bracket and flat bar welded to an I-beam. In the latter cases, lack of account of the stresses acting at the transverse element sides causes inaccuracies (Doerk et al. 2002).

### **Fixed point structural stress concentration**

Methods based on the extrapolation methods or analytical tools as mentioned above, require a post-processing of the output from the finite element analysis. In addition, it is difficult in most cases to separate the influence of the structural geometry from the weld and the gross geometry. Some empirical methods based on finite element analysis are also proposed to get a practical structural stress. One simplification is to consider barely the stress at a point within the “structural geometry affected zone” as the structural stress. Neither extrapolation nor integration is then needed. This method is also adopted by some existing design guidance such as the Lloyd’s Register in which the stress at a point  $0.5t$  in front of the weld toe is used as the design structural stress in the assessment of fatigue strength of welded joints.

When the finite element analysis are based on a model with mesh size of  $t \times t$  that is normally practiced for structure analysis, the point that is  $0.5t$  in front of weld toe would be a useful validation as this point is at the centre of the element. Obviously, this value will be smaller than that obtained by extrapolation. A simple modification of the point-wise estimate of the structural stress may be to multiply it by a constant factor. DNV proposed a factor of 1.12 (DNV 2000).

### **Structural stress design SN curves**

Fatigue assessment methods for welded joints particularly on tubular joints, based on the structural stress range approach are well-established (Hobbacher 1996). However, even though Eurocode 9 (1998) contains SN curves for the structural stress design approach, no fatigue design codes or recommendations have suggested a structural stress range approach for welded aluminium structures based on a well defined method

for the structural stress extrapolation together with a consistent definition of design SN curves.

The fatigue strength of a welded detail is dependent on several factors such as geometrical parameters including the plate thickness and the plate width, the attachment length, width and height, the specimen length, the leg length, and additional factors such as the loading mode (tensile/bending), misalignments (if not included in the finite element model where the stresses are derived from), and the condition at the weld toe (as-welded/toe-ground). The geometrical effect (thickness effect) is commonly addressed in fatigue design as a penalty factor on the form:  $f(t) = (t_{ref}/t)^n$ , where  $f(t)$  is the thickness correction factor,  $t_{ref}$  is the reference plate thickness,  $t$  is the plate thickness of the detail, and  $n$  is the thickness correction exponent. The thickness correction exponent applied in different codes and recommendations varies between 0.1 and 0.4 depending on joint category and condition. Eurocode 9 (1998) did not adapt to the scheme of a penalty factor but the geometrical effect is based on several different structural stress design SN curves depending on the actual plate thickness of the component. Poutiainen and Marquis (2006) proposed a modified structural stress method based on weld stress by which a semi-empirical thickness correction is claimed to be unnecessary.

For some details where the plate thickness is not evident (e.g. gusset plates with edge attachments, Type “b”, Figure 2.4), other geometrical parameters such as e.g. plate width or/and attachment length will govern the effects relating to the stress gradient in the crack plane. Partanen et al. (1994) derived a penalty factor for load carrying gusset plates with edge attachments as  $f(t) = (t_{ref}/t_{app})^n$ , where  $t_{ref} = 25$  mm,  $n = 0.25$ , and  $t_{app} = \min\{B, 1.5L, 15H\}$  where  $B$  is the height of the stressed member,  $L$  is the length of the attached gusset plate, and  $H$  is the height of the attached gusset plate. Niemi (1994) suggested a linear and a quadratic extrapolation method where he claimed that the geometrical effect was automatically accounted for by the quadratic extrapolation procedure, as the shape variation of the stress distribution in the crack plane due to changes in dimensions is included in the structural stress. While for the linear method, the geometrical effect has to be considered by multiplying the fatigue strength by the penalty factor,  $f(t)$ , suggested by Partanen et al. (1994).

Rather limited SN data for the validation of the structural stress approach for welded aluminium structures are available. However, some authors have presented SN data for welded aluminium structures based on a structural stress range approach. Partanen and Niemi (1999) compiled fatigue test results for a variety of aluminium test specimens with moderate thickness (up to 6 mm) subjected to pulsating tension ( $R > 0$ ) using structural stress obtained from extrapolated strain gage measurements and finite element analysis. The structural stress was based on the extrapolation procedure suggested by IIW (Hobbacher 1996). The SN data presented by Partanen and Niemi (1999) are shown in Figure 2-19 together with SN data provided by Maddox (1995).

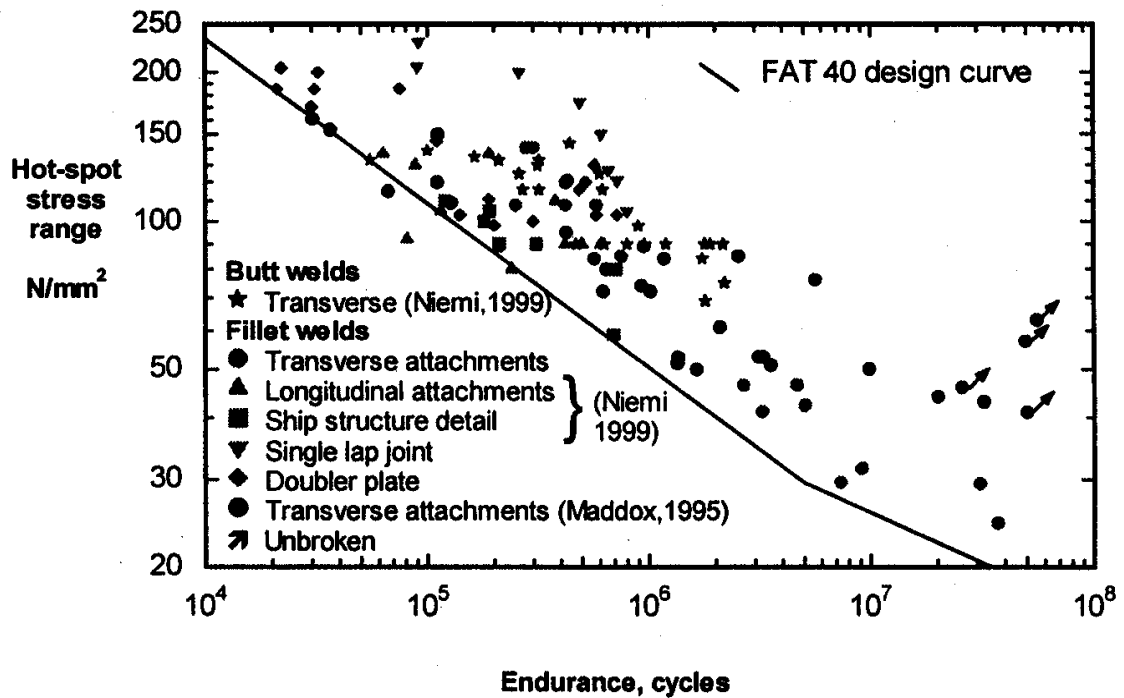
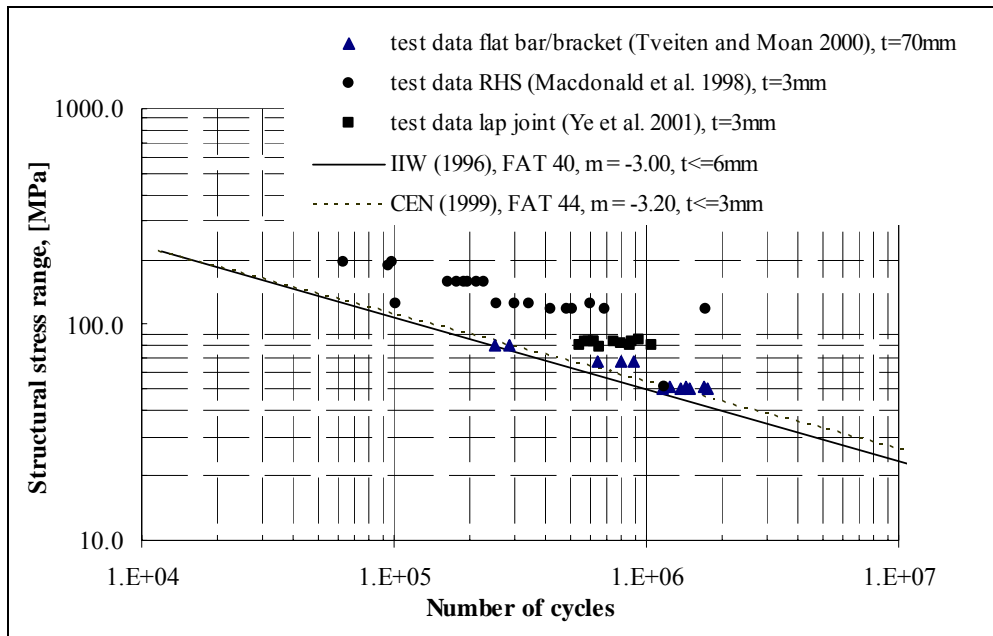


Figure 2-19 SN data expressed in terms of IIW (Hobbacher 1996) structural stress range definition (Maddox 2001)

The authors suggest that the structural stress range approach can safely be used with an SN curve of fatigue class 40 (fatigue class 40 refers to the characteristic stress range at  $2 \times 10^6$  cycles) for butt and fillet welded aluminium joints of relatively thin plates and extrusion (up to 6 mm) failing from the weld toe location. For plates with a thickness exceeding 6 mm, Niemi (2001) suggested that the fatigue strength must be reduced with a thickness penalty factor,  $f(t) = (t_{ref}/t_{app})^n$ , where  $t_{ref} = 6$  mm, and  $n$  varies between 0.1 and 0.3. Assuming a design SN curve of fatigue class 40 together with the thickness penalty factor suggested by Niemi (2001), the design fatigue strength is seen to be 10 to 15 per cent below what is suggested by Eurocode 9 (1998) for  $n = 0.3$ . For  $n = 0.1$ , the fatigue strength is seen to be 0 to 30 per cent above what is suggested by Eurocode 9 (1998). Most difference is seen for the largest plate thickness. As the difference in design strength depending on the thickness effect is rather large, it is suggested that there is a need for further research on this topic.

A numerical and experimental study by Macdonald et al. (1998) suggested a fatigue design methodology for welded aluminium space frames made of rectangular hollow sections joints using a linear or quadratic extrapolation of the structural stress according to recommendations given by the IIW (Hobbacher 1996) and a design SN curve with a fatigue class of 40. The fatigue test specimens were loaded four-point bending of the chord member at  $R = 0.1$ . The wall thickness of the test specimens (3 mm) was within the thickness range of the test specimens used for deriving the SN data presented by Partanen and Niemi (1999). The SN data are presented in Figure 2.10.

Tveiten and Moan (2000) published SN data on flat bars with fillet welded in-plane brackets (Type “b”, Figure 2-15). The structural stress was calculated using the extrapolation methods suggested by Niemi (1994) and Tveiten and Moan (2000). The SN data are presented in Figure 2-20. No thickness penalty factors are applied in the figure.



**Figure 2-20 SN data expressed in terms of the definition suggested by Tveiten and Moan (2000) and IIW (Hobbacher 1996) without thickness penalty factors**

The SN data obtained for the flat bar/bracket connections seemed to correspond well with the findings of Partanen and Niemi (1999) with respect to an appropriate structural stress design SN curve of fatigue class 40. However, the detail was also expected to be affected by geometry, which would influence the SN data. Design codes and design recommendations provide no recommendations on penalty factors for these particular types of joints. Using the penalty factor suggested by Partanen et al. (1994) with a  $t_{app} = 35$  mm, would give a  $f(t) = 0.92$  that would suggest slightly more conservative SN data compared to a design SN curve of fatigue class 40. Note, however, that the scatter of the test results was relatively narrow, the standard deviation of  $\log N$  is 0.094.

Studies on aluminium box stiffener/lap joints reported by Ye and Moan (2002a) showed that using a structural stress range approach, design SN curve of fatigue class 44 suggested by Eurocode 9 (1998) seemed to give conservative fatigue assessments (wall thickness of box stiffener and lap plate was 3 mm). The SN data are presented in Figure 2-20. The 97.7 per cent lower limit confidence regression line of the SN data was 5.5 per cent above the design SN curve at the point of two million cycles. The standard deviation of the test results was,  $STDV_{\log N} = 0.10$ . It should be noted that the structural stress extrapolation method adopted in the SN data representation was the method

suggested by Tveiten and Moan (2000). The margin will even be greater if the other extrapolation methods are applied, e.g. IIW (Hobbacher 1996).

Studies by Tveiten (1999) on longitudinal stiffener/bracket connections have shown that a possible effect on the fatigue strength due to the loading mode (tensile or bending) was assumed to be limited since this effect was mostly covered by a change in the structural stress concentration factor.

Tveiten (1999) also presented SN data on as-welded and toe ground flat bars with fillet welded in-plane brackets which suggested that there was fatigue life improvement in the low stress region (more than one million cycles). This implies a different design SN curve for toe ground details than for as-welded details. Test data of non-load carrying fillet welded cruciform joints supports the findings and suggest an increase on the fatigue class of about 30 per cent, which corresponds well to what is seen for welded steel joints (Ye and Moan 2007b).

**2.6.4 Evaluation of the structural stress calculation methods**

Some of the structural stress calculation methods have been extensively investigated recently. Results from various two-dimensional (simple) and three-dimensional (complicated) joint types have been published in the last couple of years. Most of them have been focused on the comparison between the surface extrapolation method and the method proposed by Dong et al. (2001) and Dong (2003) in which through thickness stress distribution is used to derive the structural stress. A summary of these findings published in the literature are presented in the . The comparison is based on steel structures while the conclusions are also applicable to aluminium structures.

**Table 2-1 Comparison of structural stress calculation methods**

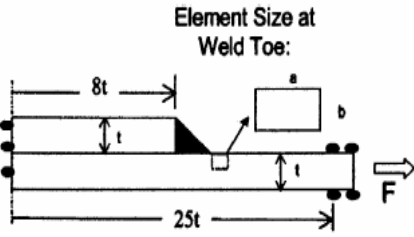
Joint type	Investigations
<div style="text-align: center;">  <p style="text-align: center;">Element Size at Weld Toe:</p> </div> <p>Dong et al. (2001)</p>	<p>The plate lap fillet joint under axial load <math>F</math> was first used by Dong et al. (2001) to demonstrate the mesh insensitivity of the method proposed by the author. Doerk et al. (2003) remodelled the joint by the same meshing schemes as used by Dong et al. (2001) while comparing the structural stress with the extrapolation method. Mesh insensitivity was achieved by both methods. No significant difference was found for the amplitude of the structural stress concentration factor.</p> <p>This joint was further investigated by Poutiainen et al. (2004) to study the limits for various structural stress calculation methods with regard to the act of mesh and loading modes. Equal results were obtained by all methods while heavily distorted finite elements should be avoided.</p>

Table continued.

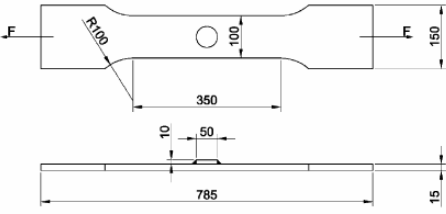
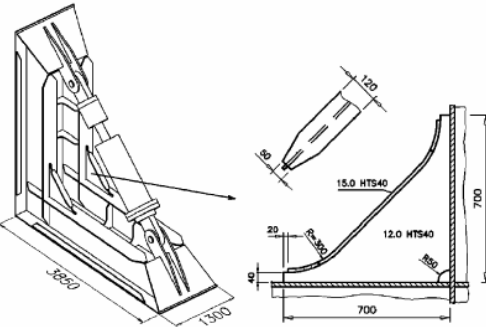
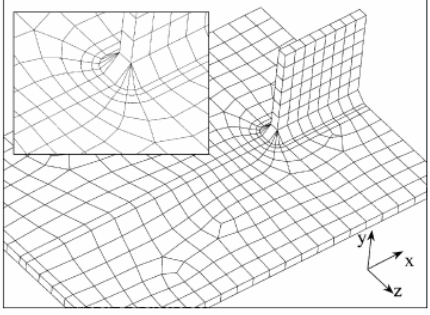
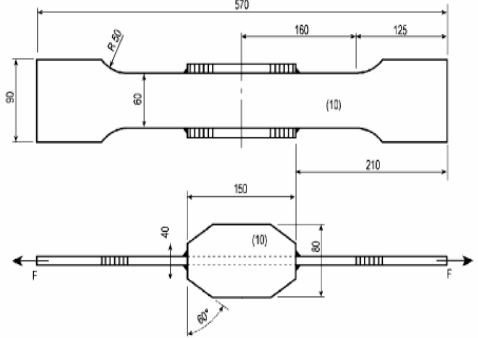
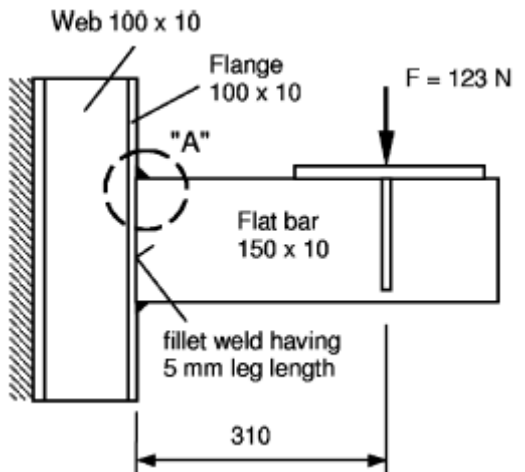
Joint type	Investigations
 <p>Yagi et al. (1991)</p>	<p>The one sided doubling plate investigated by Yagi et al. (1991). Non-uniform transverse stress distribution is present because of the round shape of the doubling plate. 6% scatter was reported by using the extrapolation method (Fricke 2002) while 10% scatter was observed by method proposed by Dong et al. (2001). It was pointed by Doerk et al. (2003) that neglecting vertical shear stresses acting on the transverse element sides in the equilibrium formulae was the reason.</p>
 <p>Paetzold et al. (2001)</p>	<p>The bracket toe from the Paetzold et al. (2001). 8-noded quadratic shell elements were used in the model by Doerk et al. (2003). Both methods were found to have problem with predicting a reasonable structural stress while the extrapolation method seemed to be able to yield a better result.</p>
 <p>Poutiainen et al. (2004)</p>	<p>The longitudinal gusset plate used as a 3D example by Poutiainen et al. (2004). The author claimed the same findings against the method by Dong et al. (2001) as by Doerk et al. (2003). All necessary shear components must be considered in order for a consistent estimation of the structural stress. Corrections for the equilibrium formulae were provide as a supplement to the method by Dong (2001, 2002).</p>
 <p>Kim and Lotsberg (2004)</p>	<p>The thick edge gussets joint was investigated by Kim and Lotsberg (2004) and Fricke (2002). Less scatter was observed for the surface extrapolation method. The method proposed by Xiao and Yamada (2004) was also compared. Slightly smaller structural stress was observed compared to the surface extrapolation method.</p>

Table continued.

Joint type	Investigations
 <p>Kim et al. (2001)</p>	<p>The joint is a flat bar welded to an I-beam investigated by Kim et al. (2001). 8-noded quadratic shell elements were used in the model. Method by Dong (2001, 2002) showed less scatter while higher than that obtained by surface extrapolation method. Both methods caused a quite conservative fatigue life prediction, with Dong's method most conservative.</p>

In addition, an extensive comparison for Floating Production Storage and Offloading (FPSO) vessel details as shown in Figure 2-21 was made by Hong and Dong (2004). The authors concluded that the structural stress concentration factors obtained by surface extrapolation methods are more dependent on the methods used and also finer meshes are needed to achieve converged values.

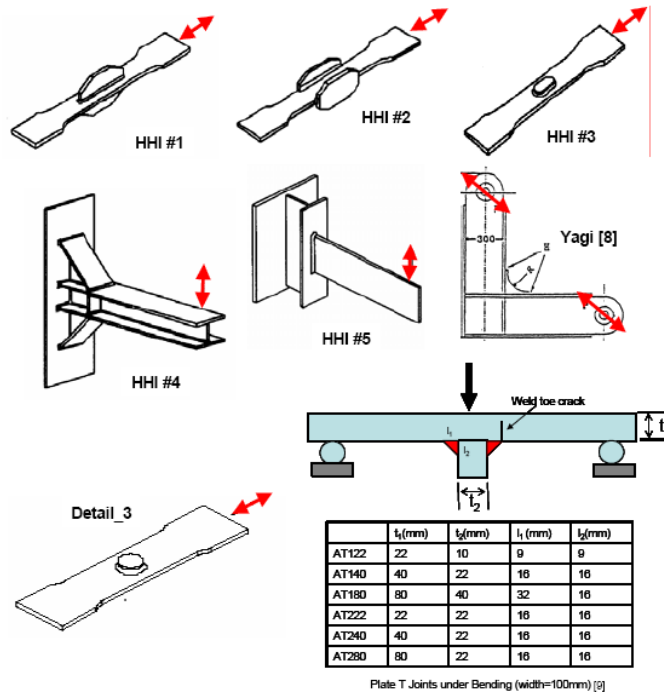


Figure 2-21 Small FPSO details analyzed by Hong and Dong (2004)



It should be noted that the surface extrapolation methods give results which are very close. Therefore, the SN curves for fatigue assessment can be theoretically applied to all methods. However, the through thickness method defines the structural stress differently and the SN curves must be accordingly modified (Dong 2003; Hong and Dong 2004). No such curves for aluminium are available.

Therefore, the surface extrapolation method will be used in this thesis to assess the fatigue properties of the aluminium welded joints because of the availability of the design curves. Furthermore, these methods have been successfully applied in the industrial applications and proven to be very practical even though there are still limitations with regard to the method itself (Doerk et al. 2003).

### 2.6.5 CEM in determining the structural stress

The surface stress adjacent to the weld toe is affected both by the structural geometry and the local weld. The stress gradient (first derivation of the stress which is a function of the distance to the weld toe) towards the weld toe is the most important parameter that reflects the stress raising gradient. Figure 2-22 is another form of the picture in Figure 2-14 with the first derivatives gradients being illustrated.

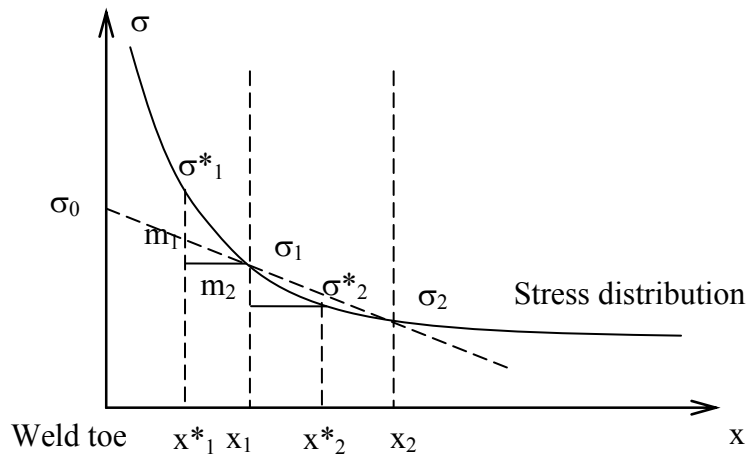


Figure 2-22 Stress near the weld toe

According to theory of geometry a line through the point  $(x_1, \sigma_1)$  with the slope  $m$ :

$$\sigma = m(x - x_1) + \sigma_1 \quad (2-14)$$

where  $\sigma$ ,  $x$  and  $m$  represent the stress, distance to the weld toe, and slope of the extrapolation path, respectively.

All the linear extrapolation methods previously described can be generalized by Equation (2-14) if the slope is defined between the corresponding extrapolation points. For example, for the method based on  $0.5t$  and  $1.5t$ , the slope is  $m = (\sigma_{1.5t} - \sigma_{0.5t}) / (1.5t - 0.5t)$ , the structural stress will be the stress value at  $x=0$  by

specifying  $x_l=0.5t$  and  $\sigma_l=\sigma_{0.5t}$  according to Equation (2-14). The fixed point method as indicated by Lotsberg and Sigurdsson (2004), can also be represented by setting the slope to zero using the same equation.

However, as indicated in Figure 2-22, various definition of the slope may be used. In practice, the stresses obtained either by FE analysis or laboratory measurements are a piece wise function of the distance. The conventional extrapolation methods attempted to implicitly postulate that  $m_2$  (as shown in Figure 2-22, the slope determined by the two extrapolating points) solely reflected the stress gradient towards the weld toe. This is true while the mesh is so fine that  $m_1$  and  $m_2$  tends to be unique. For a generally coarse FE mesh, taking  $m_1$  into account becomes necessary because the stress within the weld affected zone is influenced by both the local weld and the structural geometry and the ignorance. Ignoring  $m_1$  would underestimate the stress raising effect due to the structural geometry and therefore cause an over-conservative fatigue assessment, or non-conservative derivation of SN curves based on test results.

It is therefore suggested that the slope of the extrapolation line should take both the slopes at either side of the leading point into account.

$$m = c_1 m_1 + c_2 m_2 \quad (2-15)$$

where  $c_1$  and  $c_2$  are penalty factors. A value of 0.5 is chosen for both parameters, indicating that stress gradients at both sides of the chosen point are equally weighted.

The extrapolation is then constrained by the stress gradient on both sides of the extrapolation points and hence termed as Constrained Extrapolation Method (CEM). The predicted structural stress will be larger than or equal to the conventional extrapolation methods depending on the change of the stress gradient near the weld toe. The method can be used together with FE analysis or laboratory strain gauge measurements.

Nearly identical structural SCFs were obtained compared with previously mentioned extrapolation methods (Ye and Moan 2006) because the stress gradients adjacent to the weld toe nearly remain as constants for the studied welded joints. This proves that the conventional extrapolation methods are accurate enough for structural stress calculation. However, the application of this method is more complicated than conventional extrapolation methods and is not recommended for practical use.

## 2.6.6 Notch stress range approach

### **Definition**

By ignoring stress raising effects due to the both the structural geometry and the weld, the fatigue assessment by means of the nominal stress range approach is simplified greatly by taking only the gross geometry into account. An elastic crude beam or frame theory or crude finite element analysis is adequate for this purpose. However, fatigue is a highly localized phenomenon which is affected not only by the gross geometry but more affected by the local details of the joints. The development of finite element analysis has made it possible to accurately carry out local stress analysis.

The structural stress calculation goes one step beyond than the nominal stress by taking the influence of the structural geometry into account when the stress at the weld toe is dealt with. By extrapolating from outside of the region affected by the weld, the stress raising effect of the weld is expected to be eliminated by the structural stress. However, there still exists dispute on the validity of those proposed structural stress calculation methods. The lack of a universal method valid to all joint types prevents this approach from being widely adopted.

In addition to that, for a given joint, it has been shown that the fatigue strength depends heavily on the weld parameters (Ye and Moan 2007a). The change of the weld parameters (such as the weld leg length and the weld toe angle) can affect the fatigue strength significantly. For this reason methods that can deal with the very local behaviour in the weld affected zone are desirable. The notch stress range approach provides a possible alternative towards this aim.

**Definition of the notch stress and calculation of the notch stress concentration factor**

The notch stress is the total stress at the fatigue-prone location that accounts for all stress raising factors including structural discontinuities, attachments, and the presence of the weld. The local surface notch stress may be expressed as:

$$\sigma_{notch} = K \cdot \sigma_{nominal} \tag{2-16}$$

in which  $\sigma_{notch}$  and  $\sigma_{nominal}$  denote the notch and nominal stresses, and  $K$  is termed as the notch stress concentration factor.

DNV (1997) defines the notch stress concentration factor  $K$  as a product of stress concentration factors related to all stress risers such as the structural geometry, weld geometry, misalignment, angular mismatch, eccentricity, and thickness factor, etc. The factor is usually written as a multiplication of stress raising factors:

$$K = K_g \cdot K_w \cdot K_{te} \cdot K_{ta} \cdot K_t \tag{2-17}$$

where

$K_g$ =stress concentration factor due to the structural geometry of the detail considered

$K_w$ =stress concentration factor due to the weld geometry

$K_{te}$ =stress concentration factor due to eccentricity tolerance

$K_{ta}$ =stress concentration factor due to the angular mismatch

$K_t$ =stress concentration factor for plate thickness exceeding 25 mm

The  $K$  factor can either be selected from a list of construction details (DNV 1997) or calculated by means of finite element analysis with fine mesh in the fatigue-prone area. In the latter case, the modelling of weld geometry is of most significance. A typical weld profile is schematically shown in Figure 2-8. Weld throat thickness “a” is usually used to specify the size of a fillet weld.

Based on an investigation of the influence of factors relating to the weld geometry, initial crack size and material parameters on the fatigue strength of welded joints,

Engesvik (1981) and Engesvik and Moan (1983) concluded that the weld toe radius contributed most in the scatter in simulated fatigue life and the weld toe angle had equivalent influence as the initial crack size.

The geometry of the weld, particularly the weld toe angle and the weld toe radius, should therefore be carefully modelled when using the finite element method to calculate the notch stress concentration factor. A sub-model technique including the weld geometry is usually demanded.

Empirical equations are also proposed to calculate the notch SCF. Equation suggested by Yung and Lawrence (1985) is the most versatile one among many other equations proposed for the fillet weld profile under bending load. It is expressed as,

$$K = 1 + 0.21(\tan \theta)^{1/6}(t/\rho)^{1/2} \tag{2-18}$$

Where  $\theta$  is weld toe angle,  $\rho$  is the radius of the curvature at the toe and  $t$  is the plate thickness.

**Notch stress design SN curves**

By means of the notch stress, stress concentrations caused by either the structural geometry or the weld geometry is implemented in the stress calculation. In spite of the joint difference, one basic SN curve can therefore be applicable for all joint types. Table 2.2 lists the standard notch stress-based design SN curves. It can be seen that four SN curves are suggested, among which one curve is for base material, two curves are assigned to welded joints and one curve is suitable for welded joint under corrosive environment. These SN curves are plotted in a log-log plane in Figure 2-23.

**Table 2-2 Parameters for standard SN curves (DNV 1997)**

SN curve	Material	N≤5×10 <sup>6</sup>		N≥5×10 <sup>6</sup>	
		Log(a)	m	Log(a)	m
I	Base material	21.10	7	21.10	7
II	Welded joint	13.82	4.32	17.12	6.32
III	Welded joint	11.87	3.37	14.94	5.37
IV	Welded joint in corrosive environment	11.44	3.37	11.44	3.37

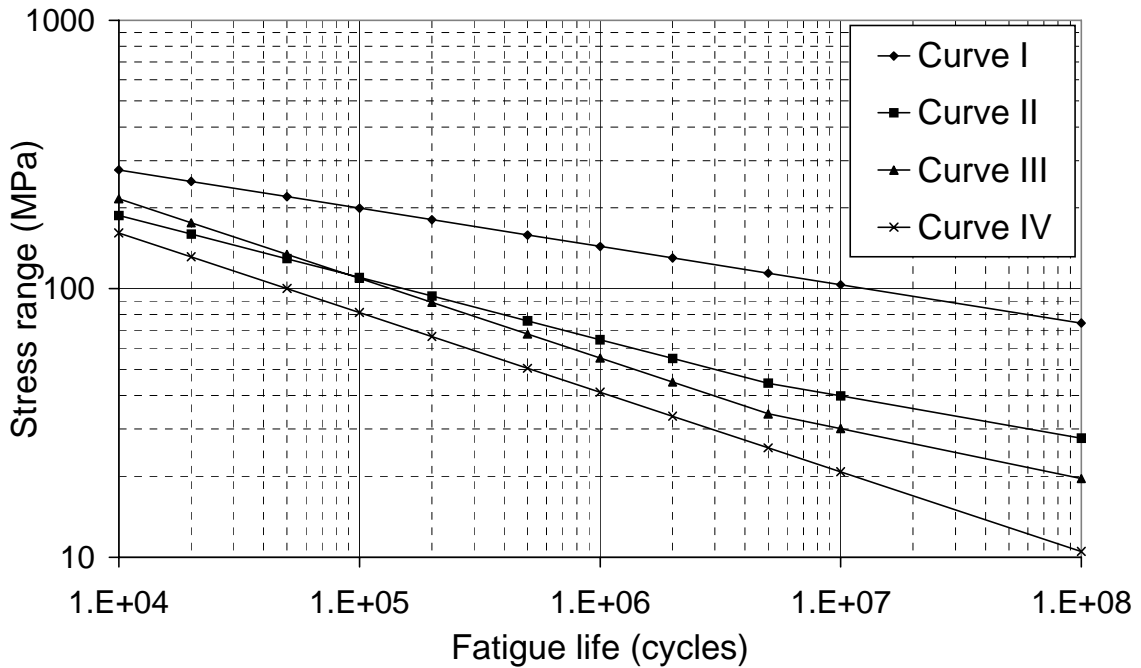


**Figure 2-23 Basic SN curves for aluminium (DNV 1997)**

The notch SN curves are derived on the basis of smooth specimens (the notch stress concentration factor  $K$  equals to 1.0) without taking the stress ratio into account. The effect of the residual stress is accounted for in the SN curves.

The characteristic fatigue strength in stress range for each SN curve can be derived through Equation (2-2), thus resulting in an equivalent “detail class” of 55 for curve II and 45 for curve III approximately.

Compared to the structural stress design SN curve 40 (without thickness correction) proposed for aluminium welded joints, the notch stress design SN curve II and III imply a further stress raising factor of 1.38 and 1.13 if these two approaches are assumed to be equivalent.

It is important to note that the notch stress range approach addressed in this study is different from “notch root approach” described for instance by Radaj (1996) and Radaj and Sonsino (1998). The “notch root approach” is used to assess the fatigue strength and service life up to crack initiation. The elastic-plastic strain amplitudes at the notch root of a notched specimen is compared to the strain SN curve of the material in the un-notched comparison specimen. The assumption is that the mechanical behaviour of the material at the notch root in respect of local deformation, local damage and crack initiation can be simulated by means of a miniaturized, axially loaded, un-notched or mildly notched specimen in respect of global deformation, global damage and complete fracture. The fatigue assessment is then to first determine the stresses and strains at the notch root in the elastic-plastic condition and then compare them with the strain SN curve of the un-notched small specimen. The expenditure of using the “notch root

approach” is high, however, simplified versions were developed to make an assessment of the “endurance limit” (Radaj and Sonsino 1998).

The notch stress range approach described here is, however, based on a similar concept as the structural stress range approach, i.e. separating the stress concentrations due to the weld geometry from the design SN curves thus simplifying the fatigue assessment procedure for welded joints. When fatigue damage is mainly due to the low stress data for a high speed light craft as reported by Heggelund et al. (1998), the notch stress range approach described here seems to be an effective method in the fatigue strength assessment.

## **2.7 Fatigue life improvement techniques**

### **2.7.1 Introduction**

Experience has shown that a large percentage of structural damage can be attributed to fatigue failure, and as a result, improving fatigue strength of structural components under cyclic loading is necessary particularly when fatigue cracking is the critical structural failure mode.

Fatigue life of welded joint is smaller than for similar joints made of base material. Sometimes, often late in the design process or during the service time of a structure, it becomes necessary to increase the fatigue life of a particular joint detail to extend the fatigue life. Use of a so-called improvement method is a viable alternative to achieve this goal.

Various methods have been developed for increasing the fatigue life of existing welded joints, as summarised by Gurney (1979), Haggensen (1992) and Haagensen and Maddox (2004). The more specific about the effect of increase in fatigue can reach 50 to 100 per cent for as-welded joints made of steel. However, limited information is available for aluminium welded joints.

### **2.7.2 Post weld treatment techniques**

Grinding (either whole profile grinding or weld toe grinding), peening (needle peening or hammer peening), tungsten inert gas (TIG) dressing, and ultrasonic impact technique (UIT), etc. have been used to improve the fatigue life of welded joints. These methods are grouped into two classes: weld geometry methods and residual stress methods. The former methods are designed to reduce the stress concentrations due to the weld geometry and remove or reduce crack-like flaws (defects) at the weld toe. The latter methods introduce compressive residual stresses in the regions where the fatigue cracking is likely to occur. These methods were first used in the steel industry and then extended to aluminium structures.

In the present study, only the effect of toe grinding pursued. This technique is briefly outlined in the subsequent section.

### 2.7.3 Weld toe grinding for aluminium welded joints

#### **Introduction**

The fatigue life of a structural consists of two phases according to fracture mechanics, namely the crack initiation and propagation phases. In an as-welded structure, the initial defects that exist make the initiation phase short because the defects size along the fusion line is believed exceed the transition crack size between the initiation and propagation. Therefore, the fatigue life of welded joints primarily comprises propagation. The aim of the grinding is to remove or reduce the size of the defects, and hence, reintroduce an initiation phase or extend the propagation phase so that the fatigue life is increased. Significant fatigue improvement can be obtained for steel welded structures because fatigue life of such joints is dominated by the crack propagation phase. However, the fatigue life of aluminium alloys is governed primarily by crack initiation, which is accelerated by the presence of microporosity in the alloy structure (Morris 1998). Hence, a significant fatigue improvement can only be achieved by successfully reintroduce an initiation phase. Partial reduction of the defect sizes may only have marginal effect.

A general weld profile of an as-welded joint is shown in Figure 2-8 and a typical weld profile after toe-grinding is illustrated in Figure 2-24. Figure 2-25 shows the photograph of real as-welded and toe-ground specimens.

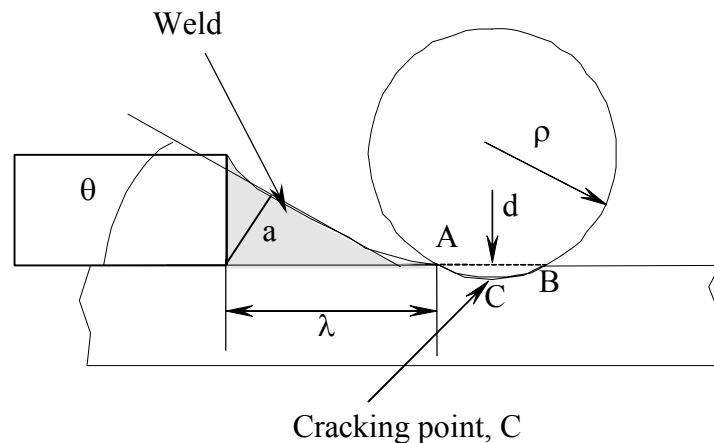


**Figure 2-24** Weld profile after toe grinding



**Figure 2-25 Photograph of as-welded (to the left) and toe-ground specimens**

The toe grinding technique implies a round undercut with a depth  $d$  into the parent plate. The original weld toe as it appears in the “as-welded” joint does not exist any more. Instead, three geometrical discontinuities  $A$ ,  $B$  and  $C$  may become the fatigue cracking point. The highest stress concentration occurs at point  $C$  and is therefore taken as the fatigue cracking point in this study.

The depth of defects in welded joints has been investigated by Maddox (1998) and Jaccard (1990) and a range from  $0.013$  mm and  $0.38$  mm was found to be representative. Therefore, the grinding should be performed with a depth of at least  $0.5$  mm, according to Haagensen and Maddox (2004).

The toe grinding has little influence on the structural details where fatigue lives are not governed by weld toe failure the removal of the crack-like defects along the weld toe is not relevant to the actual fatigue cracking site such as the weld root. It has also been found that there exists an upper bound fatigue class beyond which only limited fatigue improvement can be achieved compare to low fatigue classes. The limit for steel is fatigue class 90 below that a factor of 1.5 can be achieved in terms of stress range. Aluminium as-welded joint with fatigue class below 40 can be upgraded to class 45 when post treatment methods are applied (Haagensen and Maddox 2004). A study by Tveiten (1999), however, showed that only marginal improvement was achieved for a bracket attachment on a flat bar. In that case, the mean grinding depth of  $0.6$  mm may be insufficient to obtain a promising improvement as indicated by Haagensen and Maddox (2001).

### ***Influence on the fatigue assessment methods***

The fatigue improvement by grinding will not be achieved unless a sufficient grinding depth has been reached (Haagensen and Maddox 2004). Therefore, the reduction in thickness should be considered in determining the nominal stress in the fatigue assessment by means of the nominal stress range approach.



The structural stress range approach is primarily developed for the fatigue cracks propagating from the weld toe. Therefore, structural stress calculation is performed by reference to the weld toe. The weld toe for the “as-welded” joint is easily indentified. However, after toe grinding three possible fatigue cracking locations are introduced. Finite element analysis show that the highest stress occurs at the deepest point in the weld profile and fatigue test also showed that the fatigue cracks initiated from the deepest point. The stress at the initial weld toe (point A in Figure 2-24 is actually relaxed.

It should be noted that the fatigue cracking point for the toe-ground joint is located within the parent material rather than the transition point between the weld and parent material. The application of the structural stress defined for as-welded joint may be argued for this reason. In addition, the first element(s) in front of the cracking point may be irregular compared to brick element appeared for the as-welded joint.



### 3 Results and Recommendations

#### 3.1 General

Welded aluminium box stiffener connections are investigated by carrying out fatigue tests as well as numerical evaluations.. Important weld parameters that may affect greatly the fatigue strength are examined. Fatigue test data are presented in terms of nominal stress as well as more novel approaches based on local stresses. The test data are compared with fatigue design SN curves as illustrated in Figure 3-1. A fatigue class usually refers to the stress range value corresponding to a fatigue life of  $2 \times 10^6$  cycles. Safety margin in percentage is the difference of the stress range at a given number of cycles for instance  $2 \times 10^6$  between design SN curve and the regressed curve based on mean life minus two standard deviations. A positive margin value indicates that the design curve is conservative while a negative value means non-conservative.

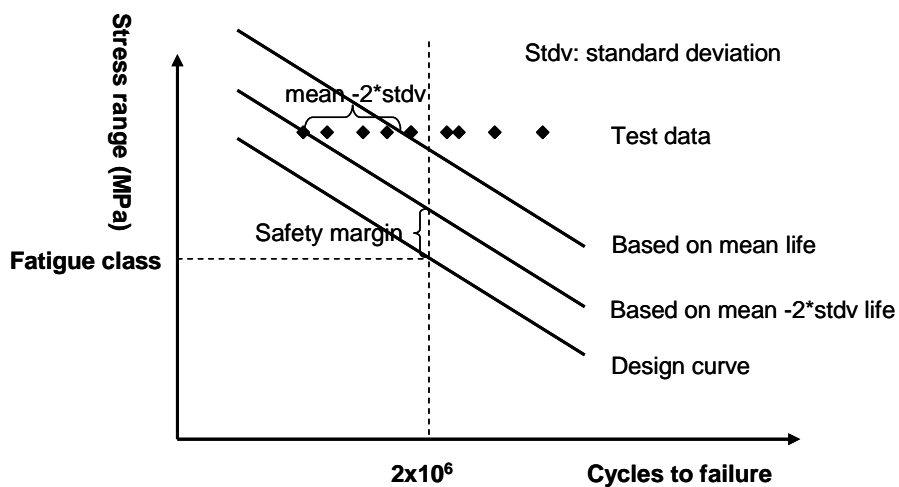


Figure 3-1 Test data against design SN curves

Fatigue improvement by weld toe grinding is evaluated by conducting fatigue tests on both the as-welded and weld toe-ground non-load carrying fillet welded cruciform joints.

The work has generally been presented in separate articles and the results are summarised in this chapter. Results are presented for each joint type in the following sections.

## **3.2 Box stiffener/web frame connections**

### **3.2.1 Introduction**

Three types of similar such connections between box stiffeners and web frame were investigated in this study. Their respective static and fatigue strength are compared to find a suitable joint solution that can reduce or minimize the fabrication costs while producing sufficient fatigue strength.

The results were presented in paper 2 by Ye and Moan (2007a) and summarized in the following context.

### **3.2.2 Joint description**

The box stiffeners are continuous and three different cut-outs in the web frame and accordingly the welding specifications are used. An excessive cut-out is used to for joint alternative Alt-1. The stiffener and web frame are joined by a double-sided fillet weld. Extra weld is performed around the cutting edge on the web frame to make a continuous welding along the joining line. Figure 3-2 is an illustration of the overview of the joints.

Compared to Alt-1, a smaller cut out is made on the web frame for Alt-2. The web frame is almost tightly fit with box stiffener with a gap of approximately 1 mm between the cutting edge and the stiffener profile. Double-sided fillet weld is also used but there is no weld around the cutting edge of the web frame. The weldment stops at a distance  $p$  from the bottom of the stiffener profile.

Alt-3 provides a watertight joint solution because the web frame is continuously welded to the box stiffener. However, more filler weld material is needed thus causing the joint the most expensive one compared to the Alt-1 and Alt-2 where intermediate weld is performed.

Among these connections, Alt-2 seems to be the most economically effective one since the least weld material as well as man hours is needed.

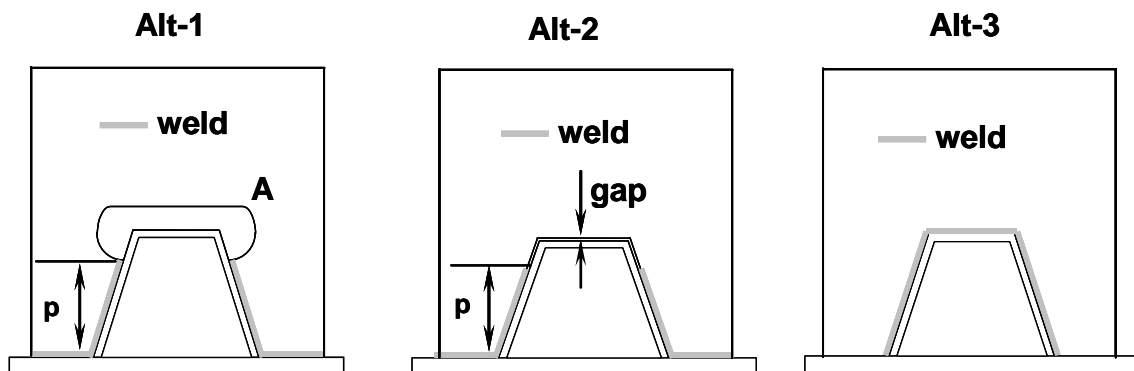
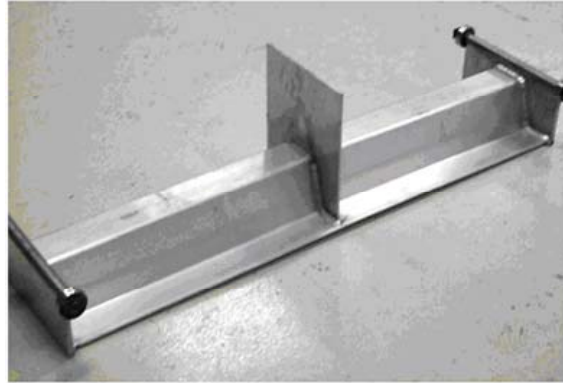


Figure 3-2 Overview of the box-stiffener/web frame connections

### 3.2.3 Static behaviour

#### *Influence of local joint geometry*

The stress distribution in the flange is not significantly influenced by Alt-1 and Alt-2 compared to a box stiffener without web frame. However, large bending effects are found in Alt-3 because of the complexity of the geometry of the box stiffener as well as the weld geometry particularly in the connecting part of the stiffener.

The stress gradient towards the fatigue cracking point (weld toe) differs greatly for the three connections. The lowest stress gradient occurs in Alt-2 due to the simplest weld geometry. Alt-1 and Alt-3, however, due to their complex weld geometry, cause a relatively high stress gradient towards the weld toe compared to Alt-1.

The influence of the local geometry extends to about  $6t$  ( $t=3$  mm) in the longitudinal direction for Alt-1 and Alt-2, while about  $4t$  for Alt-3.

#### *Influence of weld parameters*

The effect of the weld toe angle and weld throat thickness on the stress distribution in the fatigue cracking area are studied.

#### *Alt-1*

The weld throat thickness (weld leg length) plays an important role in determining the stress gradient towards the weld toe. The bigger the weld throat thickness is, the higher the stress gradient is. An increase in the weld toe angle, however, causes a reduction in the stress gradient if the weld throat thickness remains unchanged.

#### *Alt-2*

The same findings for Alt-1.

#### *Alt-3*

The influence of the weld throat thickness is the same as Alt-1. However, the change of the weld toe angle (with the weld throat thickness remaining constant) shows an opposite effect compared to Alt-1 and Alt-2. That is, an increase in the weld toe angle causes an increase in the stress gradient.

### **3.2.4 Fatigue behaviour**

#### ***Experimental program***

The same test set-up as the box stiffener lap joint was used for the box stiffener/web frame connections while the test frequency was 5Hz instead of 4Hz because of higher stiffness compared to the lap joint. Twelve specimens of each connection were tested. The standard deviations for each connection were *0.16*, *0.11* and *0.12*, respectively.

#### ***Nominal stress range approach***

##### *Design SN curve*

There is no precisely matched “detail class” in existing design codes of ship rules for these joints due to their complex geometry. Therefore, a highest “detail class” *31* referring to welded attachments on stressed members with transverse weld toe from Eurocode 9 (1998) is selected to compare the test data.

##### *Results*

The nominal stress-based design SN curve *31* is satisfied by all the connections. The fatigue strengths in terms of nominal stress range of each connection at  $2 \times 10^6$  cycles are *4.5*, *5.4* and *23.0* per cent higher than the mentioned design curve.

Although the nominal stress level of Alt-1 and Alt-2 is lower than that for Alt-3, the latter has a better fatigue performance. Intermediate welding performed in Alt-1 and Alt-2 causes stops and starts in the welding practice that may bring more unexpected defects in the weld, thus reducing the fatigue life of the connections.

#### ***Structural stress range approach***

##### *Design SN curve*

The same structural stress-based design SN curve *44* as the box stiffener lap joint is chosen to assess the fatigue strength of the three connections.

##### *Structural stress concentration factor*

The structural stress concentration factors according to the DNV rule (1993) are 1.44, 1.27 and 1.51 for Alt-1, Alt-2 and Alt-3, respectively. Methods suggested by Niemi (1994) give higher concentration factors. The former SCFs are used to present the fatigue data.

#### *Results*

The fatigue strengths in terms of the structural stress range at  $2 \times 10^6$  cycles are 7.7, -5.8 and 31.0 per cent relative to the design SN curve 44. Alt-2 does not comply with the mentioned design SN curve owing to its lowest structural stress concentration factor.

### **Notch stress range approach**

#### *Design SN curve*

According to DNV (1997), the notch stress-based design SN curve III is used in the fatigue assessment by means of the notch stress range approach.

#### *Notch stress concentration factor*

The notch stress concentration factors are 1.58, 1.62 and 1.62 for Alt-1, Alt-2 and Alt-3 based on the finite element analysis. A default value of 1.8 is suggested by the design codes (DNV 1997).

#### *Results*

The fatigue strengths at two million cycles are 33.4, 33.7 and 55.6 per cent in terms of notch stress range for Alt-1, Alt-2 and Alt-3 when the default notch stress concentration factor 1.8 is used.

The notch stress range approach is found to be the most conservative one compared to the nominal and structural stress range approaches.

## **3.2.5 Design considerations**

A weld can never be stronger than the base metal. For fillet welds, stresses are assumed to act in shear and weld strength depends on leg size, length of the weld, type of weld metal, and loading direction. In dynamically loaded parts where fatigue performance is important, the welding process and joining process are equally important for large volume products. A joining process which consumes more weld material while with possible automatic welding process may become more desirable than other joining processes which require smaller volume of manual welding.

## **3.3 Box stiffener lap joint**

### **3.3.1 Introduction**

Box stiffener lap joint provides a solution in joining two pre-fabricated panels. Compared to a transverse butt weld by which two structural components are joined together, the box stiffener lap joint requires less matching accuracy between the

components thus increasing the efficiency in fabrication. Fatigue failure from either the weld toe or the weld root is possible depending on the weld parameters.

These topics were included in paper 1 (Ye and Moan 2002a) and summarized in the text below.

### 3.3.2 Static behaviour

#### ***Influence of lapping plate***

The presence of the lapping plate has a great influence on the stress flow pattern near the lapping area. Local bending is the main phenomenon caused by the lapping plate. A higher bending effect is found in the middle part (flat) of the flange compared to curved part.

The influence of the lapping plate extends about  $10t$  ( $t=3$  mm) in the middle while a little bit more than  $2t$  in the connection part.

#### ***Influence of weld leg length***

The weld leg length plays a determining factor in the stress concentration factor at the fatigue cracking point. A leg length of 7.5 mm ( $2.5t$ ) seems to be the critical length that makes the fatigue failure equally likely to occur at the weld toe or in the root. A shorter leg length will result in a high stress peak at the curved part and a root failure more likely. A longer leg length will shift the stress peak from the curved part to the middle (flat) part of the flange and probably guarantee a weld toe failure. Further increase in the weld leg length does not reduce the stress significantly.

### 3.3.3 Fatigue behaviour

#### ***Experimental program***

Thirteen specimens were tested under a load condition of four-point bending in the fatigue test program. The stress ratio was equal to 0.44 and test frequency is 4Hz. Weld toe failures were recorded for twelve of the specimens and only one root failure was found. The findings agreed well with the static behaviour as described above. The root failure was probably due to the short weld leg length. In addition, root defects were detected after cutting out the collapsed specimen. This could be another reason of the root failure of such a joint. A standard deviation 0.09 in terms of  $\log N$  was recorded.

#### ***Nominal stress range approach***

##### *Design SN curve*

The box stiffener lap joint can be classified as “transverse cover plate welded on extruded members by load-carrying fillet weld”. A “detail class” of 31 from Eurocode 9 (1998) was selected as a basis to compare the test data.

It should be pointed out that there is no exact matching joint type in the existing design codes and classifications due to the complexity of the section profile of the box



stiffener. However, the highest “detail class” 31 classified for a general transverse load-carrying fillet welded plate joint may give a conservative estimate of the fatigue strength of the given joint.

#### *Results*

The test data satisfied the design SN curve 31. The fatigue strength at the characteristic fatigue life of  $2 \times 10^6$  cycles was 0.3 per cent higher than the design SN curve.

### **Structural stress range approach**

#### *Design SN curve*

Structural stress-based design SN curve 44 was chosen from the Eurocode 9 (1998) to compare the fatigue test data because this curve requires the thickness of the stressed plate less than 4 mm and the thickness of the flange of the box stiffener is 3 mm.

It should also be noted that the design SN curve 44 is the highest among recommended structural stress-based design SN curves. For instance, Tveiten et al. (2002) suggested a SN curve 40 to be used for aluminium welded joints.

#### *Structural stress concentration factor*

The structural stress concentration factor for the box stiffener lap joint was calculated according to three methods suggested by Niemi (1994), DNV (1993) and Tveiten and Moan (2000). A lowest factor of 1.85 obtained by means of the method proposed by Tveiten and Moan (2000) was used in the fatigue assessment for the purpose of a more “conservative” evaluation.

#### *Results*

The fatigue strength of the box stiffener lap joint was 5.5 per cent above the design curve 44 in terms of structural stress range at a fatigue life of  $2 \times 10^6$  cycles. The use of other structural stress concentration factors would cause a higher percentage above the design curve.

### **Notch stress range approach**

#### *Design SN curve*

The notch stress-based design SN curve II according to DNV (1997) was selected to compare the fatigue strength by means of the notch stress range approach. The characteristic fatigue strength specified by this curve is about 55 in terms of notch stress range at a life of  $2 \times 10^6$  cycles.

#### *Notch stress concentration factor*

The notch stress concentration factor at fatigue cracking point was 2.45 based on the finite element analysis and a default value given by DNV (1997) was 3.0.

#### *Results*

The fatigue strength was found be 14 per cent higher than the design curve II in terms of the notch stress range at  $2 \times 10^6$  cycles. The use of the default notch stress concentration factor would make the design curve more conservative to the test data.

### 3.3.4 Design considerations

As seen in Figure 2-7, box-stiffener lap joints require fillet weld all around the lapping plate. The length and width of a weld can therefore have a great effect on cost. The weld size on the parent component side is hard to control compared to the box-stiffener/web frame connections due to the welding around the edge of the lapping plate.

## 3.4 Cruciform joints

### 3.4.1 Introduction

Cruciform joint is a representative joint type found in many structures and is a standard “detail class” in most design codes and guidelines of classification societies. Fatigue strength of both as-welded and toe-ground joints was investigated in this study by means of a nominal, structural and notch stress range approach. Fatigue improvement by grinding along the weld toe was also investigated.

The weld parameters that are the weld toe angle, weld throat thickness and the weld toe radius were modelled by means of finite element method so that the influence on the stress concentration in the fatigue-prone locations could be studied. In addition, the effect of these parameters on the structural stress concentration factor and the notch stress concentration factor was also investigated.

These results were reported in a separate paper (Ye and Moan 2007b) and the results are summarized in the following context.

### 3.4.2 Static behaviour

The stress distribution pattern near the weld toe is primarily determined by the joint geometry as well as the weld geometry for the as-welded joint. The stress near the weld toe increases monotonously as the distance decreases toward the weld toe. However, the same flow pattern is not observed for the toe-ground joint. In stead, a stress peak appears at the deepest point in the toe-ground weld profile, followed by a stress trough.

### 3.4.3 Fatigue behaviour

#### ***Experimental program***

The specimens were loaded in a three-point bending condition. The tests were performed at a frequency of 12 HZ by a sinusoidal wave form in load control. The load/stress ratio was 0.5 and the fatigue life in terms of number of cycles was recorded when the specimen had been cracked through-thickness. The number of test specimens was eighteen (18) for the as-welded and thirteen (13) for the toe-ground. The nominal grinding depth was 0.8 mm.

It was found that the cracks in the as-welded specimens started from the weld toe, while failure of the toe-ground specimens was originated from the deepest point in the toe-ground weld profile.

### **Nominal stress range approach**

#### *Design SN curve*

The “detail class” for the cruciform joint ranges from 28 to 36 in different design codes and guidelines of classification societies. The weld treatment effect is not explicitly specified in codes such as the Eurocode 9 (1998) and the AA (1994). However, IIW (Hobbacher 1996; 2003) issued two individual SN curves, namely 28 for the as-welded joint and 36 for the toe-ground joint. These two curves were used as the nominal design SN curves to compare the test data.

The notch SCFs based on FE analysis of the as-welded joints were generally below those of the toe-ground joints, while the latter one had better fatigue performance than the former one. The reason for this fact is most likely the larger defects in the as-welded joint as compared to the ground joint.

The DNV notch SCFs of the as-welded joints did not vary with the change of the weld parameters. A larger weld toe radius caused a reduction in the notch SCFs for the toe-ground joints, while other parameters did not affect the value appreciably. It is also important to point out that the grinding depth should exceed a limit, for instance 0.8 mm. In this way the defects can be removed with certainty and to a reasonable fatigue life improvement can be achieved. On the other hand, excessive grinding with larger depth may cause further stress raising also because of increased nominal stress.

#### *Results*

The test data agreed quite well with the IIW nominal SN curve 28 for the as-welded joints and 36 for the toe ground joints. The fatigue strengths in terms of stress range at the characteristic fatigue life of  $2 \times 10^6$  cycles are 2.4 and 1.3 per cent lower (less than 3.0 per cent) compared to the design SN curves. The standard deviations of the  $\log N$  were 0.09 and 0.11 for the as-welded and toe-ground joints.

### **Structural stress range approach**

#### *Design SN curve*

The structural stress-based design SN curve 35 was selected from the Eurocode 9 (1998) in which six curves were issued with respect to plate thickness. The thickness of the cruciform joint plate is 12 mm. Therefore, the curve 35 is proposed because the thickness of the main-stressed member is between 10 and 15 mm as demanded by the design codes. If the design SN curve 40 is used, a thickness correction factor should be taken into account. The thickness correction factor is about 0.84 that makes the design SN curve shift 16 per cent below the curve 40, i.e. 33.6.

The Eurocode 9 (1998) structural SN curve, 35, was found to be non-conservative for the as-welded joints. The structural stress approach does not appear to be applicable to toe-ground joints due to the stress redistribution caused by the new weld profile after grinding.

#### *Structural stress concentration factor*

Three methods for calculating the structural stress concentration factor were compared in this study. The method proposed by Niemi (1994; 1995) seemed to result in a higher concentration factor than the other two methods.

The effect of the weld geometrical parameters, that are toe angle, weld toe radius, as well as the weld leg length, on the structural stress concentration factor is systematically studied by modelling these parameters by means of finite element analyses.

The weld geometrical parameters, as well as the calculation methods have little influence on the magnitude of the structural stress concentration factor for the “as-welded” joint.

The assumption for the use of the structural stress range approach in fatigue assessment of a welded joint is that the stress adjacent to the weld is increased steadily as approaching the weld toe. However, the stress distribution adjacent to the weld toe does not satisfy this assumption, hence the application of the structural stress range approach for such a joint becomes quite difficult or even impossible.

The structural stress concentration factors corresponding to the mean values of the weld geometrical parameters were used in the fatigue assessment by means of the structural stress range approach.

### *Results*

The test data of the as-welded cruciform joint did not satisfy the structural stress-based design SN curve 35 due to its low stress concentration factor, while the toe-ground joint agreed well with the design curve. From the point view of fatigue analysis, the higher the structural stress concentration factor is, the more conservative the design curve is. This is contradictory to the structure design where high stress concentration should be avoided.

It is noted that the structural stress range approach may not be suitable for the fatigue assessment for the toe-ground joint due to its complex stress gradient in front of the weld. A notch stress range approach would be more reasonable for the same assessment.

### ***Notch stress range approach***

#### *Design SN curve*

A notch stress design curve II is classified for the cruciform joint with full penetration fillet weld according to the DNV recommendation (DNV 1997). No difference is specified in choosing a design curve whether the weld toe is ground or not. However, an improvement by a factor of approximate 2 in terms of fatigue life (number of cycles at a given notch stress range) is claimed by DNV (1997).

#### *Results*

The notch stress-based design SN curve II was found to be conservative to the toe-ground joint with a large safety margin. The as-welded joint failed to satisfy the curve while only with a small margin less than 3 per cent in terms of stress range if the calculated notch stress concentration factor was used. The default concentration factor 2.4 recommended by the design code would make both the joints satisfactory to the

design curve. Test results showed that a better design SN curve should be specified for the toe-ground joints due to the fact that weld defects virtually have been eliminated.

## **3.5 Recommendations for further work**

### **3.5.1 Joint design and optimization**

Investigation of the web frame/box stiffener connections Alt-1, Alt-2 and Alt-3 showed that the fatigue strength is greatly influenced by the way the joint is designed. Easy-to-weld, reducing fabrication costs, while providing sufficient fatigue strength is the main target. However, a theoretically good design may not mean a good design in practice. Fatigue tests should be performed for the purpose of confirmation.

Investigation of the box stiffener lap joint showed that the weld parameter (weld leg length) could govern both the mode of fatigue cracking and accordingly the fatigue strength of the joint. More tests, focusing on different weld leg lengths, would be meaningful to confirm the findings in the study.

### **3.5.2 Fatigue assessment methods**

The fatigue assessment method should be accurate yet easy to apply. The stress-life method provides a satisfactory solution to assess relatively high cycle fatigue lives. A method based on SN curves is said to be both “accurate” and “practical” should at least consist of the following features:

The stress used in the design and SN curve should be consistent and reflect the real stress raising patterns by both the structural geometry and the weld geometry. The nominal stress range can provide satisfactory fatigue strength estimates if the engineering joint is similar to the joint “detail class” in the design codes or in guidelines by classification societies. Further tests of welded aluminium joints will increase confidence in using the nominal stress approach. If proper test results are available, this method can be applied.

The structural stress range approach is an attractive method for fatigue assessment for aluminium welded joints. The main challenge is to find a promising structural stress calculation method that can be used for all kinds of joint types. How to model the fatigue-prone area by finite element model and what kind of methods should be adopted are the main issues under development. In addition, investigation on the influence of the weld parameters on the structural stress concentration factor should be clarified and included in the design recommendations.

Extrapolation methods for calculating the structural stress concentration factor refer to the distance from the weld toe as a function of the thickness of the structural component through which the fatigue cracks propagate. There may not exist an apparent plate thickness in a complex welded component such as a bulb stiffener and methodology to deal more properly with this issue is needed.

The “structural geometry affected zone” can be distinguished by making use of the asymptotic behaviour of the stress near the weld toe (Tveiten and Moan 2000). It

provides a clear picture of the influence distance of the structural geometry and weld geometry while the finite element effect resorted to this method is time-consuming that may limit a further application of the method. Other structural stress concentration factor calculation methods such as the extrapolation methods may become inaccurate for very thin plate structures because the calculation is performed too close to the fatigue cracking point thus the notch effect due to the weld being included in the calculation. The calibration of the “structural geometry affected zone” in such cases is becoming necessary and reliable. Some comparison study based on several typical joints may lay a solid foundation for this purpose.

Finally, it is noted that the structural stress method is not applicable to ground joints. The notch method could in principle deal with as-welded and ground welded joints and could be further developed by establishing an more relevant SN curve for ground joints.

### **3.5.3 Fatigue design curves**

For details where the plate thickness is not evident (gusset plates with edge attachments), there are some inconsistency whether a penalty factor should be included or not, and therefore it is a need for further research on the matter.

### **3.5.4 Fatigue improvement techniques**

The fatigue improvement by weld toe grinding seems to be more affected by the grinding depth than other parameters. The impact of the grinding depth can be studied by changing the mean grinding depth of the test specimens. Further tests on various grinding depth would be helpful to define an optimized grinding depth as a fraction of the parent plate thickness.

## 4 References

- AA-The Aluminum Association (1994). Aluminum Design Manual. Washington, the United States.
- AA-The Aluminum Association (1997). Aluminum in the Marine Industry: Application to Fast Ferries. Washington, the United States.
- ALMAR-NÆSS, A. (1985). Fatigue Handbook-Offshore Structures, Tapir Publishers, Trondheim, Norway.
- AUSTAL, <http://www.austal.com/>
- BASQUIN, O.H. (1910) The exponential law of endurance tests. *Proc Ame Soc Test Mater ASTEA* 10, 625.
- BERGE, S., EIDE, O. I. AND TUBBY, P. (1994). Fatigue strength of tubular joins – some unresolved problems. In *proceedings of the International Conference on Offshore Mechanics and Arctic Engineering*. OMAE.
- BISHOP, T. (1955). Fatigue and the Comet Disasters. *Metal Progress*, 79-85.
- BS – British Standard Institution (1991). BS8118: Structure Use of Aluminium (Section 7 Fatigue). London, the United Kingdom.
- DEn (1990). Offshore Installation: Guidance on Design and Construction, Department of Energy, London, the United Kingdom.
- DNV – Det Norske Veritas. (1993). Fatigue Assessment in Ship Structures, Det Norske Veritas Classification A.S., Report No. 93-0432, Høvik, Norway.
- DNV – Det Norske Veritas. (2000). Fatigue Strength Analysis of Offshore Steel Structures. Recommendation Practice RP – C203, Det Norske Veritas Classification A.S., Report No. 93-0432, Høvik, Norway.
- DNV – Det Norske Veritas. (1997). Fatigue analysis of high speed and light craft, Det Norske Veritas Classification A.S., CN 30.9, Høvik, Norway.
- DOERK, O., FRICKE, W. AND WEISSENBORN C. (2003). Comparison of different calculation methods for structural stresses at welded joints, *Int. J. Fatigue: 25*, 359-369.
- DONG, P., HONG, J.K. AND CAO, Z. (2001). A mesh-insensitive structural stress procedure for fatigue evaluation of welded structures. IIW Doc XIII-1902-01/XV-1089-01, International Institute of Welding.
- DONG, P. (2003). A structural stress definition and numerical implementation for fatigue analysis. *Int. J. Fatigue: 23(10)*, 865-76.
- DONG, P., HONG, J.K. AND CAO, Z. (2003). Stresses and stress intensities at notches: ‘anomalous crack growth’ revised. *Int. J. Fatigue: 25*, 811-25.
- ECCS – Technical Committee 2 (1992). European Recommendations for Aluminium Alloy Structures Fatigue Design (first edition), Brussels.
- ECCS/CECM/EKS. (1985) Recommendations for the Fatigue Design of Steel Structures, Brussels.

- ENGSVIK, K.M. (1981). Analysis of Uncertainties in the Fatigue Capacity of Welded Joints. Ph. D. thesis. Department of Marine Technology, The Norwegian Institute of Technology, NTH, Trondheim, Norway.
- ENGESVIK, K. M. AND MOAN, T. (1983). Probabilistic analysis of the uncertainties in the fatigue capacity of welded joints, *Eng. Frac. Mech.* 18(4), 743-762.
- EUROCODE 3 (1992). Design of Steel Structures; Part I – General Rules and Rules for Buildings, Brussels/Luxembourg, Commission of the European Community.
- EUROCODE 9. (1998). Design of Aluminium Structures Part 2 Structures Susceptible to Fatigue. CEN – European committee for Standardisation, Brussels, Belgium.
- FISHER, J. W. (1984). Fatigue and Fracture in Steel Bridges--Case Studies, Wiley, New York.
- FREDRIKSEN, A. (1997). Fatigue aspects of high speed craft. In *Proceedings of the Fourth International Conference on Fast Sea Transportation, FAST'97*, Vol. 1,217-224, Sydney, Australia.
- FRICKE, W. AND PETERSHAGEN, H. (1992). Detail design of welded ship structures based on hot spot stresses. In *Practical Design of Ships and Mobile Units (PRADS)*, edited by Caldwell, J.B. and Ward, G., Elsevier Science.
- FRICKE, W. AND BOGDAN, R. (2001). Determination of hot spot stress in structural members with in-plane notches using a coarse element mesh. IIW-Doc. XIII-1870-01, International Institute of Welding
- FRICKE, W. (2002). Recommended hot-spot analysis procedure for structural details of ships and FPSOs based on round-robin FE analyses. *Int. J. Offshore & Polar Engng.* 12(1), 40-8.
- FRICKE, W. (2003). Review - Fatigue analysis of welded joints: state of development. *Marine Struct.* 16, 185-200.
- FRICKE, W. AND KAHL, A. (2005). Comparison of different structural stress approaches for fatigue assessment of welded ship structures. *Marine Struct.*, 18(7-8), 473-488.
- FUCHS, H. O. AND STEPHENS, R.I. (1980). Metal Fatigue in Engineering. Wiley, New York.
- GOODMAN, J. (1899). Mechanics applied to engineering. London: Longmans Green
- GURNEY, T.R. (1979). Fatigue of Welded Structures (2nd edition). London, United Kingdom: Cambridge University Press.
- GURNEY, T.R. (1992). Fatigue Design, in *Constructional Steel Design – An International Guide*, Elsevier Applied Sciences.
- HAAGENSEN, P.J. (1992). Weld improvement methods for increased fatigue strength. In *Proceedings of the International Conference Engineering Design in Welded Structures*, Madrid, Spain.
- HAAGENSEN, P.J., MADDIX, S.J. (2004). IIW Recommendations on Post Weld Improvement of Steel and Aluminium Structures, IIW Doc XIII-1815-00, Rev.5.
- HEGGELUND, S.E., MOAN, T. AND OMA, S. (2002). Determination of global design loads for large high-speed catamarans. *J. Engng. For the Maritime Environment*, 216, 79-94.



- HOBACHER, A. (1996). Recommendations for Fatigue Design of Welded Joints and Components. Cambridge, Abington Publishing.
- HOBACHER, A. (2001). Trends in science and technology of welding and joining for economic and reliable products. In the Proceedings of the International Conference - Joining Technologies of Dissimilar Materials and Structural Integrity Problems of so Jointed Structures, IIW, The International Institute of Welding, Ljubliana, Slovenia.
- HOBACHER,, A. (2003). Recommendations for Fatigue Design of Welded Joints and Components. Doc. XIII-1965-03/XV1127-03, Paris
- HONG, J.K. AND DONG, P. (2004). Hot Spot Stress and Structural Stress Analyses of FPSO Fatigue Details, Proc. *OMAE Speciality Conf. On FPSO Systems*, OMAE-FPSO'04-0023, Houston Tx, ASME Int. Petroleum Techn. Inst.
- HUTHER, M. AND HENRY, J. (1992). Recommendations for hot spot stress definition in welded joints, IIW Doc XIII-1416-91 and IIW Doc XIII-1416a-92, International Institute of Welding.
- HUTHER, M., PARMENTER, G. AND HENRY, J. (1992). Hot spot stress in cyclic fatigue from linear welded joints, IIW Doc XIII-1466-92, International Institute of Welding.
- HUTHER, M., LIEURADE, H.P., SAYHI, N. AND BUISSON, R. (1996). Fatigue strength of longitudinal non-load-carrying welded joints – Use of the hot spot stress approach. *International Conference on Fatigue of Welded Components and Structures*, 57-64.
- JACCARD, R. (1990). Fatigue crack propagation in aluminium. IIW Doc.XIII-1377-90, International Institute of Welding.
- KIM, W.S., KIM, D.H., LEE, S.G., LEE, Y.K. (2001). Fatigue strength of load carrying box fillet weldment in ship structure. In *Practical Design of Ships and Mobile Units*, edited by Wu, Y.S., Cui W.C. and Zhou, G.J., Elsevier Science.
- KNIGHT, J.W. (1978). Improving the fatigue strength of welded joints by grinding and peening. *Welding Research International* 8(6), 519-39.
- KIM, W.S. AND LOTSBERG, I. (2004). Fatigue test data for welded connections in ship shaped structures. In: International Conference Houston, OMAE-FPSO'04-0018.
- LOTSBERG, I. AND SIGURDSSON, G. (2004). Hot Spot S-N Curve for Fatigue Analysis of Plated Structures. Proc. *OMAE Speciality Conf. On FPSO Systems*, OMAE-FPSO'04-0014, Houston Tx, ASME Int. Petroleum Techn. Inst.
- MACDONALD, K., HAAGENSEN, P.J. AND SØVIK, O.P. (1998) Progress in fatigue assessment of welded hollow-section aluminium structures, *Proc. of the Int. Conf. of Aluminium Structures - INALCO'98*, United Kingdom.
- MACHIDA, S., MATOBA, M., YOSHINARI, H. AND NISHIMURA, R. (1992). Definition of hot spot stress in welded plate-type structure for fatigue assessment. IIW Doc XIII-1448-92, International Institute of Welding.
- MADDOX, S.J. (1991). Fatigue Strength of Welded Structures. Abington Cambridge, the United Kingdom.
- MADDOX, S.J. (1995). Scale effect in fatigue of fillet welded aluminium alloys, *Proc. of 6th Int. Conf. on Aluminium Weldments*, AWS.

- MADDOX, S.J. (1998). The application of fatigue life improvement techniques to steel welds. IIW Commission XIII Workshop on Improvement Methods, International Institute of Welding.
- MADDOX, S.J. (2001). Hot-spot fatigue data for welded steel and aluminium as a basis for design, Doc.IIW-XIII-1900-01, IIW-The International Institute of Welding.
- MATOBA, M., KAWASAKI, T., FUJII, T. AND YAMAUCHI, T. (1983). Evaluation of fatigue strength of welded structures – hull's members, hollow section joints, piping and vessel joints. IIW Doc XIII-1082-83, International Institute of Welding.
- MORRIS, A. (1998). Aluminium Alloys for Aerospace, *Materials World* 6(7), 407-408
- MORROW, J. (1968). SAE Advances in Engineering, *Fatigue Design Handbook*(4), 21-29.
- NVR-Naval Vessel Register, <http://www.nvr.navy.mil/nvrships/>
- NIEMI, E. (1994). On the determination of hot-spot stresses in the vicinity of edge gussets. Technical Report IIW-XIII-1555-94, IIW-The International Institute of Welding, Cambridge, the United Kingdom.
- NIEMI, E. (1995). Stress determination for fatigue analysis of welded components. Technical Report IIS/IIW-XIII-1221-93, IIW-The International Institute of Welding.
- NIEMI, E. (2001). Structural Stress Approach to Fatigue Analysis of Welded Components, Doc.IIW-XIII-1819-00, IIW-The International Institute of Welding.
- NIEMI, E. FRICKE, W. AND MADDOX, S.J. (2006). Fatigue Analysis of Welded Components – Designer's Guide to the Hot-Spot Approach, Woodhead Publishers, Cambridge.
- NORDHAMMAR, H. (1998). Experience from the construction and operation of the Stena HSS. In *The Third International Forum on Aluminium Ships*, Haugesund, Norway.
- PAETZOLD, H., DOERK, O. AND KIERKEGARD, H. (2001). Fatigue Behaviour of Different Bracket Connections, 8th International Symposium on Practical Design of Ships and other Floating Structures (PRADS'2001), Shanghai, China
- PARTANEN, T., TORVI, T. AND NIEMI, E. (1994). On size effects in fatigue of welded joints, Technical Report IIW-XIII-1535-1994, IIW-The International Institute of Welding.
- PARTANEN, T. AND NIEMI, E. (1999). *Welding in the World* 43(1), 16-22.
- PETROSKI, H. (1983). *To Engineer Is Human*. St. Martin's Press, New York, the United States.
- POUTIANEN, I. AND MARQUIS, G. (2004). A single-point structural stress assessment procedure for load-carrying fillet welds. IIW Doc XIII-2012-04/XV-1174-04, IIW-The International Institute of Welding.
- POUTIANEN, I., TANSKANEN, P. AND MARQUIS, G. (2004). Finite element methods for structural hot spot stress determination – a comparison of procedures. *Int. J. of Fatigue*, 26, 1147-57.
- POUTIANEN, I. AND MARQUIS, G. (2006). A fatigue assessment method based on weld stress. *Int. J. of Fatigue*, 28, 1037-46.

- PETERSHAGEN, H., FRICKE, W. MASSEL, T. (1991) Application of the local approach to the fatigue strength assessment of welded structures in ships. IIW Doc. XIII-1409-91, International Institute of Welding.
- RADENKOVIC, D. (1981). Stress analysis in tubular joints. In *International Conference on Steel in Marine Structures*, Paris, France.
- RADAJ, D. (1990). Design and Analysis of Fatigue Resistant Welded Structures. Abington Publication, Cambridge, the United Kingdom.
- RADAJ, D. (1996). Review of the fatigue strength assessment of non-welded and welded structures based on local parameters. *Int. J. Fatigue* 18(3), 153-170.
- RADAJ, D. AND SONSINO, C.M. (1998). Fatigue Assessment of Welded Joints by Local Approaches, Abington Publication, Cambridge, the United Kingdom.
- RICE, R.C. (1988). SAE fatigue Design Handbook (3rd edition). Society of Automotive Engineers, Warrendale.
- SCHUTZ, W. (1996). A history of fatigue. *Eng. Fract. Mech.* 54(4), 263-300
- The Welding Institute (1983). Improving the Fatigue Performance of Welded Joints. Abington, Cambridge, the United Kingdom.
- STORY, M. (1997). The design, construction and introduction of the Stena HSS 1500, IMAREST-Institute of Marine Engineering, Science & Technology.
- TVEITEN, B. W. (1999). Fatigue Assessment of Welded Aluminium Ship Details, Ph. D. thesis, NTNU, Trondheim, Norway.
- TVEITEN, B. W. AND MOAN, T. (2000). Determination of structural stress for fatigue assessment of welded aluminium ship details. *Journal of Marine Structures* 13(3), 189-212.
- TVEITEN, B.W., YE, N., MOAN, T. (2002). Recommendations on the selection of structural stress design S-N curves for the fatigue assessment of welded aluminium structures. In *Proceedings of the 8th International Congress on Fatigue*, Stockholm, Sweden, 2002.
- USS- United States Steel Corporation (2007), <http://www.ussautomotive.com>
- VAN WINGERDE, A.M., PACKER J.A. AND WARDENIER, J. (1995). Criteria for the fatigue assessment of hollow structural section connections. *Journal of Constructional Steel Research* 35, 71-115.
- SCHÜTZ, W. (1996). A history of fatigue. *Eng. Fact. Mech.* 54(2), 263-300.
- WILLIAMS, M.L. (1952). Stress singularities resulting from various boundary conditions in angular corners of plates in extensions. *Journal of Applied Mechanics* 19, 526-8.
- XIAO, Z.G. AND YAMADA, K. (2004). A method of determining geometric stress for fatigue strength evaluation of steel welded joints. *Int. J. Fatigue* 26(12), 1277-1293
- YAGI, J., MACHIDA, S., TOMITA, Y., MATAA, M. AND KAWASAKI, T. (1991). Definition of hot-spot stress in welded plate-type structure for fatigue assessment. IIW Doc XIII-1414-1991, International Institute of Welding.

- YE, N., MOAN, T. AND TVEITEN, B. W. (2001). Fatigue analysis of aluminium box-stiffener lap joints by nominal, structural and notch stress range approaches, *Proc. of PRADS'2001*, Shanghai, China.
- YE, N. AND MOAN, T. (2002a). Static and fatigue behaviour of aluminium box stiffener lap joint. *Int. J. Fatigue* 21(1), 581-589.
- YE, N. AND MOAN, T. (2002B). Fatigue analysis of aluminium box-stiffener/web frame connections by nominal, structural and notch stress range approaches. Fatigue Congress, Stockholm, Sweden.
- YE, N. AND MOAN, T. (2006). CEM in determining the structural stress. Fatigue Congress 2006, Atlanta, the United States.
- YE, N. AND MOAN, T. (2007a). Static and fatigue analysis of three types of aluminium box stiffener/web frame connections. *Int. J. Fatigue*, 29, 1426-1433.
- YE, N. AND MOAN, T. (2007b). Improving Fatigue Life for Aluminium Cruciform Joints by Weld Toe Grinding, revision submitted to *Fatigue and Fract. Of Eng. Mater. and Struct.*
- YE, N. AND MOAN, T. (2007c). Improving Fatigue Strength of Aluminium Cruciform Joints by Weld Toe Grinding, abstract accepted by *PRADS'2007*, full paper submitted, Houston, USA
- YUNG, J.Y. AND LAWRENCE, F.V. (1985). Analytical and Graphical Aids for the Fatigue Design of Weldments", *Fatigue Fract. Eng. Mater. Struct*, Vol 8(3), pp 223-241.

**5**     *Appendix A: Published and to be published papers*

---

The papers in the order given in Section 1.2 as shown in Figure 1-1 are included.



## **Paper 1**

# **Fatigue and Static Behaviour of Aluminium Box stiffener Lap Joints**

Naiquan Ye and Torgeir Moan

Department of Marine Structures, Faculty of Marine  
Technology, Norwegian University of Science and  
Technology, Trondheim, Norway

Published in International Journal of Fatigue 2002,  
Volume 24, pages 581-589





# Fatigue and static behaviour of aluminium box-stiffener lap joints

Naiquan Ye<sup>\*</sup>, Torgeir Moan

*Department of Marine Structures, Faculty of Marine Technology, Norwegian University of Science and Technology, 7491 Trondheim, Norway*

Received 1 February 2001; received in revised form 25 June 2001; accepted 27 June 2001

## Abstract

The fatigue and static behaviour of aluminium box-stiffener lap joints were investigated in this study. Finite element analysis showed that stress concentration factor (SCF) at the weld toe decreased greatly as the weld leg length increased, while the location of the greatest SCF deviated from the connecting point to the middle of the flange. It is also found that the SCF at the weld root is much less than that at the weld toe. Fatigue tests showed that weld toe cracking was the main fatigue failure mode. In addition, fatigue crack initiation site changed from the connecting point to the middle point of the flange. Weld root failure was only possible when the weld leg length was less than twice the main plate thickness (6.0 mm). The test data agree with those for toe failure given by Eurocode 9. © 2002 Elsevier Science Ltd. All rights reserved.

*Keywords:* Aluminium alloys; Box-stiffener; Lap joints; Stress concentration factor; Fatigue life

## 1. Introduction

Aluminium and its alloys are widely used in the ship building and aerospace industries due to their good mechanical properties such as the high strength/weight ratio compared with steel. Aluminium alloys have become the main building material in the development of high speed light craft (HSLC) in recent years, where speed and low weight are crucial. Another good fabrication feature is extrusion, since this makes it possible to fabricate complicated structural profiles where the advantages of the material can be utilized as much as possible. This is exemplified in this study by box-stiffeners which are extruded profiles used in the building of HSLCs and bridges.

Ships are preferably built in sections that are constructed in parallel and then joined. Lap joints are commonly used to join the sections. This is because this solution normally requires less restrictive joint dimensional tolerances and can join two components most conveniently and effectively. In the aerospace industry, adhesive and rivet lap joints are the main solutions, however, in the ship building industry, welded lap joints are widely adopted. In 1999, Tong and Steven [1] summar-

ized the analysis and design details of plate lap joints, and pointed out that for welded lap joints, the load carrying fillet welds make fatigue a main issue to consider for design. Much work has been reported relating to static stress and fatigue analysis of lap joints [2–4]. However, most of this is concentrated either on single or single-step double lap joints that are only suitable for joining simple plates such as sheets, therefore, they are normally treated as a two-dimensional problem. Furthermore, because of relatively low bending stiffness, these joints can only resist axial tensile loading in most cases.

Extruded box-stiffeners have been widely used in HSLC and bridge building practice because of their good mechanical features [5]. In the same way as simple plate lap joints have been used for joining two individual simple plates, box-stiffener lap joints have been designed to join two individual pre-fabricated box-stiffener panels. As mentioned above, avoiding fatigue is the main design criterion for such joints, especially for larger sized ships. No work has been found in the literature relating to the static and fatigue analysis of such box-stiffener lap joints.

In this study, this type of joint is first analysed numerically by the finite element (FE) method, which investigates the influences of the lap plate and the weld leg length on the stress concentration at the weld toe and root. Secondly, 13 real-scale specimens from a shipyard were tested to evaluate the fatigue strength of this joint.

<sup>\*</sup> Corresponding author. Tel.: +47-73-551103; fax: +47-73-595528.  
E-mail address: naiquan.ye@marin.ntnu.no (N. Ye).

Table 1  
Chemical composition of aluminium alloys 5083 and 6082

Alloy	S <sub>i</sub>	F <sub>e</sub>	C <sub>u</sub>	M <sub>n</sub>	M <sub>g</sub>	C <sub>r</sub>	N <sub>i</sub>	Z <sub>n</sub>	T <sub>i</sub>
5083	0.17	0.29	0.026	0.58	4.56	0.09	0.003	0.033	0.017
6082	0.98	0.18	0.1	0.55	0.66	0.25	–	0.01	0.1

Table 2  
Mechanical properties of the alloys 5083 and 6082

Alloy	5083	6082
Yield point, $R_{p0.2}$ (N/mm <sup>2</sup> )	250.8	291
Tensile strength, $R_m$ (N/mm <sup>2</sup> )	335.3	322
Elongation, $A_5$ (%)	15.27	12

The results are compared to existing nominal and structural design SN curves for fatigue analysis.

## 2. Specimen descriptions

### 2.1. Material

Two kinds of aluminium alloys were used to fabricate the lap joints. The profile of the stiffeners was made of 6082 with a T6 heat treatment and the lap material was made of 5083 tempered by H116. The chemical composition and mechanical properties are listed in Tables 1 and 2, respectively.

### 2.2. Geometrical properties

Fig. 1 illustrates the geometry of this type of box-stiffener lap joint.

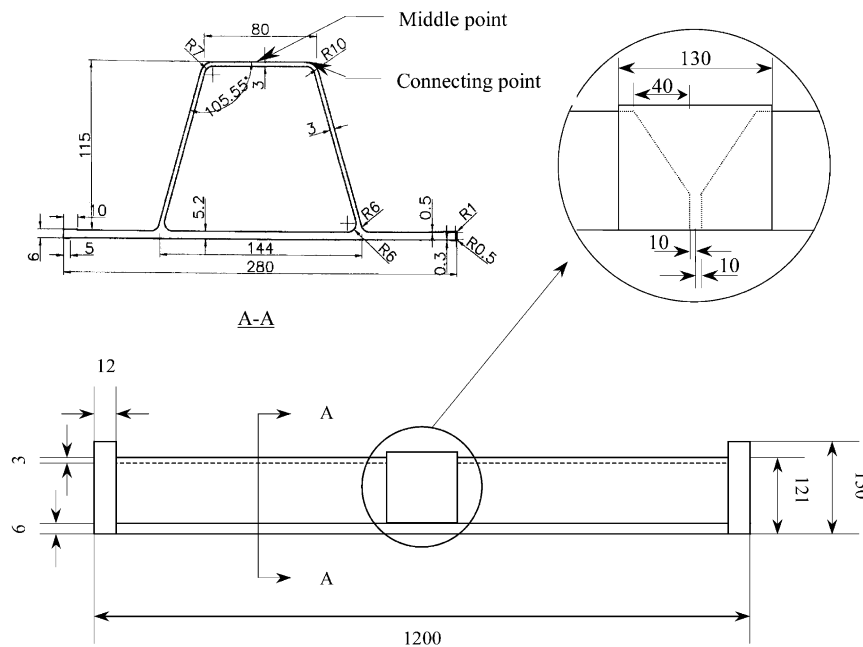


Fig. 1. Geometrical properties of box-stiffener lap joints.

### 2.3. Weld details

The lap plate was welded to the parent plates by fillet weld using AlMg4.5Mn alloy as the filler metal. A pulsed MIG technique was applied at a feeding speed of 55 cm/min. Fig. 2 shows that the weld leg length on the lap plate side  $\lambda_L$  is consistent with the thickness of the plate. The weld leg length on the main member (parent plate) side  $\lambda_m$  is set to be equal to the parent plate thickness. As the thickness of the these two plates is the same here, i.e. 3.0 mm, the nominal weld transition angle  $\phi$  is 45°. However,  $\lambda_m$  and  $\phi$  are strongly dependent on the welding procedure. Therefore, all the welds were reproduced by imprints and measured values are presented in Table 3. It can be found that the majority

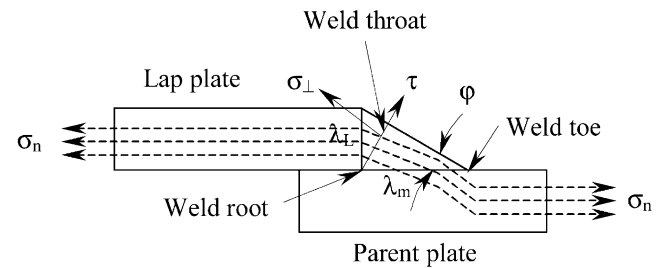


Fig. 2. Weld leg length and stress components in weld throat surface.

Table 3  
Weld parameters and fatigue test data

Specimen no.	Leg length (mm)	Transition angle (degree)	Toe radius (mm)	SCF	Cycles	Remarks
ALT-1	7.8	19.2	0.92	2.02	616,427	Toe failure
ALT-2	11.9	18.5	0.67	1.92	657,113	Toe failure
ALT-3	7.1	23.5	0.45	2.04	568,960	Toe failure
ALT-4	8.5	21.5	0.54	1.98	795,894	Toe failure
ALT-5	7.6	16.5	1.05	2.03	592,002	Toe failure
ALT-6	7.2	18.6	0.76	2.04	615,878	Toe failure
ALT-7	9.3	21.4	0.43	1.95	1,045,614	Toe failure
ALT-8	5.6	27.2	0.34	2.15	280,606	Root failure
ALT-9	10.4	17.0	0.98	1.94	864,123	Toe failure
ALT-10	6.7	23.7	0.66	2.08	933,301	Toe failure
ALT-11	9.8	21.3	0.76	1.94	546,491	Toe failure
ALT-12	7.2	18.5	0.73	2.04	877,318	Toe failure
ALT-13	7.4	17.7	0.88	2.03	738,768	Toe failure

of the specimens has a weld leg length beyond 6.0 mm, and only one specimen has a weld leg length less than 6.0 mm. It is also found that there is no evident correlation between the weld leg length and the transition angle. The latter is formed due to the cooling process of the melting filler metal. After welding was completed, the specimens were inspected visually.

A simple stress flow pattern (dash-line) through the weld in Fig. 2 shows how the fillet weld transfers loads from the parent plate to the lap plate. Stress components relating to the weld root fatigue are illustrated as well, this will be mentioned later.

### 3. Static analysis

#### 3.1. Finite element model

Finite element analysis was used to study stress raising factors that include the lap plate and the fillet weld for the lap joint. 20-node and 15-node solid elements were used to model the plates and welds, respectively. A sub-model with a minimum mesh size  $t/2 \times t/2 \times t/2$  near the weld toe was built so that the local stress raising effect due to the weld could be captured. The analysis was carried out using the SESAM package [6]. The weld leg length is a main parameter that affects the fatigue strength of the joint in this study and was varied between 1.5 and 12.0 mm with a step of 1.5 mm. An example with a leg length of 6.0 mm shows how the finite element model and sub-model were established in Fig. 3 and the local weld detail model that is also shown in the same figure.

#### 3.2. Nominal stress

Fatigue data (SN curves) can be defined with reference to a nominal, geometrical (structural), or notch

stress for steel and aluminium. Regarding the aluminium welded joints, however, the nominal stress approach is still the most widely accepted method for design and analysis. For the joint considered here, the so-called nominal stress is defined based on beam theory. Therefore the nominal stress is the axial stress (x-direction in Fig. 3) on the top of the flange surface, and can be calculated according to the following equation:

$$\sigma_n = \frac{M \cdot y}{I} \quad (1)$$

where,  $M$ ,  $I$  and  $y$  are the bending moment, inertia moment the distance to the area centre, respectively. Based on the four-point bending load case indicated in Fig. 4, the analytical beam theory solution to the nominal stress varies longitudinally on the flange top surface, as is given in Fig. 4. Also the same figure presents linear finite element results along two lines on the top of the flange surface, these are the centre line and the line along the connecting point as indicated in Fig. 1.

It is shown that the beam theory result corresponds very well with the finite element result within the area where the stiffener experiences pure bending. There is little difference from the centre line to the connecting line. The large discrepancy appearing near the boundary area results from extra restrictions due to boundary conditions. Strain gauge measurements confirm the result from these two methods by the error being less than 3%.

It is known that fatigue occurs at the point where the highest stresses exist near a weld. For the box-stiffener lap joint in this study, either weld toe failure or weld root failure through the weld throat is indicated in some codes and standards such as Eurocode 9. For the latter failure mode, however, the nominal stress refers to shear stress in the weld throat surface. But the complexity of the profile (Fig. 1) makes it very difficult to calculate the nominal shear stress. Fortunately, for the joint studied here, test results showed the weld toe failure only

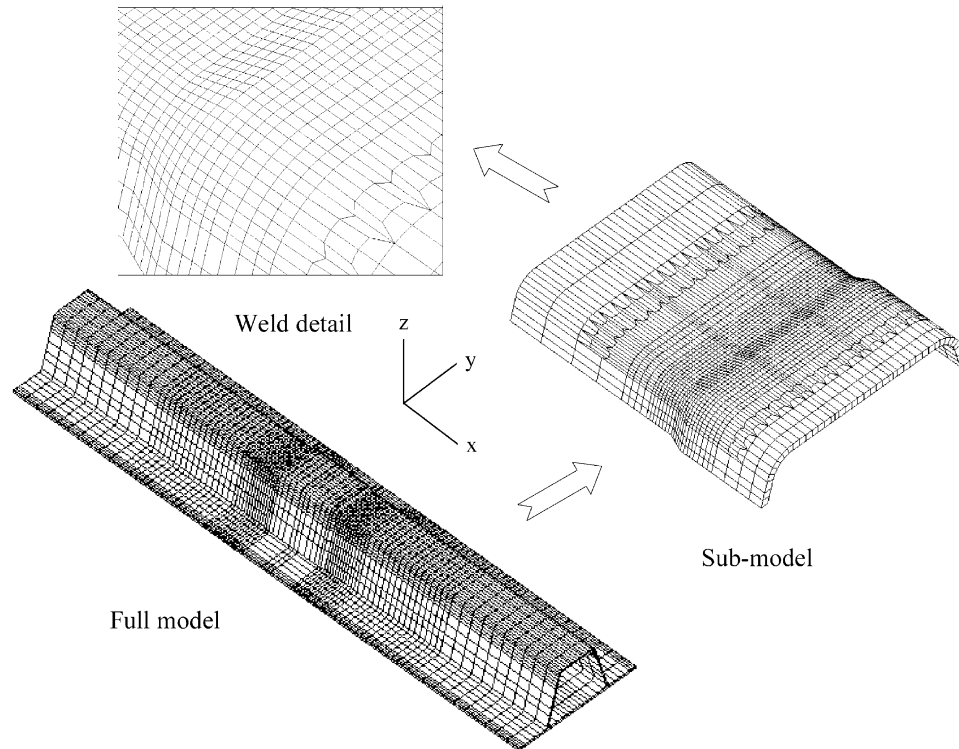


Fig. 3. Finite element model details.

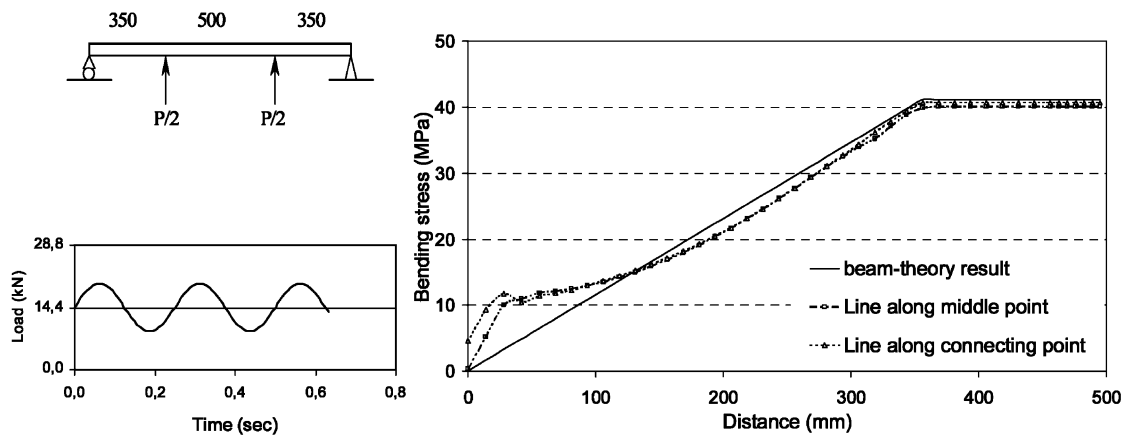


Fig. 4. Beam theory result versus finite element result (i.e. membrane stress).

occurred with 12 of the 13 specimens. The only weld root failure possibly resulted from the defects in the weld root itself that had been found after cutting out the collapsed specimen. Therefore, the static analysis will be focused on the stress concentration along the weld toe line. However, shear stress concentration in the weld root will be simply discussed as well below. Stress calculation is performed at the Gaussian points and then extrapolated to the nodes [7]. All the stresses are normalized by the axial nominal stress within the pure bending part as illustrated in Fig. 4.

### 3.3. Influence of the lap plate on SCF

The main characteristics of the joint in this study is the box-stiffener lap plate that joins two individual box-stiffeners by means of a weld. This local geometry has a great influence on the normal stress concentration close to the joining area. Figs. 5 and 6 schematically illustrate this effect along two longitudinal lines that are the line along the middle point and the line along the corner (connecting point) on the top surface of the flange. Furthermore, in order to get to know the variation of this

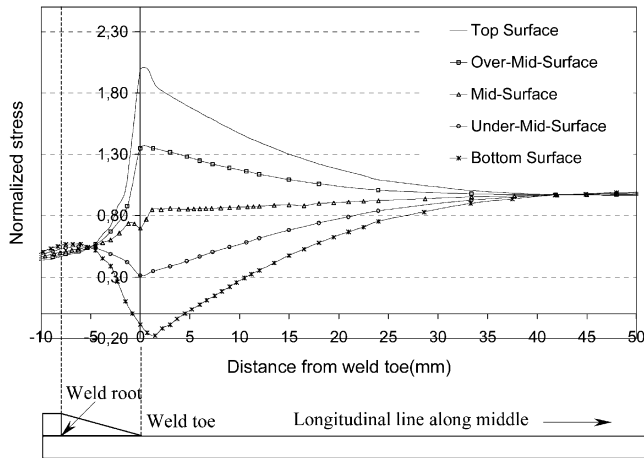


Fig. 5. Normal stress variation along middle point (Fig. 1) lines at different layers in the longitudinal direction.

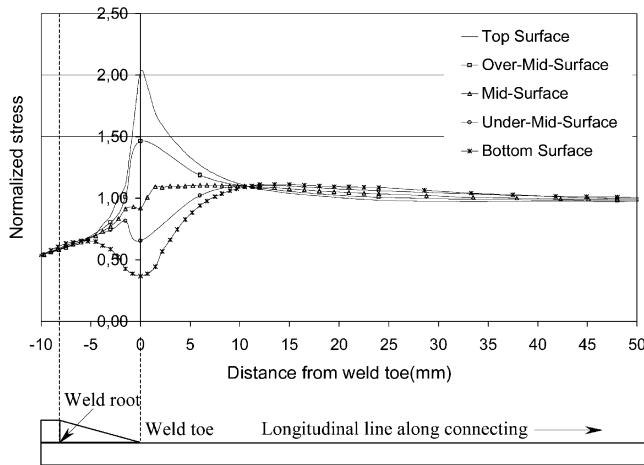


Fig. 6. Normal stress variation along connecting point (Fig. 1) lines at different layers in the longitudinal direction.

stress in the thickness direction, the same calculation is carried out on the other four layers: these are bottom surface, middle surface and the surfaces between. These surfaces evenly divide the thickness.

As expected, the peak value of the SCF for both lines appears at the weld toe on the top surface. There is no difference evident between the two peaks (less than 3%). The influence of the lap plate tends to be negligible when it is about  $10t$  (30.0 mm) away from the weld toe. These similar features have already been reported for the simple plate lap joints. The typical features of this box-stiffener lap joint appear at the weld toe.

By comparing Figs. 5 and 6, it can be seen that the SCF peak at the top surface decreases at a quite different rate towards the bottom surface. In Fig. 5, it even ends with a compressive value of  $-0.1$  at the bottom surface, however, a positive value of  $0.7$  is found in Fig. 6. After decomposing the normal stress into bending stress and membrane stress, it is found that the middle part of the

flange plate experiences a higher bending stress but a lower membrane stress. However, the lower bending stress and higher membrane stress are found in the plate at the connecting point. Actually, when it is about  $2t$  (6.0 mm) away from the weld toe, there is no evident bending component and the bending stress changes sign after this point. The phenomena reveal that the bending of the middle part of the flange is less restricted than the connecting part. The curvature of the connecting plate plays an important role in this local bending restriction.

It should be noted that the weld leg length in Figs. 5 and 6 is 8.2 mm, i.e. the mean value as indicated in Fig. 1. Other specimens with different weld leg lengths come out with the same result.

### 3.4. Influence of the weld on SCF

Local weld is another important factor that affects the SCF at the weld toe. Engesvik [8] reported that the weld toe radius and the weld transition angle are the major parameters that determine the SCF at the weld toe. The transition angle correlates theoretically with the leg length according to (Fig. 2),

$$\varphi = \arctg\left(\frac{\lambda_L}{\lambda_m}\right) \quad (2)$$

However, as shown in Table 3, the actual transition angle is almost independent of the leg length and is determined by the welding process. It was found that the weld leg length was the dominant factor for the joint studied herein. Fig. 7 illustrates how the longitudinal normal stress varies along the weld toe line for different weld leg lengths. When the leg length is shorter than 6.0 mm, it is seen that the stress varies slowly from the middle line and increases rapidly when it comes to the edge of the flange surface, reaching its peak value near

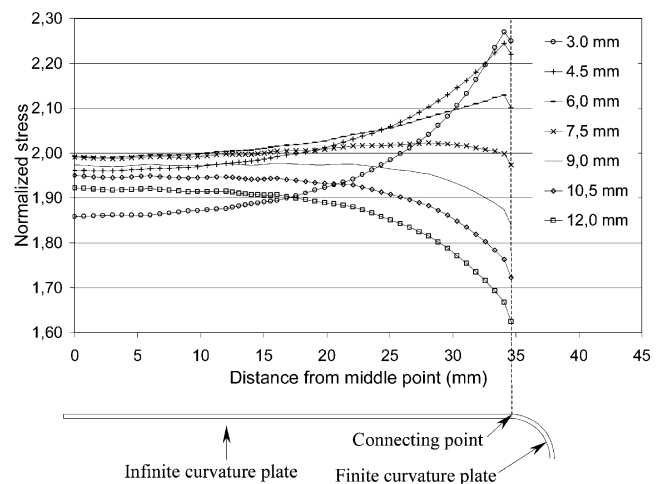


Fig. 7. Normal stress variation along the weld toe line for different weld leg lengths.

the connecting point where the curvature of the plate changes from infinite to finite value. Further weld leg length increases tend to reduce this stress raising effect near the connecting point. That is, when the weld leg length is greater than 7.5 mm, this connecting point stress peak disappears. As a consequence, the highest SCF does not then occur near the corners of the box-stiffener, but is shifted to the middle of the flange plate. Moreover, the absolute value of this peak value decreases greatly when the weld leg length increases from 3.0 to 7.5 mm. Increasing the weld leg length beyond this value, from 7.5 to 12.0 mm does not introduce more influence on the highest SCF, instead, this peak value only changes slightly. Obviously, crack growth would depend upon the initial crack size and the stress level. For equal initial crack size, fatigue failure will occur near the connecting point for those specimens with a weld leg length below 7.5 mm. However, for those with a weld leg length above 7.5 mm, the fatigue failure initiation area will be more likely around the middle line. This feature is rather important for fabricators because it will cancel out the detrimental effects due to possible defects that are easily introduced when the welding is performed manually around the finite curvature plate. Test results have confirmed this feature.

### 3.5. Shear stress in the weld root

The evident nominal shear stress for the joint is hard to assess. A practical approach to deal with the cracks initiating from weld roots and propagating through the weld throat is calculating via a vector sum of the shear stresses in the weld throat surface [9–11]. The total shear stress acting on the weld throat plane is calculated accurately based on the finite element results where all the stress components are given individually for each coordinate direction [12]. Fig. 8 shows the normalized shear

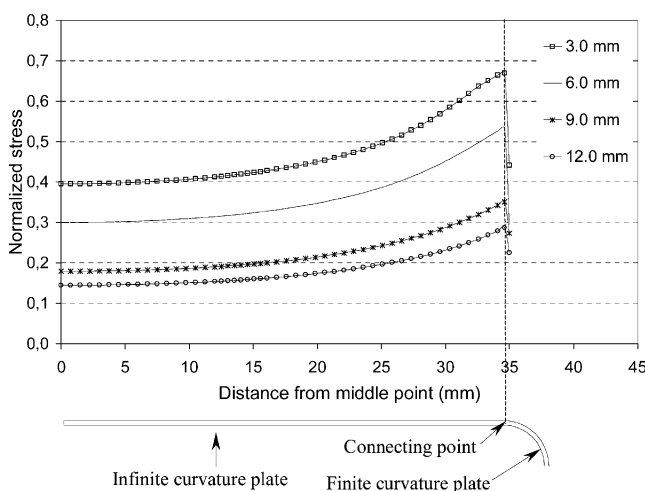


Fig. 8. Shear stress along the weld root line across the width of the flange for different weld leg lengths.

stress along the weld root line across the flange width direction, four weld leg lengths are presented so that the effect of different weld lengths can be quantified.

As experienced for normal stress at the weld toe, the shear SCF for each weld leg length increases gradually from the centre of the flange to its peak near the connecting point and then jumps abruptly after this point. As to the influence of the weld leg length, longer weld leg length results in lower SCF and vice versa.

Comparing the shear SCF with the normal SCF in Fig. 7, it can be found that the SCF peak at the weld toe is much higher than that in the weld root for each weld leg length. The ratios of the normal SCF peak at the weld toe against the shear SCF in the weld root are 3.4, 4.0, 5.7 and 6.7 with corresponding weld leg lengths being 3.0, 6.0, 9.0 and 12.0 mm, respectively. It cannot be concluded that the failure from the weld toe will be due to the axial normal stress since different SN curves are involved for these two failure modes [9–11], even though the weld toe failure was the main failure mode recorded in the test. However, it is seen that this ratio seems to rise with the increase in the weld leg length. Therefore, it is reasonable to presume that this welded joint would fail at the weld toe when the leg length increases. The assumption coincides with the test results.

## 4. Experimental analysis

### 4.1. Test set-up

In the test, the specimens were subjected to four-point bending under constant amplitude conditions in a computer controlled servo-hydraulic fatigue testing machine. In order to match the actual residual stress level which exists in the vicinity of the welds in real situation, the specimens were tested in load control with a nominal load (stress) ratio  $R$  of 0.44. The frequency used in the test was 4 Hz. All the tests were carried out at ambient conditions with room temperature (about 24°C). As far as possible each test was completed without intermediate stops. The specimens were set up in four-point bending as illustrated in Fig. 9.

### 4.2. Test results

Thirteen specimens were tested in this investigation. Fatigue lives were recorded when the specimens failed with full penetration cracks in the plate thickness direction (Table 3). As expected from the finite element analysis, the weld toe failure was the main failure mode, i.e. 12 of a total 13 specimens experienced this mode of failure. Another one failed at the weld root with much fewer cycles. The corresponding weld leg length of this specimen was 5.6 mm (<6.0 mm).

Fig. 11 schematically illustrates the correlation

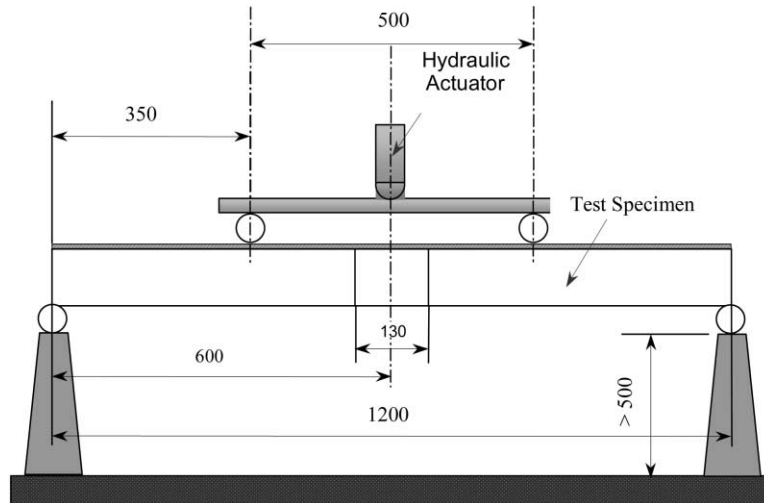


Fig. 9. Test set-up.

between the fatigue life and the transition angle, no evident correlation factor is found. This confirms the assumption that the weld leg length is the dominant factor that has the most significant influence on the fatigue life of the box-stiffener lap joints.

The most common method of fatigue analysis and design by far is the use of SN curves in which nominal axial stress in the structural component is used as design stress. Following the nominal stress approach, the geometrical similarity between the test specimen and detail in the codes and standards is required so that the fatigue life prediction can be trustworthy. Unfortunately, the relevant joint considered herein is not classified in any existing codes. However, for the load carrying fillet weld, among the existing codes and recommendations Eurocode 9 requires the highest fatigue strength for the weld toe failure mode. Therefore, detail class 25 in Eurocode 9 corresponding to weld toe failure was chosen as the basis for comparing the fatigue test results in Fig. 10.

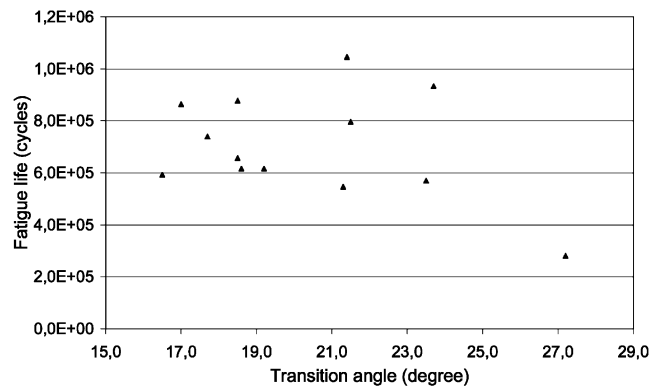


Fig. 11. Weld transition angle versus fatigue life.

Both the mean curve and the mean minus two standard deviation curves are plotted. The standard deviation obtained from the test data is 0.092 in terms of logarithmic cycles. Fig. 10 shows that the test data satisfy this

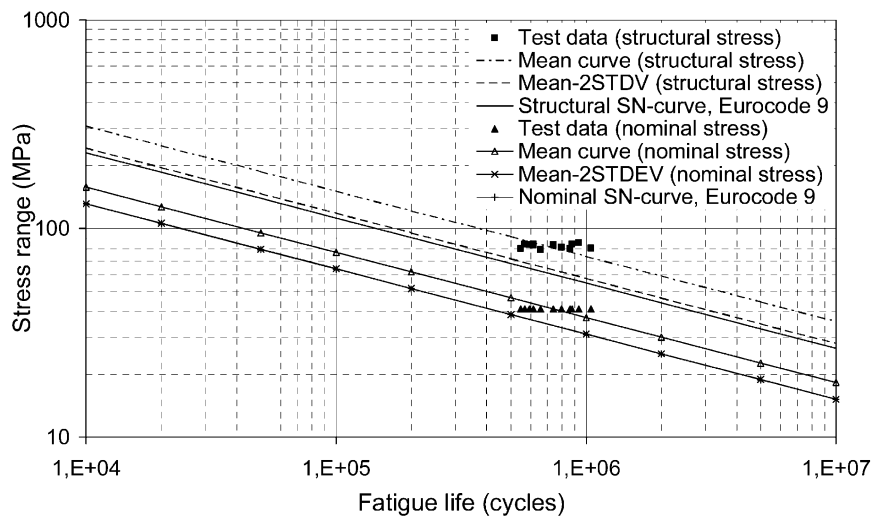


Fig. 10. Fatigue test data against Eurocode 9.

code. The mean minus two standard deviation line is just over the class 25 SN curve in the Eurocode 9. These two curves appear to overlap in the figure due to the safety margin being only about 5% at the characteristic  $2 \times 10^6$  cycles.

As another fatigue design and analysis method, a structural stress approach has been proposed and developed in recent years. Stress extrapolation is required in order to apply this method. Even though various methods have been suggested, there is still a lack of consistent stress extrapolation methods for different joint details. Furthermore, the accuracy is strongly affected by the element size and type close to the weld toe [13]. Nevertheless, as a comparison to the nominal stress approach, a structural SN curve with a characteristic structural stress range of 44 MPa recommended by Eurocode 9 [11] is plotted in Fig. 12. Thereby the fatigue test data are re-plotted by means of structural stress. The structural stress concentration factors are calculated according to the DNV extrapolation method [14] and the results are found in Table 3. The safety margin is increased compared with the nominal stress approach. The scatter of the test data (standard deviation) is changed from 0.09 to 0.07.

Since there was only one specimen that failed because of weld root failure mode, it is meaningless to plot it against any SN curve. However, the weld leg length of this corresponding specimen was the shortest one among all the specimens. Therefore, this failure mode may much more likely give rise to the short weld leg length. In other words, the weld root failure could possibly be avoided by barely increasing the weld leg length to a reasonable range, i.e. larger than 6.0 mm. The FE analysis in the study have confirmed that the shorter the leg length is, the higher the shear stress at root and normal stress at toe SCF are. However, the shear SCF seems to be increasing with a higher ratio. This makes the weld throat failure more likely when the leg length decreases. It can be simply understood by the stress flow pattern in Fig. 2. That is, the shorter the leg length is, the less

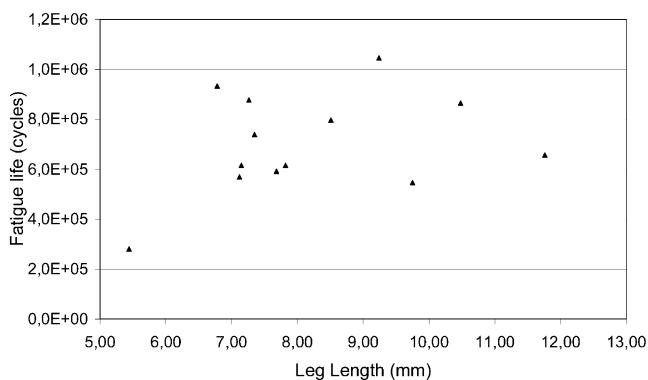


Fig. 12. Weld length versus fatigue life

throat area is used to transfer the forces, implying higher shear SCF at root.

It should be noted that the recorded fatigue life for this specimen was only one-third of the mean fatigue life of those that failed from the weld toe. This relative low fatigue life may result from the defects inside the weld itself that were found after cutting out the failed specimens.

It is also shown in Fig. 12 that there was no obvious correlation between the individual fatigue life and weld leg length when the failure is at the weld toe. This is because the leg lengths are fairly long and the sensitivity to the weld length is relatively small, as is shown in Fig. 7. Therefore, further increase in the weld leg length does not contribute to longer fatigue life. However, the crack initiation site was affected by further increase in the weld leg length. The fatigue failure occurred around the connecting point for those specimens with short weld leg lengths and a shift to the middle point was observed when the weld leg length was increased. This confirms the stress analysis result in Fig. 7 where it is said that the greatest SCF shifts from the connecting point to the middle point with regard to the weld leg length increase. Therefore, a weld leg length that is slightly longer than 7.5 mm is suggested so that the drawback from any manual welding imperfections around the connecting point can be eliminated.

## 5. Conclusions

On the basis of the results obtained from this laboratory investigation, and the corresponding results from the finite element analysis, it seems reasonable to draw the following conclusions:

The weld leg length is a decisive parameter in determining both the fatigue failure mode and fatigue life of the type of box-stiffener lap joint in this investigation. In addition, the fatigue crack initiation site is also influenced by this leg length. The experiments show that weld toe failure dominates when the weld leg length is twice the main plate thickness or more. Also, it is found that only marginal improvements in the fatigue strength can be achieved by further increasing the leg length. In addition to that, when the weld leg length increases, on the one hand, the highest SCF reduces rapidly, and on the other hand, the crack initiation site shifts from the connecting point to the middle of the flange plate.

## Acknowledgements

The experiments reported in this paper were a part of the project Aluminium in Ships funded by Hydro Aluminium Maritime a.s. The authors gratefully acknowl-



edge this financial support and the technical support provided by Jon Ersland and Eirik Smedstad.

## References

- [1] Tong L, Steven PS. Analysis and design of structural bonded joints. Boston, MA: Kluwer, 1999.
- [2] Ono M et al. Static and fatigue strength of laser-welded lap joints in thin steel sheet. *Welding International* 1995;11:462.
- [3] Wang H, Grandt A. Fatigue analysis of multiple site damage in lap joint specimens. ASTM Special Technical Publication 1360 1999;214–26.
- [4] Hsu C, Albright CE. Fatigue analysis of laser welded lap joints. *Engineering Fracture Mechanics* 1991;39:571–80.
- [5] Mazzolani FM. Aluminium alloy structures. London: E. & F.N. Spon, 1995.
- [6] SESAM SYSTEM. Det Norske Veritas SESAM AS. Norway, 1993.
- [7] Cook RD. Concepts and applications for finite element analysis. New York: John Wiley and Sons, 1989.
- [8] Engesvik KM. Analysis of uncertainties in the fatigue capacity of welded joints. Ph.D. thesis. Department of Marine Technology, The Norwegian Institute of Technology, NTH, Trondheim, Norway, 1981.
- [9] Hobbacher A. Recommendations for fatigue design of welded joints and components. ISO standard proposal, 1996.
- [10] BS8181: structural use of aluminium. London: British Standards Institution, 1991.
- [11] Eurocode 9: design of aluminium structures. Part 2: structures susceptible to fatigue. Brussels: CEN—European Committee for Standardisation, 1998.
- [12] Dally JM, Riley WF. Experimental stress analysis. New York: McGraw-Hill, 1991.
- [13] Niemi E. On the determination of hot spot stresses in the vicinity of edge gussets. Technical report IIW-XIII-1555-94, Cambridge, 1994.
- [14] DNV-Det Norske Veritas. Fatigue assessment in ship structures. Det Norske Veritas Classification A.S., No 93-0432, Høvik, Norway, 1993.



## **Paper 2**

# **Static and Fatigue Analysis of Three Types of Aluminium Box stiffener/Web Frame Connections**

Naiquan Ye and Torgeir Moan

Department of Marine Structures, Faculty of Marine  
Technology, Norwegian University of Science and  
Technology, Trondheim, Norway

Published in International Journal of Fatigue 2007,  
Volume 29, pages 1426-1433



# Static and fatigue analysis of three types of aluminium box-stiffener/web frame connections

Naiquan Ye<sup>\*</sup>, Torgeir Moan

*Department of Marine Structures, Faculty of Marine Technology, Norwegian University of Science and Technology, 7491 Trondheim, Norway*

Received 24 February 2006; received in revised form 23 October 2006; accepted 15 November 2006

Available online 30 January 2007

## Abstract

Static and fatigue behaviour of three types of aluminium box-stiffener/web connections are investigated in this study. The main purposes are to provide a connection solution that can reduce the fabrication costs by changing the cutting shapes on the web frame and correspondingly the weld process and meanwhile sufficient fatigue strength can be achieved. Finite element analyses (FEA) show the influence of local geometry and weld parameters on the stress gradient near the fatigue cracking area. The influence of the weld parameters on the structural stress concentration factors is also studied. Twelve specimens of every type were tested and the test data are compared both to a nominal stress based design SN curve Eurocode9/31 and a structural stress based design SN curve Eurocode9/44. © 2006 Elsevier Ltd. All rights reserved.

*Keywords:* Aluminium alloys; Box-stiffener; Stress concentration; Fatigue life

## 1. Introduction

Aluminium has been widely used due to its good mechanical properties. For example, the light weight of the aluminium structure may reduce the load level acting on the structures when the loading is proportional to the mass of the structure such as automotive frames and some ship structures [1]. Some alloys of aluminium are preferred particularly when the structures survive in corrosive environment.

Compared to steel, aluminium and its alloys are suitable for extrusion which often makes them to be the designer's first choice. Extrusions avoid extra welding or machining to achieve unique section shapes and enable an optimised structure design. In the point view of fatigue, the joints or discontinuities can be located in areas of lower stress level, thus improving fatigue resistance.

Fatigue was not separately taken into consideration in the design of aluminium structure before, instead, it was

assumed to be sufficient if the requirements given in the design codes are fulfilled [2]. Larger-sized ships (with length more than 120 m) have been built in recent years owing to the development of new fabrication methods and structural detail solutions. The former design codes in which only small-sized vessels were considered, can no longer satisfy the new needs for the large vessels in the point view of fatigue. Fatigue becomes the governing criteria in the design of the mid-ship stiffener/web frame connections at the top and bottom of a high speed large aluminium catamaran [3].

Stiffener/web frame connection is a most common joint in structure design. A great number of such joint can be found in a middle-sized ship. Therefore, a slight improvement on design may benefit the fabricator a lot economically. The extruded box-stiffener provides a good solution to the top and bottom structure in the design of high speed light crafts (HSLCs). The box-stiffener is connected to the web frame by welding and fatigue may be the determining limit state for design [3]. In this study, the static and fatigue behaviour of three similar types of box-stiffener/web frame connections are investigated.

<sup>\*</sup> Corresponding author.

*E-mail address:* [Naiquan.Ye@marintek.sintef.no](mailto:Naiquan.Ye@marintek.sintef.no) (N. Ye).

Table 1  
Chemical composition and mechanical properties of the alloys 5083 and 6082

Alloy		5083	6082
Chemical composition	Si	0.17	0.98
	Fe	0.29	0.18
	Cu	0.026	0.1
	Mn	0.58	0.55
	Mg	4.56	0.66
	Cr	0.09	0.25
	Ni	0.003	–
	Zn	0.033	0.01
	Ti	0.017	0.1
Mechanical properties	Yield point, $R_{p0.2}$ [MPa]	250.8	291
	Tensile strength, $R_m$ [MPa]	335.3	322
	Elongation, A5 [%]	15.27	12

2. Box-stiffener/web frame connections

2.1. General

The general geometrical requirements for an aluminium stiffener under bending are the depth of the stiffener and space between stiffeners so that excessive deflection is avoided and stresses in the part would be lowered. The extruded box-stiffener in this study meets both of the above requirements. The stiffness against bending is increased by a hollow section, besides, the space between the stiffeners is reduced by the twin-wall section shape compared to the single-wall stiffeners e.g. T-shaped or L-shaped.

A cutting is made on the web frame and fillet weld is performed to join the box-stiffener with the web frame.

2.2. Material

Two kinds of aluminium alloys were used in building the connections. The main body of the stiffener was made of alloy 6082 with a T6 heat treatment and web frame was 5083 H116 tempered. The chemical composition and mechanical properties of the two alloys are listed in Table 1.

2.3. Geometrical and welding specifications

The three types of connections are termed as, for simplification, Alt-1, Alt-2 and Alt-3. The main difference of each alternative was made on cutting shape on the web frame, and thus causing a different welding procedure. Alt-1 was cut with a largest opening so that the welding can easily be performed. Fillet welding on both sides of the web frame was performed, in addition, extra welding around the cutting edge on the web frame ensures a continuity of the weldment. The web frame was tightly joined with the box-stiffener for Alt-2 and Alt-3. The same fillet weld as Alt-1 was applied, however, Alt-3 was continuously welded around the stiffener with no interruption along the cutting edge and the welding for Alt-2 was performed from the bottom of the stiffener along the joining line but stop at a height of  $p$ . Fig. 1 schematically illustrates the geometrical specifications together with an indication of the fatigue cracking point.

The type of joint affects its fatigue strength greatly. Among the fatigue influencing factors, weld geometry is of great importance. Study by Engesvik and Moan [4] showed that the weld parameters affect the scatter of the constant amplitude fatigue data more than other factors such as the crack size and the material properties. Fig. 2 represents a typical profile of a weld between the stiffener and the web frame. The weld toe radius  $\rho$ , weld toe angle  $\theta$  and the weld throat thickness  $a$  (or the weld leg length  $\lambda$ ) on the stressed member as illustrated in Fig. 2 are the key parameters that may affect the fatigue performance of the joint [4,5]. The weld leg length  $\lambda$  correlates with the weld throat thickness  $a$  by  $\lambda = a/\sin\theta + \rho \tan(\theta/2)$  and it can be simplified as  $\lambda = a/\sin\theta$  if the effect of the weld toe radius can be neglected in the finite element analysis.

The web frame was welded to the box-stiffener by fillet weld using a pulsed MIG technique with AlMg4.5Mn alloy as the filler metal. The feeding speed is 50 cm/min. The nominal weld toe angle is  $45^\circ$  and the weld throat thickness is equal to 3 mm that corresponds to the weld leg length,  $\lambda$  of 4.24 mm. After completion of welding, the specimens

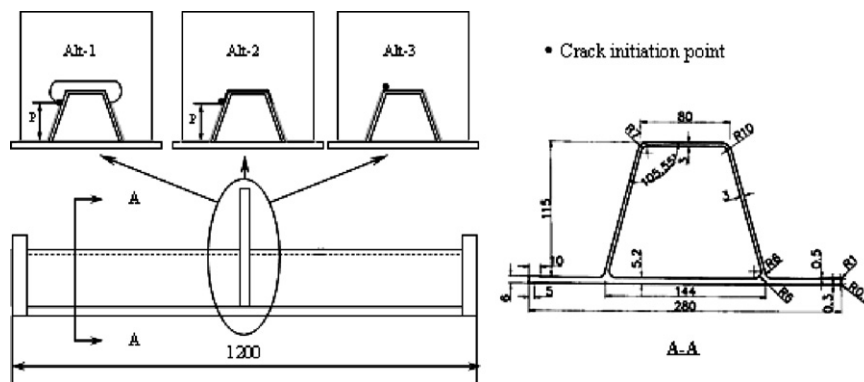


Fig. 1. Geometrical specifications.

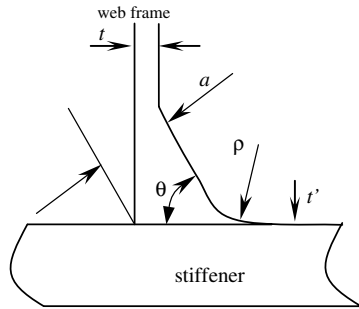


Fig. 2. Weld profile between the web frame and the stiffener,  $t = 6$  mm,  $t' = 3$  mm.

were visually inspected. All the welds were reproduced by imprints and measured at the testing place. The statistical data of the weld parameters are listed in Table 2.

It is seen that the measured mean value of weld toe angle corresponds quite well to the nominal angle. However, the measured weld throat thickness is larger than the nominal value. Besides, sensitivity analysis shows that the weld toe angle and the weld throat thickness seem to be independent of each other.

3. Stress analysis by FEM

Fig. 3 is an illustration of the finite element model of the joints. Twenty-node solid elements are used in the FE models, and the mesh size is half of the thickness of the stiffener flange. The weld details are also shown in the same figure.

Fig. 4 reflects the normal stress distribution on the outer surface of the box stiffener flange at a distance of 4.24 mm from the web frame. For the Alt-1 and Alt-2, it is the extending line of the weld toe line and for Alt-3 it is the line along the weld toe.

It is found that the weld of the Alt-1 and Alt-2 does not have significant influence on the normal stress on the outer surface of the box stiffener. However, the continuous weld of Alt-3 causes obvious stress concentration near the connecting point. Later analysis will show that fatigue cracking for the Alt-3 is always originated from the connecting region.

Table 2 Geometrical parameters of the weld

Parameter	Connection	Minimum	Maximum	Mean	Standard deviation
$\rho$ (mm)	Alt-1	1.47	1.91	1.62	0.10
	Alt-2	1.47	1.91	1.67	0.13
	Alt-3	1.32	1.52	1.42	0.09
$\theta$ (degrees)	Alt-1	34	57	45	6.36
	Alt-2	30	59	45	5.78
	Alt-3	36	55	45	5.55
$a$ (mm)	Alt-1	3.12	5.72	4.33	0.75
	Alt-2	2.70	6.23	4.09	0.87
	Alt-3	2.70	5.20	3.80	0.68

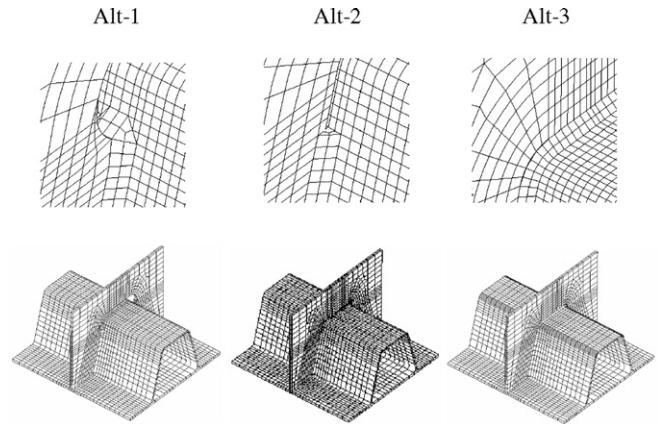


Fig. 3. Finite element models with weld details.

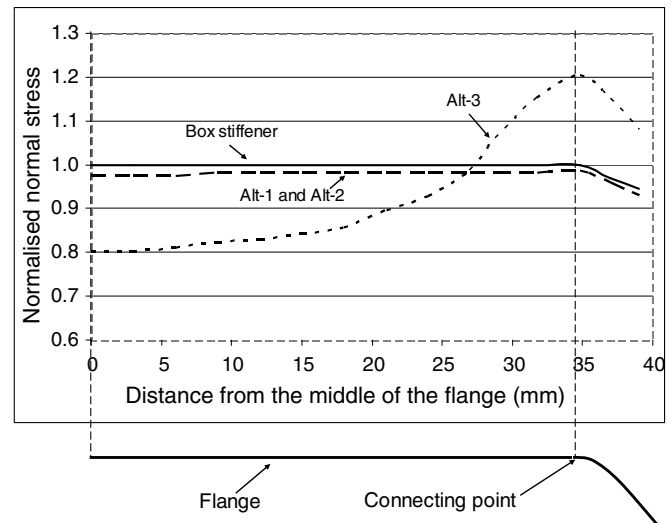


Fig. 4. Normal stress distribution on the outer surface of the flange at a distance of 4.24 mm from the web frame.

The geometry of the joint may have some influence on its local stress distribution, and hence the fatigue behaviour. The cuttings on the web frame as well as the corresponding weldments may cause redistribution of the stresses. It is seen from Fig. 4 that Alt-1 and Alt-2 does not significantly change the stress pattern on outer fiber on the surface of the stiffener flange because there is no weld on the flange. However, the continuous weldment around the stiffener of Alt-3 causes a stress concentration of 1.2 at the connecting point compared to Alt-1 and Alt-2. This is mostly because of geometry resulting from the weldment around the curved part and a secondary bending introduced by the weldment at the curved part will cause high bending stress near the connecting point.

Furthermore, Fig. 5 illustrates the longitudinal stress from the fatigue cracking point for each joint type. The stresses are normalised by the stresses far enough ( $10t$ ,  $t = 3$  mm) from the weld toe. It should be noted that Alt-1 and Alt-2 have a different nominal stress from that of Alt-3 because of their different distance of the fatigue cracking point to the neutral axis of the cross section.

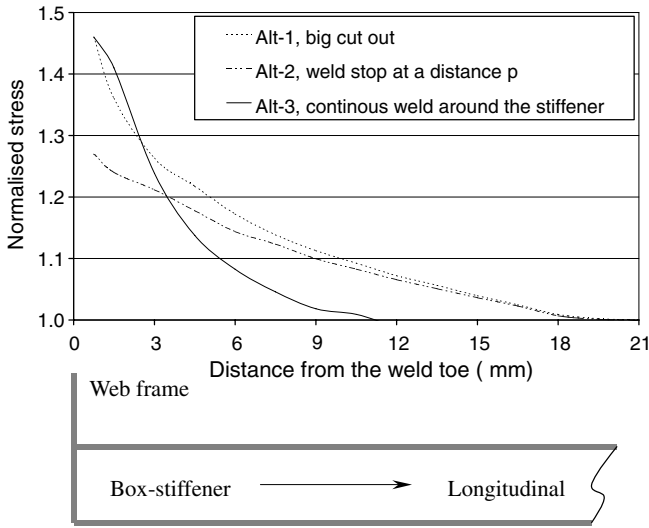


Fig. 5. Normalised stress from the fatigue crack initiating point for joints, see Fig. 1.

### 3.1. Effect of weld parameter

The effect of the weld geometry is investigated by changing the weld toe angle and the weld throat thickness (weld leg length) because these parameters were found to be most important in determining the stress distribution near the weld [5,7] and the weld throat thickness is commonly used as a measurement of the size of a weldment in practice. First, the mean weld toe angle (Table 2) is fixed while the weld throat thickness ranges from the minimum, mean and maximum values. Then while changing the weld toe angle from the minimum, mean and maximum values, the weld toe throat thickness is kept as its mean value. Therefore, five cases for each type of joint are simulated. The results are presented in Figs. 6–8. The legends and the curves in each figure are presented in the same order for convenient visualisation. For instance, the uppermost curve in Fig. 6 corresponds to the first item in the legend where the leg length, weld toe angle, and the weld throat thickness are 8.09 mm, 45° and 5.72 mm, respectively.

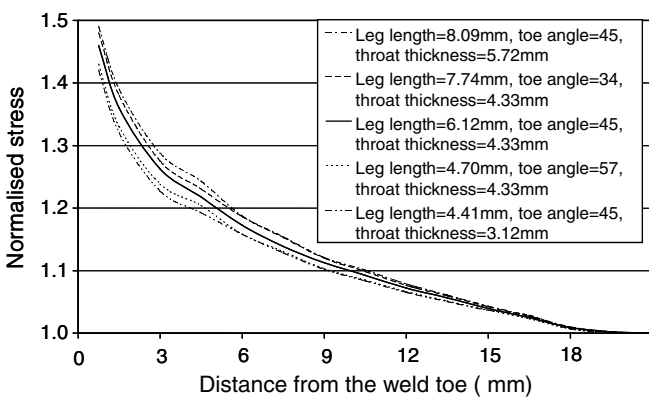


Fig. 6. Effect of weld geometry for Alt-1.

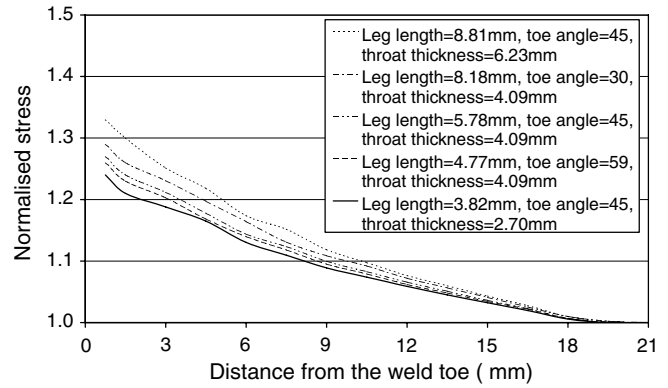


Fig. 7. Effect of weld geometry for Alt-2.

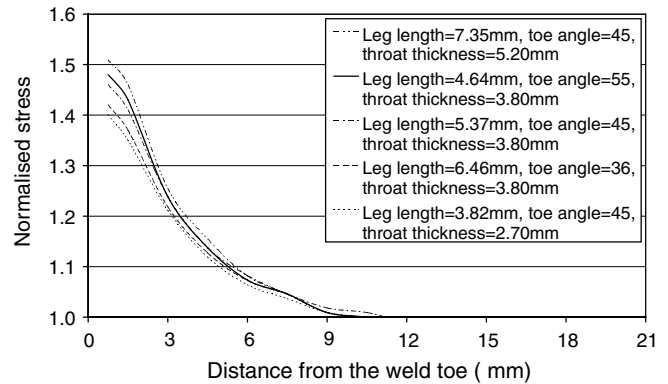


Fig. 8. Effect of weld geometry for Alt-3.

It is seen from Figs. 6–8 that, for all joint types, the highest stress at the weld toe happens for the largest weld throat thickness  $a$  (Fig. 2), and the lowest stress corresponds to the smallest weld throat thickness. This can be attributed to the fact that, on one hand, the increase of the weld throat thickness “extends” the influence of the joint geometry on the stress field, and on the other hand, a bigger weldment draws more stress flowing into the weld that causes higher stress concentration. Since the weld throat thickness is commonly used as the measurement of the size of the fillet weldment, it is accordingly suggested that the weld throat thickness should be controlled in fabrication to avoid extra stress concentration for non-load carrying fillet welded joints. It must be remembered that the transverse load through the web frame is not taken into account and this may also affect the choice of a suitable weld throat thickness if it is considered. For example, the Alt-3 with continuous weld around the stiffener would be preferable due to its better performance in transferring the load through the web frame than the other two alternatives.

It is also found in Figs. 6 and 7 that the trend of the stress gradient is in the same order as the weld leg length for Alt-1 and Alt-2. The longer the weld leg length is, the higher the stress concentration is. In addition, if the weld throat thickness remains the same, for instance, 4.33 mm in Fig. 6, it is found that an increase in the weld toe angle causes a drop in the stress for Alt-1 and Alt-2.



But this is not the case for Alt-3. Even though the highest stress appears when there is a longest weld leg length and the lowest corresponds to the shortest, a leg length of 4.64 mm (weld angle = 55°, weld throat thickness = 3.80 mm) has a larger stress than the cases with the leg length being 5.37 mm and 6.46 mm as shown by Fig. 8. In contrast to the influence of the weld toe angle on stress gradient of Alt-1 and Alt-2, the increase of the weld toe angle does not lower the stress gradient, in stead, as shown by Fig. 8, a larger toe angle corresponds to a larger stress concentration when the weld throat thickness remains unchanged (3.80 mm).

The fatigue cracking point for Alt-3 has been found to be situated near the connecting point between a flat and curved part (Fig. 4), the complexity in both the joint and weld geometry near the point may give reason to the difference of the stress level compared to Alt-1 and Alt-2.

## 4. Fatigue behaviour

### 4.1. Test set-up

The specimens were loaded in the condition of four-point bending by a computer controlled servo hydraulic testing machine (Fig. 9). The load (stress) ratio was 0.44 so that the residual stress in the vicinity of the welds in real situation can be simulated. Constant amplitude test was carried out at a frequency of 5 Hz under an ambient condition.

### 4.2. Test results

Twelve specimens of each joint type were tested. Fatigue life was recorded as the number of cycles when the specimen was fully cracked through thickness of stiffener profile.

In general, stress range determines the fatigue behaviour of a structural component through the SN curve equation,  $\log N_f = \log A - m \log \Delta \sigma$ , where  $N_f$  is number of cycles to failure,  $A$  is a constant which depends also on the joint features and load parameters,  $m$  is the inverse slope and  $S$  is

the stress range. Accordingly, a longer fatigue life is expected if the structural component is exposed to a lower stress range. In this study, the three types of joint were loaded at the same load level, therefore, Alt-1 and Alt-2 should have longer fatigue life due to their lower stress range level compared to Alt-3.

Fatigue assessment can either be based on a nominal or structural range depending on the stress range embedded in the design SN curves. The nominal stress range approach has been used since fatigue was considered as a design criterion. However, the structural stress range approach is a more refined method that requires more detailed stress calculation implementing the structural design.

#### 4.2.1. Fatigue assessment based on the nominal stress range approach

A number of “detail classes” is included in a nominal stress based fatigue assessment method. A “detail class” usually refers to a characteristic fatigue strength in terms of stress range corresponding to a characteristic fatigue life of two million cycles and is classified according to the geometry of the joint detail, weld specification, load condition as well as the location where fatigue cracking occurs. The stress used herein does not reflect the stress raising effects due to the structural geometry nor the weldment. Instead, these stress raising effects are implicitly embedded in the design SN curves. Therefore, the stress can either be derived by a simple elastic beam or frame theory or the FEM using a rather coarse mesh size. The accuracy of fatigue life prediction by using this method depends on how much the desired joint detail and load condition matches the one given in the design codes. Fatigue tests are required if mismatching exists.

The box-stiffener/web frame connections in this study are described as attachment welded on stressed members with transverse non-load-carrying fillet weld in the design codes, however, no exact matching is found in existing design codes because of the complexity of the extruded particular box-stiffener section profile. A design SN curve given by Eurocode 9 was calculated using the highest detail class 31 (denoted as Eurocode9/31) [8,9]. The fatigue test data are presented in Fig. 10.

As described in the previous section that the nominal stress level for Alt-3 is higher than that of Alt-1 and Alt-2, and furthermore, the local geometry for Alt-3 implies a higher stress concentration compared to Alt-1 and Alt-2 (Fig. 4), the joint type Alt-3 should theoretically have a shorter fatigue life if the joints are equally loaded. However, it was found in Fig. 10 that Alt-3 had a longer fatigue life than Alt-1 and Alt-2. This is probably because of different defects in the weld. As stated above, a start or stop of weld is required for Alt-1 and Alt-2. This may introduce more detrimental defects in the area where the weld starts or stops and this caused a reduction in the fatigue life. It is seen that the stress for a stress range at 2 million cycles for Alt-1, Alt-2 and Alt-3 are 4.5%, 5.4% and 23.0% above the Eurocode9/31, respectively.

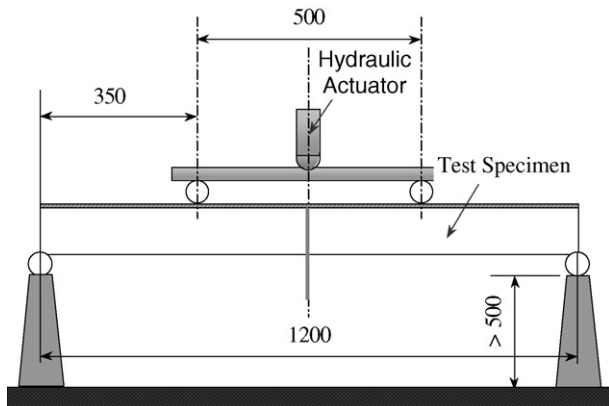


Fig. 9. Four-point-bending test set-up.

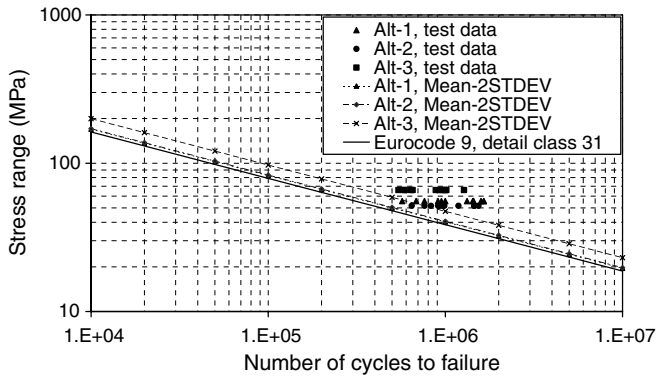


Fig. 10. Test data based on the nominal stress range approach.

4.2.2. Fatigue assessment based on the structural stress range approach

Since fatigue is a highly localised phenomenon, more refined fatigue assessment methods have been developed recently [6,12,13]. Even though the structural stress range approach has been used successfully for tubular joints since 1970 s [10], its application on aluminium welded joints is still under development. The main focuses are to find a suitable structural stress calculation method based on FEA and consistently select a corresponding design SN curve for a given joint.

Unlike the nominal stress range approach, the stress raising effect due to the structural geometry is explicitly reflected in the calculation of a structural stress concentration factor (SCF) but the stress raising factor by the weld is still embedded in the structural design SN curves. Various solutions have been proposed to separate the influence of the structural geometry in the calculation of the structural SCF [10–13]. All these methods assume that the weld has an influence zone of  $0.3t$  to  $0.5t$  on the stress near the weld toe. However, Tveiten and Moan pointed out that this zone may vary with the joint detail [12]. Moreover, the structural SCF obtained by means of extrapolation methods is not significantly affected by changing the weld geometry [7].

One advantage by using the structural stress range approach is that the number of the design SN curves can be greatly reduced compared to the nominal stress range approach because the difference in structural geometry is explicitly reflected in the structural stress calculation. Tve-

iten et al. collected the most recent information on how to select a consistent structural design SN curve for given aluminium welded joints [14].

The structural SN curve Eurocode9/44 is chosen for the box-stiffener/web frame connections because this curve represents the highest requirement among the available structural design SN curves. However, since no corresponding procedure for calculating the structural SCF was suggested in Eurocode 9, an extrapolation method by using the stress values at  $0.5t$  and  $1.5t$  according to the classification society Det Norske Veritas (DNV) rule [15] was used in the structural SCF calculation because it was found that this method would provide a relatively conservative estimation of the fatigue strength of the joints [16]. 20-node solid finite elements with a mesh size of  $t \times t \times t$  were requested for modelling. The structural SCFs for the three types of joints obtained by this method are listed in Table 3.

As it is seen in the stress analysis, Alt-1 and Alt-3 have higher structural SCFs compared to Alt-2. The change of the weld parameters influence the results of the structural SCFs, however, the factor (standard deviation) is only about three per cent. It is also found that the mean SCFs agree quite well to the SCF with the weld parameters being the mean values. When the fatigue test data are compared to the structural stress based design SN curve, the structural SCFs corresponding to the mean weld parameters are therefore used, as illustrated in Fig. 11.

It is found that the fatigue strength in terms of stress range at 2 million cycles for the three joints is 7.7%, –5.8% and 31.0% relative to the SN curve Eurocode9/44. More details on the selection of the design SN curve as well as the structural SCF calculation for the joints can be referred to [8].

4.3. Influence of the weld geometry on the fatigue behaviour

It has been found in Figs. 6–8 that the weld geometry has influence on the stress concentration near the fatigue cracking point. It is therefore expected that the weld geometry would have an influence on the fatigue behaviour of the joints. Figs. 12–14 illustrate how the weld throat thickness and the weld toe angle correlate to the fatigue strength of each joint. The horizontal axis represents the fatigue life.

Table 3  
Structural stress concentration factors

Alt-1		Alt-2		Alt-3	
$\lambda$ (mm), $\theta$ , $a$ (mm)	SCF	$\lambda$ (mm), $\theta$ , $a$ (mm)	SCF	$\lambda$ (mm), $\theta$ , $a$ (mm)	SCF
8.09, 45, 5.72	1.46	8.81, 45, 6.23	1.34	7.35, 45, 5.20	1.61
7.74, 34, 4.33	1.45	8.18, 30, 4.09	1.29	4.64, 55, 3.80	1.58
6.12, 45, 4.33 <sup>a</sup>	1.44	5.78, 45, 4.09 <sup>a</sup>	1.27	5.37, 45, 3.80 <sup>a</sup>	1.51
4.70, 67, 4.33	1.39	4.77, 59, 4.09	1.26	6.46, 36, 3.80	1.49
4.41, 45, 3.12	1.38	3.82, 45, 2.70	1.23	3.82, 45, 2.70	1.47
Mean value	1.43	–	1.28	–	1.53
Standard deviation	0.04	–	0.04	–	0.06

<sup>a</sup> Mean values of the weld parameters.

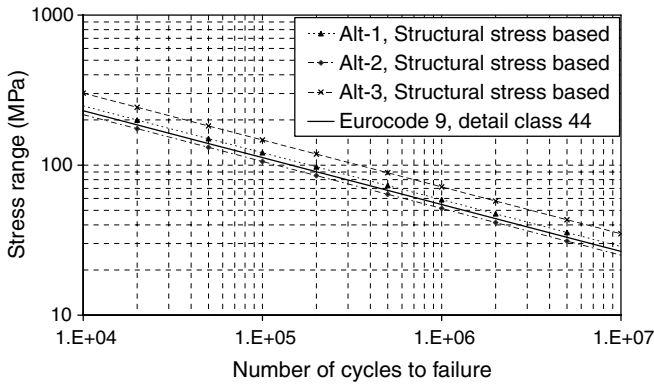


Fig. 11. Test data based on the structural stress range approach.

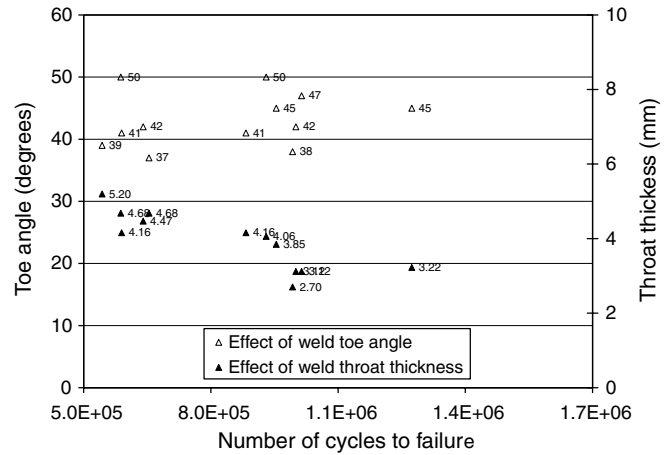


Fig. 14. Influence of the weld throat thickness and toe angle on fatigue strength of Alt-3.

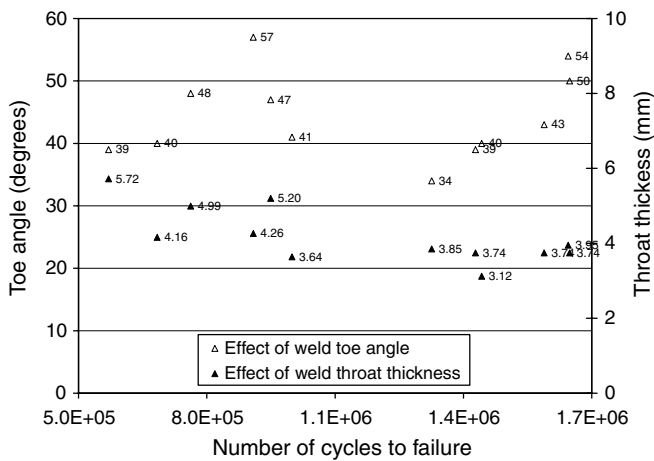


Fig. 12. Influence of the weld throat thickness and toe angle on fatigue strength of Alt-1.

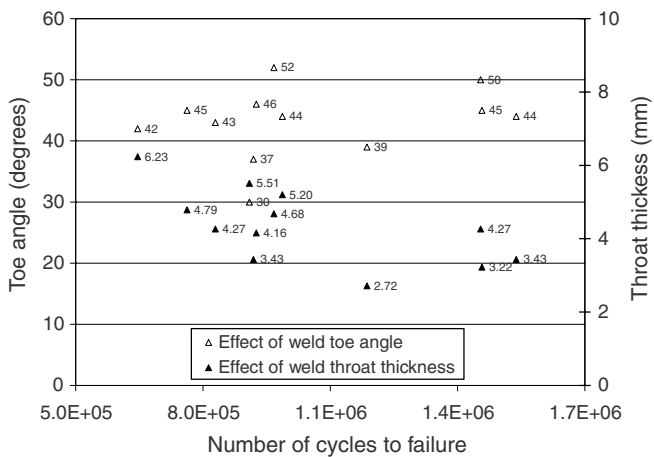


Fig. 13. Influence of the weld throat thickness and toe angle on fatigue strength of Alt-2.

The vertical axis to the left represents the weld toe angle ranging from 0° to 60° while to the left the weld throat thickness ranging from 0 to 6 mm. The numbers beside the empty (Δ) and solid (▲) triangles represent the measured weld toe angle and throat thickness, respectively.

#### 4.3.1. The influence of the weld throat thickness

Generally, an increase in the weld throat thickness causes a reduction in the fatigue strength for all the three types of joints although scatter exists. This correlates quite well with the findings in the stress concentration in Figs. 6–8 where it was stated that the increase of the weld throat thickness would cause larger stress concentration and will accordingly shorten the fatigue life of the joint. As an example, five (5) tests were recorded in the sequence of (weld toe angle, weld throat thickness, number of cycles to failure) for Alt-2 for a given weld toe angle range of  $40 \pm 1^\circ$  that were (40, 3.12, 1,442,736), (41, 3.64, 999,082), (39, 3.74, 1,428,156), (40, 4.16, 683,928) and (39, 5.72, 570,395). It is seen that number of cycles to failure decreased from 1,442,736 to 570,395 while increasing the weld throat thickness from 3.12 mm to 5.72 mm. The third record (39, 3.74, 1,428,156) was an exception that did not follow the trend is perhaps due to some uncertainties relating to many complex factors such as the welding and transportation, etc.

However, too much reduction on the size of the weld throat thickness should be avoided because that causes shorter fatigue life as illustrated by the figures where throat thickness 3.12 mm for Alt-1, 2.72 mm for Alt-2 and 2.70 mm for Alt-3 relates to a shorter fatigue life that is against the general trend. Too much reduction in the weld throat thickness may cause insufficient penetration of the weld into the parent material (box-stiffener). An additional local stress concentration caused by the insufficient weld penetration would have shortened the fatigue lives as recorded in the test.

Therefore, for any of the joint type, there exists an optimised range for the magnitude of the weld throat thickness and here it is roughly equal to 4 mm for all the joint types.

#### 4.3.2. The influence of the weld toe angle

For Alt-1 and Alt-2, the fatigue strength is increased by increasing the weld toe angle while keeping the weld throat thickness as constant. For example, the fatigue

lives for Alt-1 were recorded as 1,428,156, 1,588,764 and 1,648,224 cycles corresponding to the weld toe angles being equal to 39°, 43°, and 50° while the weld throat thickness is equal to 3.74 mm for all three test cases, respectively. This agrees well with the conclusions from Figs. 6 and 7 where it was said that for a given weld throat thickness, an increase of weld toe angle results in a reduction of stress level.

For Alt-3, it was found in Fig. 8 that for a constant weld throat thickness, an increase of the weld toe angle yields an increase of stress level. One would therefore expect a reduction in fatigue strength by increasing the weld toe angle. However, it is not always true as found in Fig. 14. For example, the fatigue life reduces from 653,988 to 587,537 cycles when increasing the weld toe angle from 37° to 50° while keeping the weld toe thickness as 4.68 mm. For another two test cases, the fatigue life increases from 1,000,606 to 1,013,806 cycles when increasing the weld toe angle from 42° to 47° while keeping the weld toe thickness as 3.12 mm.

The formation of the weld toe angle is very much depended on the welding procedure and cooling time history and other factors. In practice, the weld throat thickness is the controlling parameter in the welding process. Therefore, the findings for the influence of the weld toe throat thickness can generally be extended to other welded joints while care should be taken when the conclusion from the effect of weld toe angle is applied to other joints.

## 5. Conclusions

The following conclusions can be drawn based on the above study:

The welding procedure plays a determinant role in the fatigue strength of the box-stiffener/web frame connections. In spite of costs saving by intermediate welding in Alt-1 and Alt-2, these two types of joints should be avoided otherwise detrimental defects introduced by start and stop in the weldment which significantly reduce the fatigue strength of the joint, despite their limited nominal stress.

The nominal design SN curve Eurocode9/31 is conservative to all the three joints by means of the nominal stress range approach. However, Alt-2 failed to satisfy the structural SN curve Eurocode9/44, nevertheless, this curve is more conservative to Alt-1 and Alt-3 compared to the nominal stress range approach.

The smaller the size of the fillet weldment (weld throat thickness) is, the longer the fatigue life of the joint will be. Therefore, larger-sized weldment should be avoided while in practice very tiny weldment should also be avoided to maintain sufficient weld penetration.

## Acknowledgements

The study here was a part of the project “Aluminium in Ships” funded by Hydro Aluminium Maritime a.s. The authors gratefully acknowledge the financial support and especially the support provided by Jon Erslund and Eirik Smedstad to this work. Thanks are also extended to engineers Roar Skjetne, Erik Fleischer and technician Johan Terje Lines who provided on-time help when the tests were performed in the Structural Laboratory at the Marine Technology Centre.

## References

- [1] The Aluminium Association, Aluminium design manual. Washington, US, 1994.
- [2] Pettersen N, Wilklund KM. Det Norske Veritas requirements for direct calculation methods of high speed and light crafts. In fifth international conference on fast sea transportation, FAST'99, 399–407, New Jersey, USA, 1999.
- [3] Heggelund SE, Tveiten BW, Moan T. Fatigue analysis of high speed aluminium catamarans. In The third international forum on aluminium ships, Kent, UK: 1998.
- [4] Engesvik KM, Moan T. Probabilistic analysis of the uncertainties in the fatigue capacity of welded joints. Eng Frac Mech 1983;18(4):743–62.
- [5] Ye N, Moan T. Fatigue and static behaviour of aluminium box-stiffener lap joints. Int J Fatigue 2002;24(5):581–9.
- [6] Hobbacher A. Recommendations for fatigue design of welded joints and components. ISO standard proposal, Technical Report IIW doc. XIII-1539-96/XV-845-96, IIW, 1996.
- [7] Ye N, Moan T. Improving fatigue life for aluminium cruciform joints by weld toe grinding, Fatigue Fract Eng Mater Struct, in press.
- [8] Ye N, Moan T, Tveiten BW. Fatigue analysis of aluminium box-stiffener/web frame connections by nominal, structural, and notch stress range approaches. In: Proceedings of the eighth international conference on fatigue, Stockholm, Sweden, 2002.
- [9] Eurocode 9. Design of aluminium structures. Part 2 Structures susceptible to fatigue. CEN – European committee for Standardisation, Brussels, Belgium, 1998.
- [10] HSE, Offshore installations: guidance on design, construction and certification, London, 1995.
- [11] Hobbacher A. Recommendations for fatigue design of welded joints and components. Iso standard proposal 1996.
- [12] Tveiten BW, Moan T. Determination of structural stress for fatigue assessment of welded aluminium ship details. Int J Marine Struc 2000;13:189–212.
- [13] Fricke W. Recommended hot-spot analysis procedure for structural details of FPSOs and ships based on round-robin FE analysis. Stavanger, Norway: ISOPE; 2001.
- [14] Tveiten BW, Ye N, Moan T. Recommendations on the selection of structural stress design S–N curves for the fatigue assessment of welded aluminium structures. In Proceedings of the eighth international congress on fatigue, Stockholm, Sweden, 2002.
- [15] DNV-Det Norske Veritas, Fatigue strength analysis of offshore steel structures. RP-C203, Høvik, Norway, 2000.
- [16] Ye N, Moan T, Tveiten BW. Fatigue analysis of aluminium box-stiffener lap joints by nominal, structural and notch stress range approaches. In Proceedings of PRADS'2001, Shanghai, China, 2001.

## **Paper 3**

# **Improving Fatigue Life for Aluminium Cruciform Joints by Weld Toe Grinding**

Naiquan Ye and Torgeir Moan

Department of Marine Structures, Faculty of Marine  
Technology, Norwegian University of Science and  
Technology, Trondheim, Norway

Accepted by Fatigue and Fracture of Engineering Materials and  
Structures, Decision made on 22-November-2007



# Improving Fatigue Life for Aluminium Cruciform Joints

## by Weld Toe Grinding

N. Ye and T. Moan

*Institute of Marine Technology, Faculty of Civil Engineering, Norwegian University of Science and Technology, NO-7491 Trondheim, Norway*

### Abstract

The increase of the fatigue life in aluminium cruciform joints by weld toe grinding was in the focus of the current study. The test data are presented by both a nominal stress range approach and by the more refined structural and notch stress range approaches. The influence of the weld toe angle, weld leg length, and weld toe radius on the structural and notch stress concentration factor was systematically studied by means of finite element analysis. Experimental data based on eighteen (18) pieces of as-welded and thirteen (13) pieces of weld toe ground specimens made of 12 mm thick plates showed a significant improvement in fatigue life in aluminium by grinding the weld toe and confirmed the permitted improvement in fatigue life by design codes.

**Keywords:** fatigue life; aluminium alloy; weld; stress concentration factor

### Nomenclature

$C_1, C_2, C_3,$  and  $C_4$  = possible fatigue cracking sites

$d$  = weld toe grinding depth in mm

$K_g$  = structural stress concentration factor

$K$  = notch stress concentration factor

$t$  = thickness in mm

$\lambda$  = weld leg length in mm

$\theta$  = weld toe angle in degrees

$\rho$  = weld toe radius in mm

$\sigma_{\text{nominal}}$  = nominal stress

$\sigma_{\text{structural}}$  = structural stress

$\sigma_{\text{notch}}$  = notch stress

## Introduction

The fatigue life of a welded joint is substantially reduced compared to its parent material due to the presence of inherent defects along the fusion line of the weld. In addition to the defects, the weld geometry has also been reported to be a determining factor since fatigue has been proven to be a highly localised phenomenon. A probabilistic uncertainty analysis by Engesvik and Moan<sup>1</sup> using steel joints showed that weld geometry was the greatest contributor as compared to other factors, such as initial crack size and material parameters, on the scatter of constant amplitude fatigue life of welded joints. The reduction factors pertaining to fatigue life can be generally classified into two groups: 1) the weld geometry and 2) the imperfections caused by the welding procedure. The imperfections include crack-like defects along the weld path and the tensile residual stress in the weld region.

Sometimes, often late in the design process or during the service time of a structure, it is necessary to increase the fatigue life of a particular joint detail to extend the service life of the structure through an improvement method. The improvement methods are normally classified as: 1) weld geometry modification methods that reduce stress concentration and 2) residual stress methods that introduce a compressive stress field in the region where cracks are likely to be initiated.<sup>2</sup> The application of various methods, such as grinding, peening, and tungsten gas dressing, has been reported extensively in the literature for decades.<sup>3-5</sup> The post-weld improvement of steel and aluminium structures was summarised most recently in an International Institute of Welding (IIW) recommendation by Haagensen and Maddox.<sup>6</sup> However, the effort devoted to aluminium structures is still insufficient compared to steel structures.

The grinding technique is a widely accepted fatigue life improvement method due to the reliability and ease by which it can be performed. The main purpose of weld toe grinding is to reintroduce a fatigue initiation period by removing possible defects at the weld toe. The general view today is that a crack initiation period in “as-welded” steel joints is insignificant due to the existing weld defects (i.e., slag intrusions at the fusion line), which allow the crack growth to initiate very early in the fatigue life. However, the same is not absolutely agreed on for aluminum welded structures, where studies have indicated that the fatigue initiation period may account for a larger portion of the total fatigue life. For this reason, it is argued that the crack initiation period becomes more dominant for aluminum welds than for steel welds. This implies that the weld toe grinding method for aluminum weldments could have a lesser effect on the improvement of fatigue life compared to that of steel joints. In addition, weld toe grinding changes the local weld toe geometry, which alters the stress concentration factor (SCF). It is therefore an open question whether the weld profile of aluminium and steel welds is comparable so that the modification of the weld notch by the grinding process has a comparable effect on the fatigue life.

Some studies presented in the literature have indicated that the effect of grinding on steel and aluminium welds may show different improvement potentials.<sup>7, 8</sup> Tveiten<sup>9</sup> reported that little improvement was achieved by grinding the weld toe of an aluminium flat bar with a welded bracket. However, in a summary of fatigue improvement methods, Haagensen and Maddox<sup>6</sup> suggested that approximately 50% of fatigue life improvement could be targeted by using one or a combination of several improvement methods.



The main purpose of the current study was to further investigate the benefit of toe grinding as applied in welded aluminium joints and thereby contribute more data for design standards. In addition to that, fatigue assessment approaches based on local stresses, the most discussed issues recently, were evaluated in presenting the test results.

## **Experimental program**

### ***Specimen descriptions and weld profiles***

Thirty-one (31) specimens made of aluminium alloy 5083 were involved in the test program, among which eighteen (18) specimens were as-welded and the rest were toe-ground. Fig. 1 shows photo copies of the test specimen. Burr grinding technique was used to obtain grooves perpendicular to the weld line. The specimens were 206 mm wide, with the other geometrical properties are illustrated in Fig. 3 (a).

Weld geometry has a great influence on the fatigue behaviour of welded joints. The weld profiles were first reproduced by duplication material as shown in Fig. 2. Five (5) slices evenly along the weld profile were made and magnified by a microscope camera and the weld parameters were measured based on the magnified photos. Figs. 3(b) and 3(c) show typical as-welded and toe-ground weld profiles. Table 1 is a list of the corresponding measured data. A study by Engesvik and Moan<sup>1</sup> indicated that among the weld geometrical parameters, the weld toe radius and the weld toe angle affect more than the other factors on fatigue performance. In addition, Ye et al.<sup>10</sup> found that the weld leg length,  $\lambda$ , had a great influence on the stress concentration for a box-stiffener lap joint. Therefore, the effect of these three parameters on the structural and notch SCFs were investigated in this study.

It should also be emphasized that fatigue cracking for a cruciform joint may occur at any of the four possible locations from  $C_1$  to  $C_4$  (Fig. 3) as a result of tensile residual stresses introduced by welding. However, by introducing a load/stress ratio of 0.44, only pure tensile stresses occurred at  $C_1$  and  $C_2$  in the test program and it was found that all fatigue cracking occurred at either  $C_1$  or  $C_2$ .

It should also be pointed out that the weld toe for an as-welded specimen can be easily detected at point C in Fig. 3(b). However, the original weld toe is removed by grinding and two possible cracking points are introduced, specifically A and B, as shown in Fig. 3(c). The weld toe usually refers to a melting line between the weld material and the parent material. According to this definition, therefore, point A would become the new weld toe. However, tests have shown that fatigue cracking originating from point B is the deepest point after grinding. In this study, point B was used for the calculation of the stress concentration factors for the toe-ground joint.

After grinding, the mean weld toe radius is increased by about two and half times and the standard deviation is greatly reduced. The weld toe angle is increased by grinding, however, the weld leg length is reduced by the material removal at the weld toe. The mean grinding depth is about 0.8 mm into the thickness and this depth is the least requirement in the IIW documentation to assure satisfactory fatigue life improvement.<sup>6</sup>

### **Stress and fatigue design curves**

Stress at the weld toe is usually raised by the structural geometry as well as by the weld itself. The structural and notch stresses are correspondingly defined to capture stress raising factors relating to the structural and weld geometry. As a consequence, different fatigue assessment methods have been developed depending on the stress range used in design SN curves. Fig. 4 schematically illustrates how these stresses are defined for a general joint detail.<sup>11</sup> Fig. 5 shows how different stress definitions are used together with corresponding fatigue design SN curves for welded joints. The more accurate the stress calculation is, the fewer design SN curves are needed. If no other uncertainties than the weld exists, the notch stress based design SN curve will be identical to the base material SN curve.

### **Nominal stress and design SN curves**

The failure of the non-load carrying fillet welded cruciform joints occurred at the weld toe. The nominal stress range at the weld toe can be obtained either by simply using elastic beam theory or coarse finite element analysis. For complex joint details, difficulty may arise in calculating the nominal stress and care should be taken to use the calculated nominal stress in the fatigue analysis.<sup>12</sup>

For the three point bending load case [Fig. 3 (a)] in this study, the nominal stress was simply obtained by a beam solution under bending, i.e.,  $\sigma = M/I \cdot y$ , where M, I, and y represent the bending moment, inertia moment, and the distance of the interested point to the neutral axis of the section, respectively. The difference between the analytical solution and the measured value by strain gauge was less than 2% for both the as-welded and toe-ground joints. The nominal stress applied to the test specimen was 37.7 MPa. It should be noted that the thickness reduction effect of the toe-ground joint was not taken into account while calculating the nominal stress, rather it was reflected in the SCFs.

The detail classes for the investigated cruciform joints from different codes based on nominal stress are summarized in Table 2 and it is seen that the lowest detail class for a non-load carrying cruciform joint was 28, given by Eurocode 9<sup>18</sup> and the IIW,<sup>14</sup> however, a clear indication of as-welded condition is only specified by the IIW. The highest class, 36, is given by both the IIW and Aluminium Association<sup>20</sup> and toe-grinding is clearly indicated by the IIW. It should be noted that the IIW is the only code in which the as-welded and toe-ground joints are clearly classified into two detail classes, 28 for as-welded joints, and 36 for ground joints; as a consequence, there is an improvement of approximately 29% in terms of stress range at a given number of cycles. In other words, by applying the above SN curve equation, the fatigue life in terms of cycles at a given stress range level for a toe-ground joint is about twice that of the as-welded joint.

### **Structural stress and design SN curves**

The nominal stress only reflects the response of the joint to global forces. A traditional fatigue assessment uses this stress as a design stress by including all the other factors, such as the effect of the structural geometry and the weld geometry implicitly in the design of the SN curves. Some more refined fatigue assessment methods have been developed recently based on

a deeper understanding of the influence of the structural geometry and weld on the stress at the fatigue cracking area, such as the weld toe.

The structural stress range approach has recently been one of the most interesting methods by which structural stress is used to capture the stress raising factor due to structural geometry, however, the contribution of the weld to stress concentration is excluded by performing an extrapolation to the weld toe within the structural geometry affected zone, as shown in Fig. 4. Various methods have been proposed, however, a universal method that can be applied to all kinds of joint types is still needed. The structural SCF can be obtained either by strain gauge measurements or finite element analysis; the latter method was used in this study to calculate the stress concentration. A full model was built in the analysis. However, only a quarter portion of the full finite element models, as well as the sub-models, are shown in Fig. 6 for the sake of symmetry.

The structural stress range approach is designed so that the stress raising effects due to the weld can be excluded from the structural SCF. It has been agreed based on experience that the influence of the weld on the stress concentration at the weld toe is confined to a short distance of  $0.3-0.5t$ , i.e., 3.6-6 mm for the specimens studied herein. Three representative structural SCF calculation methods were investigated in this study for the as-welded specimens. Method 1 is a linear extrapolation method in which the stresses at  $0.4t$  and  $1.0t$  were used to perform the extrapolation. Niemi<sup>13</sup> reported this method after investigating a gusset attachment joint and this is used as a standard method by IIW<sup>14</sup>. Method 2 is another linear extrapolation method used by DNV<sup>15, 16</sup> in which the points  $0.5t$  and  $1.5t$  were used. No extrapolation was required for Method 3, rather the stress value at  $0.5t$  was taken as the structural stress. This method is used by Lloyd's Register. It is seen that in the aforementioned methods, the distance of the leading point is either  $0.4t$  or  $0.5t$ . However, this distance is dependent on the joint type, as reported by Tveiten and Moan.<sup>17</sup>

Fig. 7 shows typical stress distributions near the fatigue cracking point.. It should be noted that different origins were used for the illustration in order to compare the SCFs at the fatigue cracking point. The origins refer to C (weld toe) for the as-welded joints and the deepest point B for the toe-ground joints, as shown in Figs. 3(b) and 3(c).

The structural stress range approach is based on an assumption and observation that there exists a consistent stress gradient near the weld toe, as shown in Fig. 4. The stress gradient for the as-welded joint, as shown in Fig. 7, reveals the same pattern, therefore it was reasonable to apply the structural stress range approach. However, as also shown in Fig. 7, the toe grinding caused redistribution of the stress adjacent to the cracking point B in Fig. 3(c). A consistently increasing stress gradient no longer appeared. This made the application of the structural stress range approach to the toe-ground joint more difficult or even impossible. For instance, a structural SCF of 1.02 was obtained if the stresses at  $0.5t$  and  $1.5t$  were used as the basis for a linear extrapolation. This value was unreasonably small compared to the as-welded cases, which is also in contrast to experience. For instance, a recent IIW documentation pointed out that grinding may introduce further stress concentration at the weld toe<sup>6</sup>. Therefore, the structural SCF appears unable to capture the real stress concentration at the fatigue cracking point.

Very little information regarding the influence of weld parameters on structural SCFs is available in the open literature. Moreover, no public literature exists related to the effect of

weld parameters for a toe-ground joint when the structural stress range approach is used to present the fatigue test results.

The weld toe radius, weld leg length, and weld toe angle were modelled in the FEM. In each case, the minimum, mean, and maximum values of each of the parameters were chosen to investigate the influence of that parameter, while the mean values of the other parameters were utilized in the model. The results are shown in Tables 3, 4 and 5, respectively.

It is shown in Tables 3, 4 and 5 that, in general, the closer the distance of the leading point in the extrapolation methods to the weld toe, the higher the structural SCF. It can be easily understood that extrapolation points at a short distance from the weld toe may bring the notch effect into the extrapolation procedure and result in a higher stress value at the leading point. The distance necessary to avoid this from occurring has been further clarified by Tveiten and Moan.<sup>17</sup> The extrapolation points must fall within the structural geometry affected zone (Fig. 4) to obtain a reasonable structural SCF. A procedure to calibrate this structural geometry affected zone and the notch affected zone has also proposed.

The change of weld parameters had little influence on the structural SCFs by all the methods used for the as-welded joint, and the use of different methods did not cause a significant change in the structural SCFs.

Fatigue assessment based on structural stress range has been used in the design of steel tubular joints since the 1970s.<sup>23</sup> The structural stress,  $\sigma_{\text{structural}}=K_g \times \sigma_{\text{nominal}}$ , is taken as the design stress, where  $K_g$  represents the structural SCF. However, the derivation of a universal structural SCF calculation method and consistent design SN curves are still needed for both steel and aluminium plate structures. Moreover, rather limited data for aluminium structures are available up to now.

Eurocode 9 issued six structural stress design SN curves.<sup>18</sup> for aluminium welded joints. The choice of SN curve is dependent on the thickness of the stressed member of the structure, for instance, detail class 35 is proposed for structures with the thickness of a stressed member between 10 and 15 mm. However, no corresponding structural stress calculation process is specified in the code. A detail class of 40 has been accepted, to some extent, as a suitable design SN curve<sup>24, 25</sup> for butt and fillet welded aluminium joints of relatively thin plates (up to 6 mm) failing from the weld toe location. A thickness penalty factor was suggested by Niemi<sup>13</sup> to further apply the detail class 40 to the structures with a thickness exceeding 6 mm. In the case of a 12 mm thickness, a modified detail class will be approximately 35. Tveiten et al.<sup>26</sup> commented that the use of the penalty factor should be further investigated since the reduction in design fatigue strength would be unacceptably large once the large thickness appears. More description on the choice of a suitable structural stress design SN curve was summarised recently by Tveiten et al.<sup>26</sup>

### Notch stress and design SN curves

The notch stress concentration factor included not only the structural geometry related stress raising factors, but also the stress raising factors due to the weld. This factor was assessed by direct finite element calculation by means of the sub-modelling technique (Fig. 6). The notch refers to the weld toe for the as-welded joints (point C in Fig. 3 (b)) and the deepest point in the

ground profile (point B in Fig. 3 (c)). It should be pointed out that no reduction of thickness for the ground joints was applied in the calculation of the nominal stress because it had already been captured in the stresses obtained by FE analysis. The results are summarised in Tables 6, 7 and 8. 20-nodes solid elements were used with an element size of about  $\frac{1}{4}$  of the weld toe radius. Fig. 14 shows an example of the mesh detail for the minimum weld toe radius  $\rho=0.1$  mm for the as-welded joint. Element size adjacent to the weld toe on both the normal and tangential directions is approximately 0.02 mm.

It was found, in principle, that the notch SCFs for the toe-ground joint were greater than those of the as-welded joint when the weld toe radius exceeds the mean value of each category.

The notch SCF can also be roughly estimated according to the equation  $K = 1 + 0.21(\tan \theta)^{1/6}(t/\rho)^{1/2}$  for cruciform joints under bending, in which  $t$  represents the parent plate thickness while  $\theta$  and  $\rho$  have the same meaning as indicated in Fig. 3, as suggested by Yung and Lawrence<sup>18</sup>. For instance, the notch SCF will be 3.38, 1.67 and 1.37 for weld toe radius  $\rho=0.1, 1.3$  and  $4.2$  mm, respectively ( $\lambda=9.0$  mm,  $\theta=52.1$  degree). The FE results are consistent to the values obtained by the empirical equation. Figs. 3 and 6 showed that a “notch” was introduced by grinding that caused more severe stress concentration compared to the as-welded joint. This is revealed in Fig. 7 as well. Moreover, it was also found that the change of weld parameters did not have as significant an influence on the notch SCFs as for the as-welded joint.

Table 6 shows that the increase of the weld toe radius for the toe-ground joint caused a reduction of the notch SCFs for the same reason as the influence of the weld toe radius on the structural SCFs. This also confirms the IIW requirements that the new weld toe radius should not be too small, otherwise a sharp discontinuity may appear accompanied by a high SCF.<sup>6</sup> The change of the other two parameters had little influence on the notch SCFs for the toe-ground joint, as shown in Tables 7 and 8.

The notch stress,  $\sigma_{\text{notch}}=K \times \sigma_{\text{nominal}}$  is taken as the design stress in the notch stress range fatigue assessment method, where  $K$  represents the notch SCF.

Four notch stress based SN curves were issued by DNV<sup>1</sup> among which curve I is base material, curve II is for welded joints, and the remainder is for a welded joint in corrosive environment.

## ***Fatigue tests and results***

### **Test set-up**

Fig. 3 (a) is an illustration of the test set-up of three point bending. The test was carried out at room temperature with a load frequency of 12 Hz by a constant sinusoidal waveform. A random input signal and its corresponding output signal were compared to assure that no waveform peak “cut-off” occurred in the testing program as shown in Fig. 8. Fig. 9 shows the measured stress agreed quite well with the beam theory solution. The fatigue life was recorded when the specimen was fully cracked through the thickness of the plate.

## Test data

The test data are summarized in Table 9. The fatigue life in terms of the number of cycles was recorded when a full thickness crack developed. Eighteen (18) as-welded and thirteen (13) toe-ground specimens were tested.

## Fatigue analysis based on nominal stress

The IIW SN curves, 28 and 36, were chosen in this study to compare the test data for the as-welded and toe-ground joints in Figs. 10 and 11. The nominal stress applied to the test specimen was 37.7 MPa as can be seen in those two figures.

It seems that that the tested data agreed quite well with the IIW SN curves. The fatigue strength of the as-welded and toe-ground joints was approximately 2.4% and 1.3% below the SN curves, 28 and 36, respectively. The grinding improved the fatigue strength by about 30% in terms of stress range, which was nearly equivalent to a doubling in fatigue life improvement in terms of the number of cycles. This occurred despite the fact that the notch SCF of the toe-ground joint was generally greater than the as-welded joint. The contribution of grinding in improving fatigue life is therefore primarily due to the removal of the defects. The grinding depth is therefore the decisive parameter in determining the effect of grinding. This is also reflected by the test data in Fig. 11 where a rather low fatigue life was recorded and the corresponding grinding depth was found to be the smallest one, that is 0.2 mm.

It should be mentioned that, as indicated in Fig. 3(c), the original weld toe disappeared after grinding and the fatigue cracking was found to be located at point B, which is the deepest point in the ground profile. The effect of the thickness reduction on the determination of the nominal stress was not taken into account when presenting the data against the nominal SN curves. This effect should have been embedded in the specified SN curves for the toe-ground joints. The grinding effect will tend to be more significantly conservative if the nominal stress is corrected by the thickness reduction, i.e., a higher nominal stress was used in the presentation of the test data.

It should also be noted that the standard deviations of  $\log N$  for the as-welded and toe-ground joints were 0.09 and 0.11, which indicates that the grinding did not reduce the scatter of the test data, rather the scatter was slightly expanded. This was probably due to the scatter of the grinding depth, which was from 0.2-1.6 mm, as shown in Table 1. An insufficient grinding depth may cancel off the fatigue life improvement effect compared to those sufficiently ground specimens. As can be seen in Table 9, the lowest fatigue life of toe-ground specimen did not improve significantly compared to the mean fatigue life of the as-welded specimens.

## Fatigue analysis based on structural stress

The test data of the as-welded specimens are presented against the Eurocode 9 SN curve 35 in Fig. 12. The structural SCFs correspond to the mean weld parameters. The as-welded joint falls quite below the SN curve 35 because the structural SCFs of the as-welded joint is low as shown in Table 2. It should be remembered that the application of the structural stress range approach to the toe-ground joint can bring uncertainties because there is no consistent stress gradient towards the fatigue cracking point.

## Fatigue analysis based on notch stress

Curve II is assigned to the cruciform joint and Fig. 13 is an illustration of the test data against this curve. The notch SCFs are taken from the direct calculation by FEA using a sub-model technique and correspond to the mean values of the weld parameters. It should also be noted that no indication of the selection of different SN curves for the as-welded and toe-ground joints was given in the code. Curve II from DNV<sup>1</sup> was found to be conservative to the toe-ground joint. The improvement factoring fatigue life was about 34% in terms of stress range at a specified fatigue life, i.e., two million cycles. The as-welded joint based on the calculated notch SCF did not satisfy the curve II while the margin of stress range at two million cycles was less than 3%. If the default notch SCF of 2.4 in the DNV classification notes<sup>1</sup> was used, curve II would be more conservative for the two joint types because 2.4 was higher than the notch SCFs in Table 8.

Due to difficulties in applying both the nominal and structural stress range approaches to the toe-ground joint, the notch stress range approach based on the notch stress at the fatigue cracking point appeared to be more reasonable to assess its fatigue performance. However, the application was accompanied by a time-consuming SCF calculation.

The notch SCFs of the ground joints were generally greater than that of the as-welded joints as shown in the Tables 6-8. For instance, the SCFs corresponding to the mean statistical weld parameters were 1.91 for the toe ground joints and 1.83 for the as-welded joints. The difference of the notch SCFs is quite marginal. This may explain why no distinction was given in the design codes in choosing notch stress based design SN curves for as-welded and toe-ground joints. The fatigue performance for the as-welded and toe-ground joints would expect to be similar if the stress concentration factor plays a decisive role. However, the test results were contradictory to the prediction by indicating that the toe-ground joints had a nearly doubled fatigue life compared to the as-welded joints. The effect of the relatively higher stress concentration introduced by the grinding for the toe ground joints was compensated by the removal of the defects introduced by welding. By assuming the slope of the fatigue curve to be 3.0, the stress range level at any given number of cycles of the toe-ground joint design curve should be at least be shifted above the as-welded joints by about 30 per cent. This is consistent with the IIW<sup>14</sup> which clearly assigns different nominal stress design curves for the as-welded and toe-ground joints and the increase of the stress level at any given number of cycles is also about 30%, as discussed in previous sections.

In addition, the effect of grinding depth on the notch SCF was further studied by keeping the weld leg length  $\lambda=9.0$  mm, weld toe angle  $\theta=72.9$  degrees and weld toe radius  $\rho=3.2$  mm. Fig. 15 shows that the notch SCF increases nearly linearly proportional to the increase of the grinding depth. Therefore, excessive removal of the parent material by grinding should be prohibited to avoid further increase of the stress raising.

## Conclusions

The following conclusions can be drawn based on the stress analysis and fatigue tests, which corresponds very well to the IIW recommendation:<sup>6</sup> 1) the weld toe grinding significantly improved the fatigue life of the cruciform joint based on a nominal stress range approach and

2) a near doubling of the fatigue life was observed in terms of the number of cycles for the toe-ground joint.

The test data agreed quite well with the IIW nominal SN curve 28 for the as-welded joints and 36 for the toe ground joints.

The weld parameters had little influence on the structural SCFs for the as-welded joint.

The Eurocode structural SN curve, 35, was found to be non-conservative for the as-welded joints. The structural stress approach appears to be not applicable to toe-ground joints due to the stress redistribution caused by the new weld profile after grinding.

The notch SCFs based on FE analysis of the as-welded joints were generally below that of the toe-ground joints, while the latter one had better fatigue performance than the former one. Therefore, the defects introduced by the welding procedure played a decisive role in determining the fatigue behaviour of the welded joints. The removal of those defects by grinding significantly improved the fatigue life of the joints.

The DNV notch SCFs of the as-welded joints did not vary with the change of the weld parameters. A larger weld toe radius caused a reduction in the notch SCFs for the toe-ground joints, while other parameters did not affect the value appreciably. It is also important to point out that the grinding depth should exceed a lower limit, for instance 0.8 mm, while within a reasonable upper limit to avoid further stress concentration, so that the defects can be removed with certainty and to achieve a reasonable fatigue life improvement. The notch SN curve II was found to be conservative to the toe-ground joints with a large margin. The as-welded joints failed to meet the requirement of the design curve II while only with a small margin. A default notch SCF of 2.4, as suggested by DNV,<sup>1</sup> will satisfy both joints with the specified SN curve II.

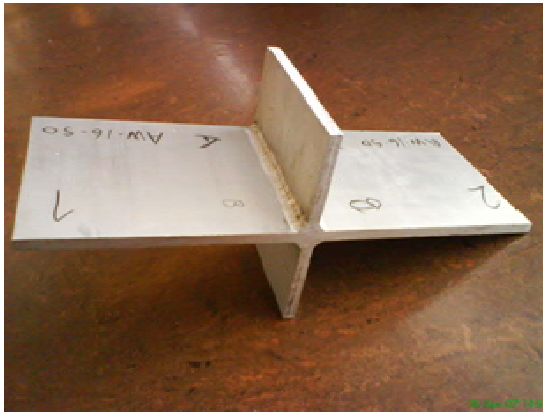
## References

1. Engesvik, K. M., Moan, T. (1983). Probabilistic analysis of the uncertainties in the fatigue capacity of welded joints. *Eng. Frac. Mech.*, 18(4), 743-762.
2. Haagenen, P. J. (1994). Effectiveness of grinding and peening techniques for fatigue life extension of welded joints. *OMAE-Vol. III, Material Engineering*, 121-127.
3. Cledwyn-Davies, D. N. (1954). *The Effect of Grinding on the Fatigue Strength of Steels*. Institution of Mechanical Engineers, London.
4. Watkinson, F., et al. (1970). The fatigue strength of welded joints in high strength steels and methods for its improvement. *Proc. Conf. On Fatigue of Welded Structures*, 97-113, Brighton.
5. Fisher, J. W., Dexter, R. J. (1993). Weld improvement and repair for fatigue life extension. *OMAE-Vol. III, Material Engineering*, 875-881.
6. Haagenen, P. J., Maddox, S. J. (2004). Recommendations on Post Weld Improvement for Steel and Aluminium Structures. *Doc.IIW-XIII-1815-00*, Rev. 5.
7. Smith, I.F.C. and Smith, R.A. (1982). Defects and crack shape development in fillet welded joints. *Fatigue Eng. Mater. Struct.*, 5(2), 151-165.

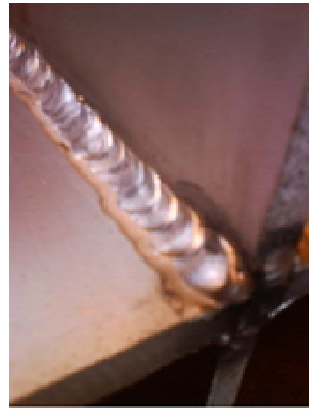


8. Valaire, B. (1993). Optimisation of weld toe burr grinding to improve fatigue life, *OMAE-Vol. III\_B, Material Engineering*, 869-873.
9. Tveiten, B. W. (1999). *Fatigue Assessment of Welded Aluminium Ship Details*. Doctoral thesis, Department of Marine Structures, Norwegian University of Science and Technology, Trondheim, Norway.
10. Ye, N., Moan, T. (2002). Fatigue and static behaviour of aluminium box-stiffener lap joints. *Int. J. Fatigue*, 39, 581-589.
11. Ye, N., Moan, T. and Tveiten, B. W. (2001). Fatigue analysis of aluminium box-stiffener lap joints by nominal, structural, and notch stress range approaches. *Proceedings of the 8<sup>th</sup> International Symposium on Practical Design of Ships and Other Floating Structures*. Shanghai, China.
12. Niemi, E. Fricke, W. and Maddox, S. J. (2006). *Fatigue Analysis of Welded Components – Designer’s Guide to the Hot-Spot Approach*, Woodhead Publ., Cambridge.
13. Niemi, E., (1995). *Recommendations Concerning Stress Determination for Fatigue Analysis of Welded Components*, Abington Publ., Abington, Cambridge.
14. Hobbacher, A. (2003). Recommendations for Fatigue Design of Welded Joints and Components. *Doc. XIII-1965-03/XVII127-03*, Paris
15. DNV-Det Norske Veritas (2000). *Fatigue Strength Analysis of Offshore Steel Structures*. Høvik, Norway.
16. DNV-Det Norske Veritas (1993). *Fatigue Assessment in Ship Structures*, No 93-0432, Høvik, Norway.
17. Tveiten, B. W., Moan, T. (2000). Determination of structural stress for fatigue assessment of welded aluminium ship details. *J. of Marine Struct.*, 13(3), 189-212.
18. Yung, J.Y. and Lawrence, F.V. (1985). Analytical and graphical aids for the fatigue design of weldments. *Fatigue Fract. Eng. Mater. Struct.*, 8(3), 223-241.
19. Eurocode 9 (1998). *Design of aluminium structures-Part 2: Structures susceptible to fatigue*, EC-ENV 1999-2, CEN, Brussels.
20. The Aluminium Association (1994). *Aluminium Design Manual*. Washington, D.C., U.S.A.
21. BS-British Standard (1991). *BS 8118, part 1*. England.
22. ECCS (1992). *European Recommendations for Aluminium Alloy Structures Fatigue Design*, first edition.
23. HSE (1995). *Offshore Installations: Guidance on Design, Construction and Certification*, London.
24. Partanen, T., Niemi, E. (1999). Hot spot S-N curves based on fatigue tests of small MIG-welded aluminium specimens, *Welding in the World*, 43(1), 16-22.
25. Maddox, S. J. (2001). Hot-spot fatigue data for welded steel and aluminium as a basis for design, *Doc.IIW-XIII-1900-01*, IIW.

26. Tveiten, B.W. et al. (2002). Recommendations on the selection of structural stress design S-N curves for the fatigue assessment of welded aluminium structures, *The 8th International Fatigue Congress*, Stockholm, Sweden.
27. DNV-Det Norske Veritas (1997). *Fatigue Analysis of High Speed and Light Craft*, Classification Notes, CN30.9, Høvik, Norway.



(a)



(b)



(c)

**Fig. 1 Test Specimen (a) Overview; (b) as-welded ; (c) toe-ground**

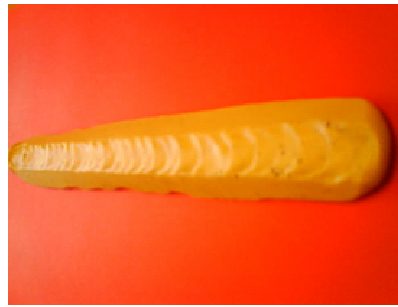
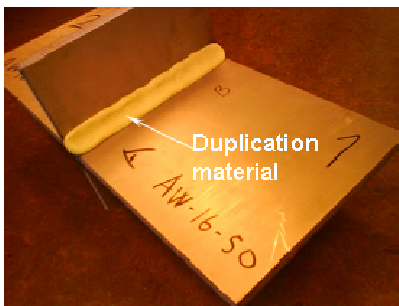


**Fig. 2 Duplication of the weld profile**

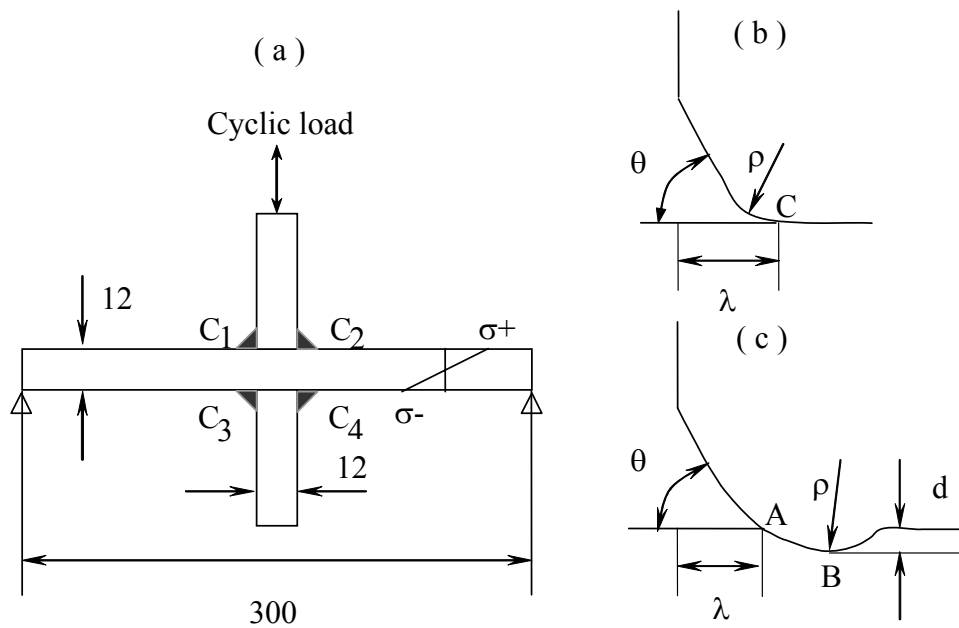


**Fig. 3 (a) Geometrical properties (mm); (b) as-welded toe profile; (c) weld toe profile after grinding**

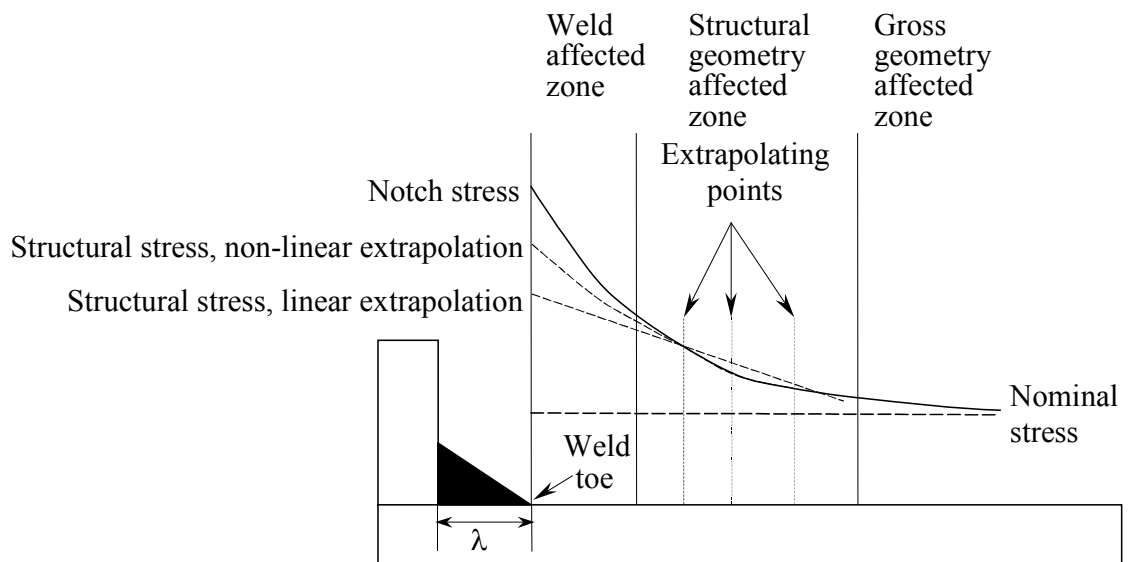


**Fig. 4 Stress components at the weld toe**

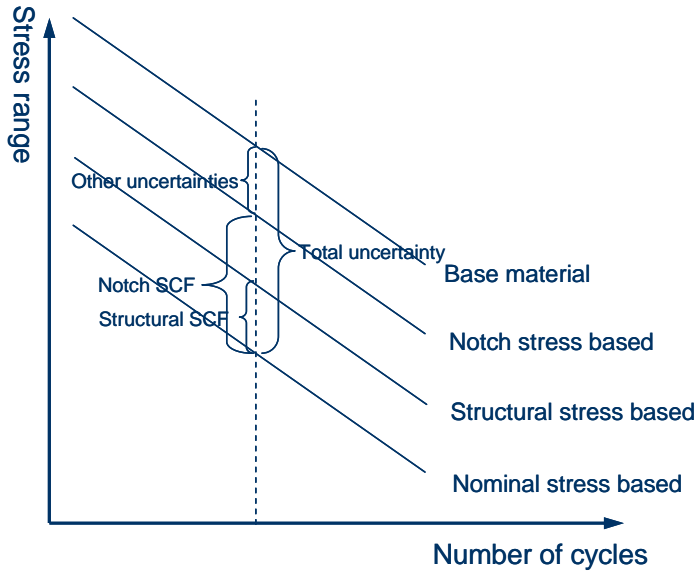


**Fig. 5 Stress definitions and associated design SN curves for welded joints**

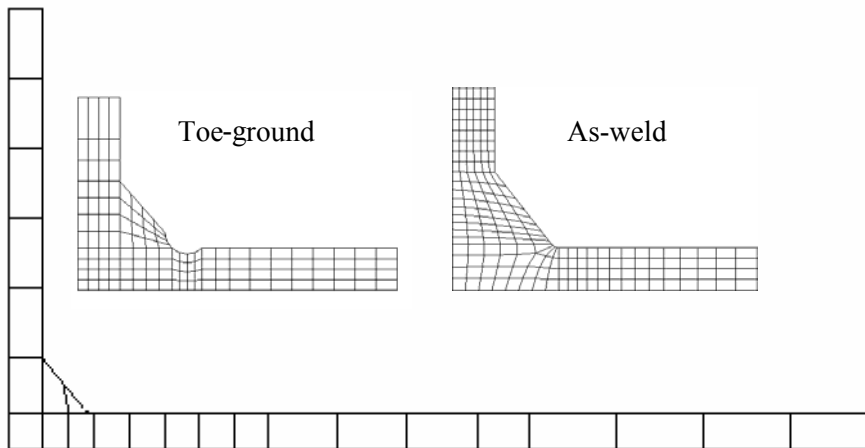


**Fig. 6 A quarter portion of the finite element model and sub-models**

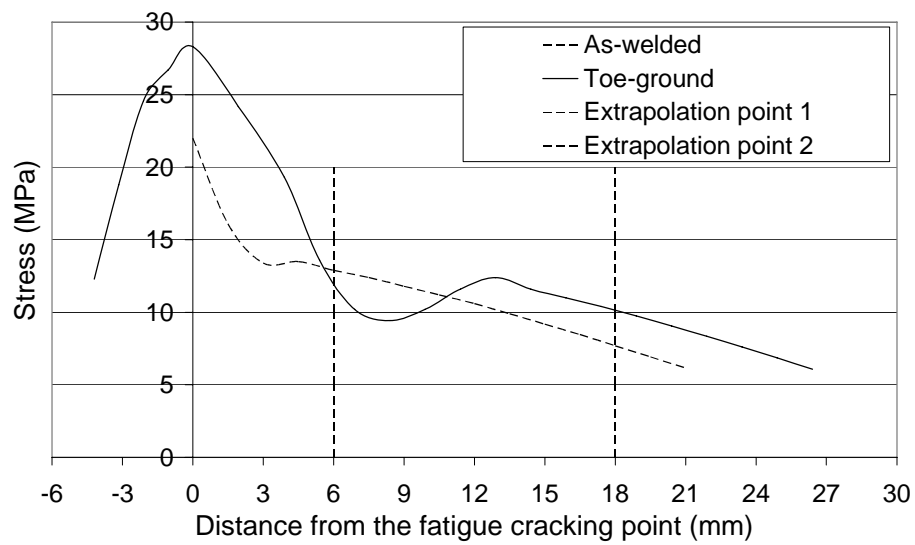


**Fig. 7 Stress gradient near the cracking point for the as-welded and toe-ground joints**  
 $(\lambda=5.9 \text{ mm}, \theta=72.9^\circ, d=0.8 \text{ mm}, \rho=3.2 \text{ mm})$

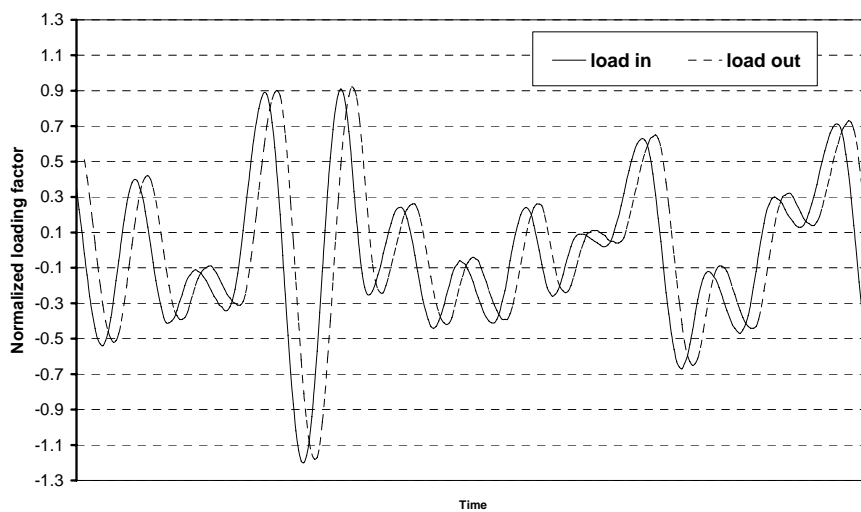


**Fig. 8 Comparison of input and output signals to ensure no peak “cut-off”**

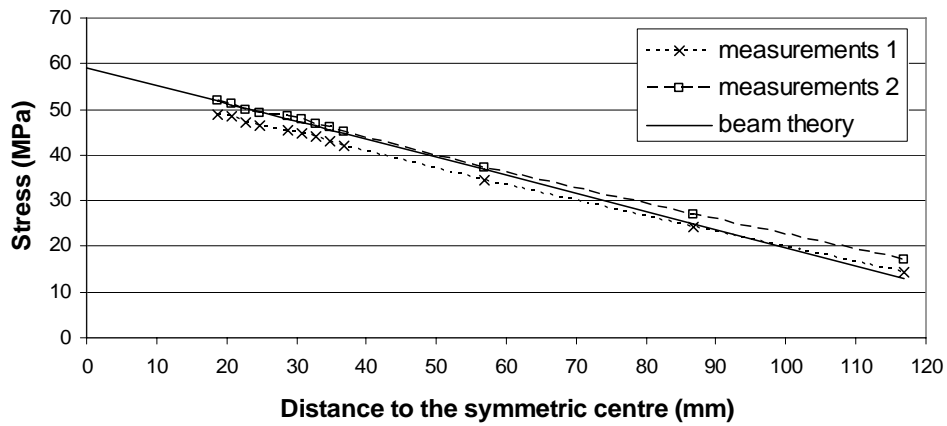


**Fig. 9 Comparison of measured stress and beam theory analytical result**

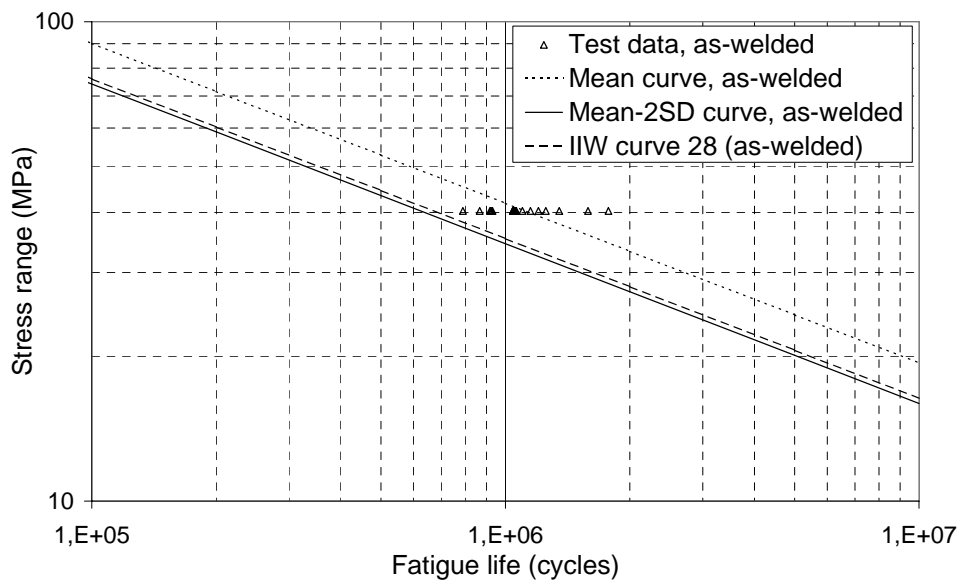


**Fig. 10 Test data of as-welded specimens compared with IIW SN curve 28 based on nominal stress**

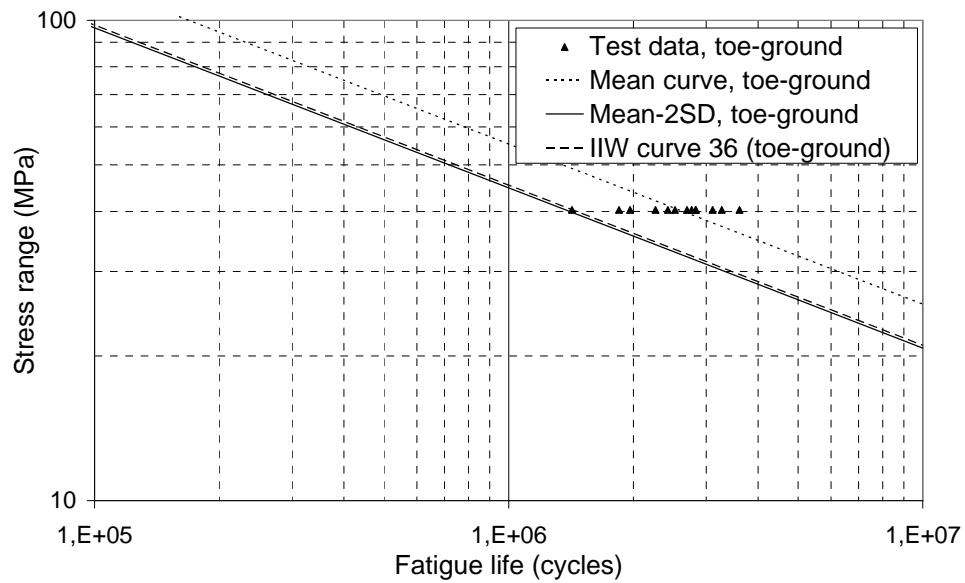


**Fig. 11 Test results of toe-ground specimens compared with IIW SN curve 36 based on nominal stress**

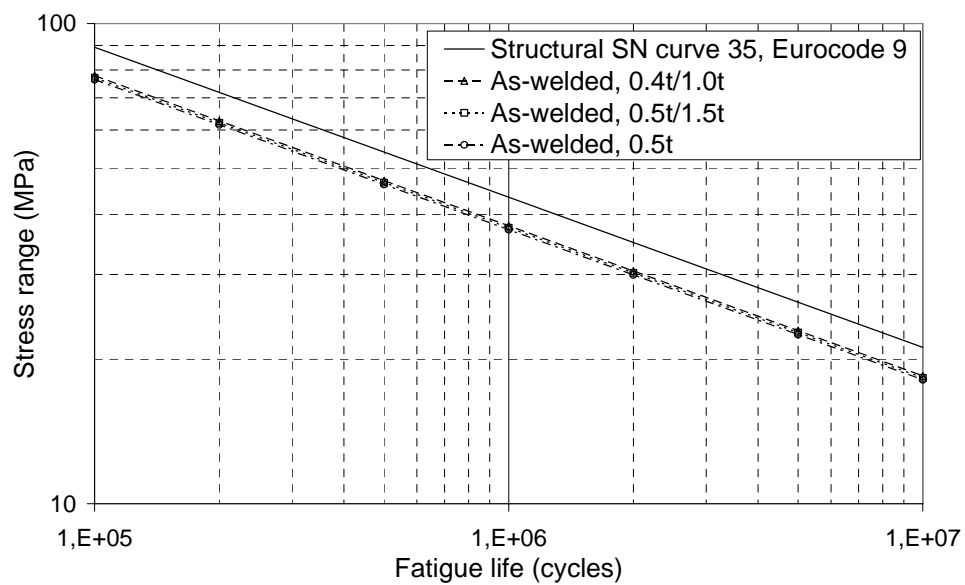


**Fig. 12 Test results compared with Eurocode 9 SN curve 35 based on structural stress**



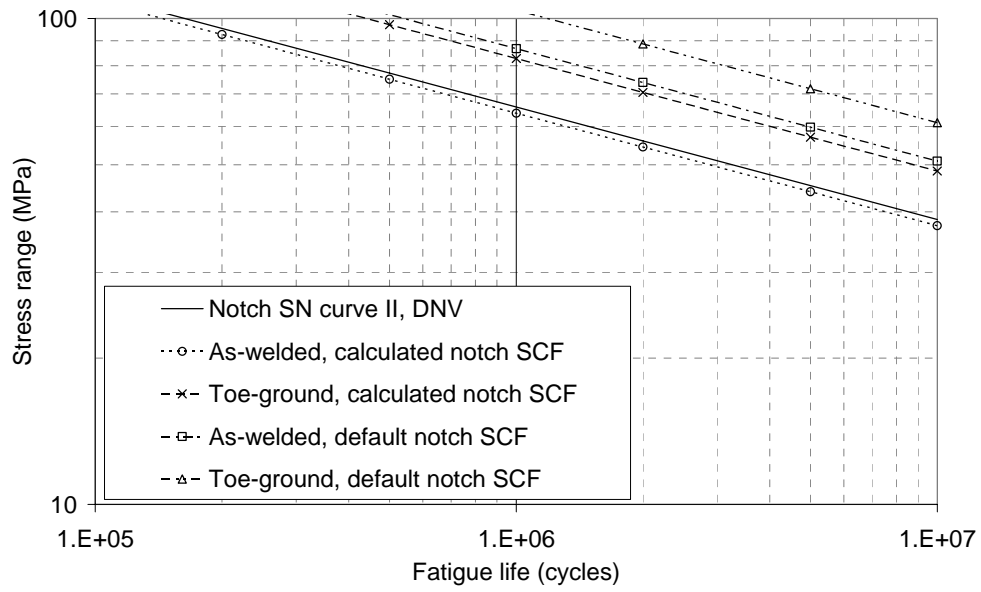


**Fig. 13 Test results compared with DNV SN curve II based on notch stress**

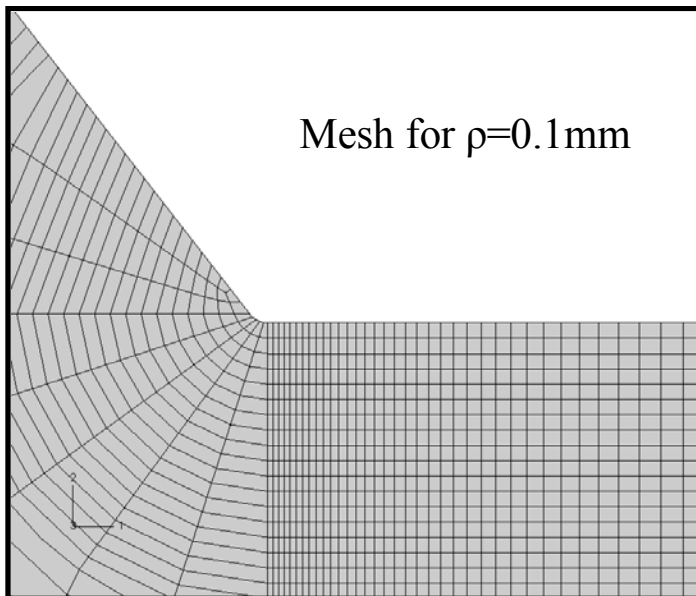


**Fig. 14 Finite element model for 0.1 mm weld toe radius**

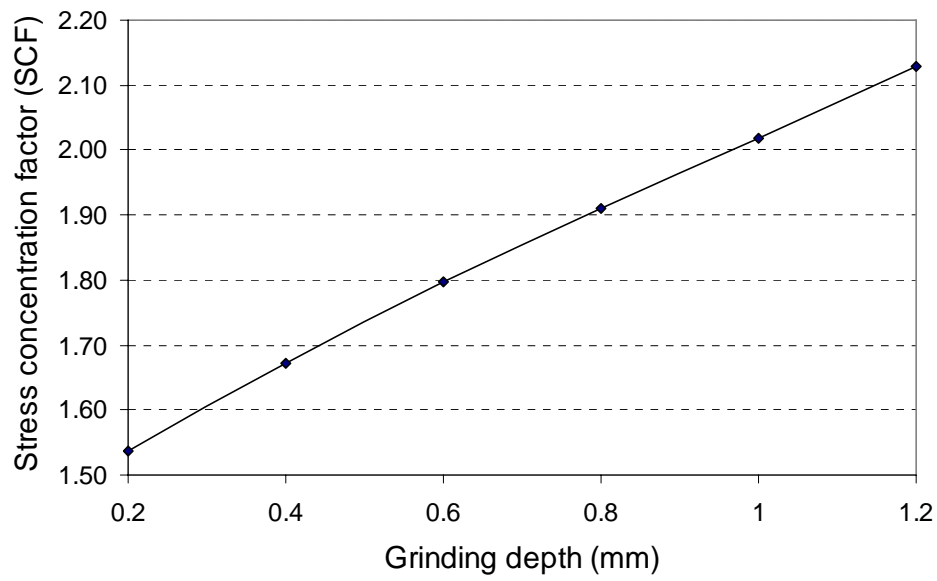


**Fig. 15: Influence of grinding depth on notch SCF**

**Table 1. Statistical results of weld parameters**

Parameter		Minimum	Maximum	Mean	STDV
$\rho$ (mm)	As-welded	0.1	4.2	1.3	0.90
	Toe-ground	2.5	4.8	3.2	0.38
$\theta$ (degree)	As-welded	17.0	90.0	52.1	14.40
	Toe-ground	28.0	100.0	72.9	12.92
$\lambda$ (mm)	As-welded	7.2	11.8	9.0	1.05
	Toe-ground	5.9	9.5	7.5	0.81
d (mm)	Toe-ground	0.2	1.6	0.8	0.28

**Table 2. Detail class in different design codes for aluminium cruciform structures**

Design code	Detail specification		Class/parameter m
Eurocode 9, part 2 [18]	Members with welded attachment; attachment length, 12mm and thickness, 12mm		28/3.2
International Institute of Welding [14]	Non-load carrying attachments, fillet welds	As-welded	28/3.0
		Toe ground	36/3.0
British Standard, part 1 [21]	Welded details on surface of member, with the length of attachment < 25 mm		29/3.0
ECCS [22]	Cruciform joint, toe-crack failure		30/4.32
Aluminium Association [20]	Attachments by fillet welds in the direction parallel to the stress, the dimension of attachments < 50 mm		36/3.64

**Table 3. Influence of weld toe radius on the structural SCF**

Extrapolation methods	As-welded ( $\lambda=9.0$ , $\theta=52.1$ )		
	$\rho=0.1$	$\rho=1.3$	$\rho=4.2$
0.4t/1.0t	1.09	1.09	1.09
0.5t/1.5t	1.08	1.08	1.08
0.5t	1.07	1.07	1.07

**Table 4. Influence of weld leg length on the structural SCF**

Extrapolation methods	As-welded ( $\rho=1.3$ , $\theta=52.1$ )		
	$\lambda=7.2$	$\lambda=9.0$	$\lambda=11.8$
0.4t/1.0t	1.09	1.09	1.09
0.5t/1.5t	1.07	1.08	1.08
0.5t	1.06	1.07	1.06

**Table 5. Influence of weld toe angle on the structural SCF**

Extrapolation methods	As-welded ( $\rho=1.3$ , $\lambda=9.0$ )		
	$\theta=17.0$	$\theta=52.1$	$\theta=90.0$
0.4t/1.0t	1.09	1.09	1.09
0.5t/1.5t	1.08	1.08	1.08
0.5t	1.06	1.07	1.06

**Table 6. Influence of the weld toe radius on the notch SCF**

As-welded ( $\lambda=9.0, \theta=52.1$ )			Toe-ground ( $\lambda=9.0, \theta=72.9, d=0.8$ )		
$\rho=0.1$	$\rho=1.3$	$\rho=4.2$	$\rho=2.5$	$\rho=3.2$	$\rho=4.8$
3.78	1.83	1.32	2.01	1.91	1.82

**Table 7. Influence of the weld leg length on the notch SCF**

As-welded ( $\rho=1.3, \theta=52.1$ )			Toe-ground ( $\rho=3.2, \theta=72.9, d=0.8$ )		
$\lambda=7.2$	$\lambda=9.0$	$\lambda=11.8$	$\lambda=5.9$	$\lambda=7.5$	$\lambda=9.5$
1.88	1.83	1.80	1.91	1.91	1.91

**Table 8. Influence of the weld toe angle on the notch SCF**

As-welded ( $\rho=1.3, \lambda=9.0$ )			Toe-ground ( $\rho=3.2, \lambda=7.5, d=0.8$ )		
$\theta=17.0$	$\theta=52.1$	$\theta=90.0$	$\theta=28.0$	$\theta=72.9$	$\theta=100.0$
1.62	1.83	1.79	1.93	1.91	1.93

**Table 9. Fatigue test data**

Specimen No.	Fatigue life	
	As-welded	Toe-ground
1	930806	2423027
2	1042485	2830036
3	916920	1846428
4	1057019	1421794
5	1774631	2694688
6	1050289	3268021
7	923797	3609481
8	1348637	2765445
9	1051069	3108286
10	1150013	2520398
11	866263	1963157
12	1099022	2262469
13	1041857	2827378
14	1252033	-
15	1063280	-
16	789209	-
17	1202075	-
18	1582690	-
Mean fatigue life	1119005	2580047
STDV of log( $N$ )	0.09	0.11

## **Paper 4**

# **RECOMMENDATIONS ON THE SELECTION OF STRUCTURAL STRESS DESIGN S-N CURVES FOR THE FATIGUE ASSESSMENT OF WELDED ALUMINUM STRUCTURES**

Bård Wathne Tveiten<sup>a</sup>, Naiquan Ye<sup>b</sup> and Torgeir Moan<sup>b</sup>

<sup>a</sup> SINTEF Materials Technology, Department of Fracture Mechanics and Materials Testing, Richard Birkelands vei 2B, N-7465 Trondheim, Norway.

<sup>b</sup> Department of Marine Structures, Faculty of Marine Technology, Norwegian University of Science and Technology, N-7491 Trondheim, Norway

Published in Fatigue Congress 2002, Session: Weld,  
Stockholm, Sweden





# RECOMMENDATIONS ON THE SELECTION OF STRUCTURAL STRESS DESIGN S-N CURVES FOR THE FATIGUE ASSESSMENT OF WELDED ALUMINUM STRUCTURES

Bård Wathne Tveiten<sup>a</sup>, Naiquan Ye<sup>b</sup> and Torgeir Moan<sup>b</sup>

The main object of this paper is a review of published structural stress S-N data of welded aluminum structures together with finite element analysis results in order to discuss the various effects that influence a consistent selection of design S-N data. The two key issues addressed in this paper are the definition and the calculation of the structural stress used in fatigue design and the appropriate selection of a structural stress design S-N curve. In addition, some general modeling principles and techniques with respect to structural stress calculations by means of finite element calculations are discussed.

## INTRODUCTION

Fatigue design codes of welded aluminum structures are normally based on a nominal stress range S-N curve approach where the design stress referred to is the local nominal stress range that does not include any stress raisers due to local weld geometry or local geometrical changes. Thus, all structural discontinuity effects and local notch effects (including fabrication defects and workmanship) are implicitly included in the fatigue strength S-N curves.

However, for welded structures characterized by relatively complex geometry, varieties of structural details, or complex combinations of loads, fatigue strength assessment may become rather cumbersome when a traditional nominal stress range S-N curve approach based on standard detail classes of typical welded details is applied. As an alternative, a design principle based on a structural stress range S-N curve approach has been suggested as a more suitable fatigue assessment procedure in that the design stress is based on the structural stress that also captures the geometrical features of the joint geometry. This reduces the number of design S-N curves since the geometrical features of the design classes are included in the design stress range rather than in the design S-N curves. However, the local notch effects are still embedded in the design S-N curves.

<sup>a</sup> SINTEF Materials Technology, Department of Fracture Mechanics and Materials Testing, Richard Birkelands vei 2B, N-7465 Trondheim, Norway.

<sup>b</sup> Department of Marine Structures, Faculty of Marine Technology, Norwegian University of Science and Technology, N-7491 Trondheim, Norway



## **CALCULATION OF STRUCTURAL STRESS IN WELDED STRUCTURES**

### **Introduction**

The structural stress is defined as the linearized through-thickness stress at the weld toe location that includes the stress raising effects due to structural geometry, excluding the stress concentrations due to the presence of the weld notch. Excluding the weld notch effects can be achieved by carrying out an extrapolation procedure of the structural stress from outside the region which is influenced by the local notch. The extrapolation points must be located such that the nonlinear stress variations caused by the local notch at the weld are not included in the stress results. At the same time, the points should be sufficiently close to capture the global geometrical effects. The structural stress range approach assumes that the fatigue crack will initiate at the weld toe location. Fatigue failures that initiate from other locations such as the weld root have to be treated separately by means of e.g. the stress referred to at the weld throat section. In general, three types of weld toe failure can be identified (Fricke [1]), Type a, b, and c (Figure 1) where the different joints have different behavior and may require different extrapolation approaches. Type a and c differ from Type b behavior as the fatigue failure of Type a and c depends amongst other things, on the plate thickness, whereas fatigue failure of Type b usually does not. Type b characterizes those failures at which the fatigue cracks initiate at the plate edge and propagate across the stressed member as through-thickness cracks. In such “2-dimensional” cases the stress distribution approaching the weld does not depend on the plate thickness.

All existing structural stress extrapolation procedures proposed in the open literature are based on surface stress extrapolation. The stress at the extrapolation points can either be obtained by strain gage measurement, or by means of numerical stress analysis. To calculate the local stress distribution that captures the stress raising effects due to the structural discontinuities, a local finite element model with a refined mesh is required. In contrast to the calculation of the nominal stresses where only frame models or coarse global finite element models are sufficient, the calculation of the structural stress requires more complex finite element models and consequently higher computational efforts. The mesh refinement of large, global finite element models at fatigue prone areas is not feasible. However, the structural geometry at the hot-spot locations can be reanalyzed by means of the submodeling technique. The displacements on the cut boundary of the global model are then specified as boundary conditions of the local finite element model.

### **Modeling principles**

The analyst has several possibilities of modeling the structural geometry, ranging from finite solid elements, thick or thin finite shell elements, or a combination of these. Finite shell element models as well as coarse finite solid element models are

⊥

□

characterized by a linear stress distribution over the plate thickness. Therefore, both types of finite element modeling are suitable for the calculation of the structural stress since the nonlinear stress distribution due to the presence of the weld notch in the thickness directions is excluded. The main problem which arises when finite shell elements are used is that the finite shell element formulation only provides a model for the mid-plane of the plates (the element thickness is given as an element property) and thus the local change of the stiffness associated with the weld shape can not be modeled.

A comparative study of ship structural details including strain gage test results and numerical stress analyses (Sumi [2]) has shown that extrapolated stresses are highly dependent on whether a finite shell element model or a finite solid element model have been used in the stress analysis, or in particular how the weld has been modeled. There have been several attempts to solve the problem of representing the actual stiffness of the weld seams in finite shell element models. The shell elements have been joined by using some sort of rigid elements, thicker elements at the weld area, or by inclined shell elements to account for the “missing” weld, or by an extrapolation to the intersection line that lies “inside” the material and hence an extrapolation which potentially predicts the structural stress at a fictitious position. Tveiten [3] has shown by finite shell and solid element analyses combined with strain gage measurements of longitudinal stiffener/bracket connections that extrapolated structural stress values were rather sensitive to how the weld stiffness had been accounted for in the finite shell element model. It was therefore recommended that finite solid element models should be used for the calculation of the structural stress, or at least to verify methods based on finite shell elements.

Fricke [1] has recently presented recommendations regarding structural stress analysis. The study included a round-robin FE analysis of typical FPSO details (steel) where 5 typical details were investigated. Various finite element models were developed by the participants, using different types and sizes of finite elements, different modeling and stress evaluation techniques as well as different finite element software. The study suggested that both solid and shell element models, preferably 8-noded shell elements, might be used together with extrapolation procedures for the calculation of structural stress. When using shell elements the welds are not necessarily needed, however, vertical or inclined elements with appropriate stiffness or constrained equations to couple node displacements to model the weld stiffness need to be considered for cases where the results are affected by a high degree of local bending.

### **Methods for structural stress extrapolation**

Stress extrapolation methods proposed in the open literature are traditionally based on the assumption that the effect of the weld notch is localized within a distance close to the weld, where the distance is normally expressed as a function of the main plate thickness. In addition, the extrapolation methods are very often quite

⊥

□

joint dependent. That is, the method is easily calibrated to a given joint type but may fail to get an accurate assessment of different joint configurations and dimensions (Tveiten [3]). Obviously, the extrapolation scheme can not guarantee that the real influence of the weld notch on the structural stress has been removed. Furthermore, the joint-dependence narrows the application range of the methods as many joint types usually differ greatly from the proposed one. These restrictions are, however, overcome by Tveiten and Moan [4] by proposing an analytical solution to obtain the structural stress at the weld toe based on the asymptotic behavior of stresses adjacent to an idealized notch. Different from existing extrapolation methods suggested by IIW [5] and Niemi [6] that applies to either Type a/c failure or Type b failure (Figure 1), the proposed method suggested by [4] applies to all types of weld toe failure (Type a, b and c). Studies ([3] and Ye et al. [14]) have shown that the suggested extrapolation method proposed by [4] provides a lower bound value of the structural stress compared to the extrapolation methods suggested by [5] and [6].

A reliable structural stress analysis procedure is dependent on a well-defined link between the calculation of the structural stress and the stress implicitly used as the design stress in the S-N curve. Assuming that the structural stress is accurately predicted, the same calculation procedure should be used to calculate the structural stress at an actual detail that was used when the structural stress design S-N curve was derived from test data. Existing extrapolation methods suggested by [4], [5], and [6] require a mesh refinement such that any further refinement does not result in significant change of the stress distribution inside the area between the extrapolation points. The extrapolation method suggested by [4] will also require a further mesh refinement close to the weld toe such that the singularity at the notch is accurately accounted for. Hence, the stress extrapolation procedures are linked to specific requirements for use of finite element types and finite element meshes. However, for practical design the aim is to use coarser finite element models and clearly it is a conflict of interests between the accuracy of the resolved structural stress and the required model complexity and thus the computing time.

Structural stress extrapolation procedures such as those presented by [4], [5] and [6] are based on surface stress extrapolation with the assumption that the structural stress is linearly distributed across the plate thickness. With basis in fracture mechanics, the stress field across the plate thickness will also govern the crack growth. Different details showing the same extrapolated structural stress value may show different stress fields in the plate and, thus, also different crack growth lives are predicted. Due to this, a uniquely determined design S-N curve based on a structural stress derived from extrapolated surface stresses might be questioned. However, the discrepancy from a single design S-N curve for different details will likely be dependent on the failure criterion used (amount of crack growth into different stress fields for different details). A method to estimate the structural stress based on the stress distribution through the thickness and on the surface has recently been launched by Battle (Dong [7]). The method is said to be mesh-size insensitive

⊥

□

and it is said that the method can be implemented in both solid and shell element models. However, all details of this method have not yet been published.

### **STRUCTURAL STRESS DESIGN S-N CURVES**

The structural stress range approach has been implemented in the fatigue design codes and recommendations of tubular steel joints, and steel plate and shell structures (e.g. IIW [5]). However, even though CEN [8] have presented some structural stress design S-N curves, no fatigue design codes or recommendations have suggested a structural stress range approach for welded aluminum structures based on a well defined method for the structural stress extrapolation together with a consistent definition of a design S-N curve.

The fatigue strength of a welded detail is dependent on several factors such as geometrical parameters including the plate thickness and the plate width, the attachment length, width and height, the specimen length, the leg length, and additional factors such as the loading mode (tensile/bending), misalignments (if not included in the finite element model where the stresses are derived from), and the condition at the weld toe (as-welded/toe-ground).

The geometrical effect (thickness effect) is commonly addressed in fatigue design as a penalty factor on the form:  $f(t) = (t_{ref}/t)^n$ , where  $f(t)$  is the thickness correction factor,  $t_{ref}$  is the reference plate thickness,  $t$  is the plate thickness of the detail, and  $n$  is the thickness correction exponent. Recent research (e.g. Maddox [11]) has shown that thickness effects in aluminum structures also apply for structural stress approaches and are similar to those found for steel structures. In line with these findings the same thickness correction is implemented in the IIW [5] rules for aluminum structures as in those for steel. In these rules the thickness correction exponent,  $n$ , varies between 0.1 and 0.3 depending on joint category and condition. The lowest values apply to un-welded plates or highest categories of welded joints, e.g. flush ground butt welds. This is consistent with the fact that part of the thickness effect is due to the steep stress gradient that is present in joints with a low fatigue strength. CEN [8] has not adopted the scheme of a penalty factor but the geometrical effect is based on several different structural stress design S-N curves depending on the actual plate thickness of the component. For some details where the plate thickness is not evident (e.g. gusset plates with edge attachments, Type b, Figure 1), other geometrical parameters such as e.g. plate width or/and attachment length will govern the effects relating to the stress gradient in the crack plane. Partanen et al. [9] have derived a penalty factor for load carrying gusset plates with edge attachments as  $f(t) = (t_{ref}/t_{app})^n$ , where  $t_{ref} = 25$  [mm],  $n = 0.25$ , and  $t_{app} = \min\{B, 1.5 \cdot L, 15 \cdot H\}$  where  $B$  is the height of the stressed member,  $L$  is the length of the attached gusset plate, and  $H$  is the height of the attached gusset plate. As demonstrated by [11], a thickness effect is shown for structural stress S-N data of fillet welded aluminum details. However, Niemi [6] has suggested a linear and a

⊥

□

quadratic extrapolation method for Type b details where he claims that the geometrical effect is automatically accounted for by the quadratic extrapolation procedure, as the shape variation of the stress distribution in the crack plane due to changes in dimensions is included in the structural stress. While for the linear method, the geometrical effect has to be considered by multiplying the fatigue strength by the penalty factor,  $f(t)$ , suggested by [9].

Rather limited test S-N data for the validation of the structural stress approach for welded aluminum structures are available. However, some authors have presented test S-N data for welded aluminum structures based on a structural stress range approach. Partanen and Niemi [10] have compiled fatigue test results for a variety of aluminum test specimens with moderate thickness (up to 6 [mm]) subjected to pulsating tension ( $R > 0$ ) using structural stress obtained from extrapolated strain gage measurements and finite element analyses. The structural stress was based on the extrapolation procedure suggested by IIW [5]. The test S-N data presented by [10] are shown in Figure 2 together with test S-N data provided by Maddox [11]. The authors suggest that the structural stress range approach can safely be used with an S-N curve of fatigue class 40 (fatigue class 40 refers to the characteristic stress range at  $2 \cdot 10^6$  cycles) for butt and fillet welded aluminum joints of relatively thin plates and extrusion (up to 6 [mm]) failing from the weld toe location. For plates with thickness exceeding 6 [mm], Niemi [12] has recently suggested that the fatigue strength must be reduced with a thickness penalty factor,  $f(t) = (t_{ref}/t_{eff})^n$  where  $t_{ref} = 6$  [mm],  $t_{eff}$  is equal to  $t$  for  $L/t > 2$  else  $0.5 \cdot L$  where  $L$  is the attachment length, and  $n$  varies between 0.1 and 0.3. Assuming a design S-N curve of fatigue class 40 together with the thickness penalty factor suggested by [12], the design fatigue strength is seen to be 10 [%] to 15 [%] below what is suggested by CEN [8] for  $n = 0.3$ . For  $n = 0.1$ , the fatigue strength is seen to be 0 [%] to 30 [%] above what is suggested by [8]. Most difference is seen for the largest plate thickness. As the difference in design strength depending on the thickness is rather large, it is suggested that there is a need for further research on the matter.

A numerical and experimental study by Macdonald et al. [13] has suggested a fatigue design methodology for welded aluminum space frames made of rectangular hollow sections joints using a linear or quadratic extrapolation of the structural stress according to recommendations given by the IIW [5] and a design S-N curve with a fatigue class of 40. The fatigue test specimens were loaded in 4-point bending of the chord member at  $R = 0.1$ . The wall thickness of the test specimens (3 [mm]) was within the thickness range of the test specimens used for deriving the S-N data presented by Partanen and Niemi [10]. The test S-N data are presented in Figure 3.

Tveiten and Moan [4] have published test S-N data on flat bars with fillet welded in-plane brackets (Type b, Figure 1). The structural stress was calculated using the extrapolation methods suggested by [4] and Niemi [6]. The test S-N data are presented in Figure 3. The test S-N data obtained for the flat bar/bracket

⊥

□

connections seemed to correspond well with the findings of Niemi and Partanen [10] with respect to an appropriate structural stress design S-N curve of fatigue class 40. However, the detail was also expected to be affected by geometry, which would influence the fatigue strength. Design codes and design recommendations provide no recommendations on penalty factors for these particular types of joints (Type b, Figure 1). Using the penalty factor suggested by Partanen et al. [9] with a  $t_{app} = 35$  [mm], would give a  $f(t) = 0.92$  that would suggest slightly more conservative S-N data compared to a design S-N curve of fatigue class 40. Note, however, that the scatter of the test results was relatively narrow,  $STDV_{\log N} = 0.094$ .

Studies on aluminum box-stiffener/lap joints reported by Ye et al. [14] showed that using a structural stress range approach, design S-N curve of fatigue class 44 suggested by CEN [8] seems to give conservative fatigue assessments (wall thickness of box-stiffener and lap plate was 3 [mm]). The test S-N data are presented in Figure 3. The structural stress extrapolation method adopted in the test S-N data representation was the method suggested by Tveiten and Moan [4]. The 95 [%] lower limit confidence regression line of the test S-N data was 5.5 [%] above the design S-N curve at the point of  $2 \cdot 10^6$  cycles. Note that the margin will be greater if other extrapolation methods are applied, e.g. IIW [5]. The standard deviation of the test results was,  $STDV_{\log N} = 0.10$ .

Studies by Tveiten [3] on longitudinal stiffener/bracket connections have shown that a possible effect on the fatigue strength due to the loading mode (tensile or bending) was assumed to be limited since this effect was mostly covered by a change in the structural stress concentration factor. [3] has also presented test S-N data on as-welded and toe ground flat bars with fillet welded in-plane brackets which suggested that there is fatigue life improvement in the low stress region (more than  $10^6$  cycles). This implies a different design S-N curve for toe ground details than for as-welded details. Additional, however, not yet published test S-N data of non-load carrying fillet welded cruciform joints supports the findings and suggest an increase on the fatigue class of about 30 [%], which corresponds well to what is seen for welded steel joints (Ye et al. [15]).

## CONCLUSIONS

Studies suggest that extrapolated structural stress values are rather sensitive to how the weld stiffness has been accounted for in the finite shell element models. Shell elements may be used in cases of low degree of local bending, however, it is recommended that preferably finite solid element models should be used in the calculation of the structural stress, or at least to verify methods based on finite shell elements.

Suggested procedures for structural stress extrapolation are linked to specific requirements for use of finite element types and finite element meshes. Thus, there is a need for further research on possible new procedures and/or further

⊥

□

development of existing extrapolation methods in order to obtain structural stress procedures that are mesh-size and finite element type insensitive.

Fatigue S-N data support the use of a structural stress design S-N curve of fatigue class 40 for the fatigue assessment of aluminum fillet welded in-plane bracket connections when the structural stress has been derived from the extrapolation methods suggested by Tveiten and Moan [4] or Niemi [6], and for butt and fillet welded aluminum joints of relatively thin plates and extrusion (up to 6 [mm]) failing from the weld toe location with the extrapolation method suggested by IIW [5]. It has been shown that a structural stress design S-N curve of fatigue class 44 for the fatigue assessment of aluminum lap joints can be used when the structural stress has been derived from the extrapolation methods suggested by [4] or [5].

For joints with a well-defined plate thickness, it is also suggested that a fatigue strength penalty factor should be used together with the design S-N curve of fatigue class 40 for plate thickness exceeding 6 [mm]. However, it is seen a difference between suggestions proposed by different authors. For details where the plate thickness is not evident (Type b, e.g. gusset plates with edge attachments), there are some inconsistency whether a penalty factor should be included or not, and therefore it is a need for further research on the matter.

## **REFERENCE LIST**

- (1) Fricke, W., Recommended Hot Spot Analysis Procedure for Structural Details of FPSOs and Ships Based Round-Robin FE Analyses, *Proc. of the 11<sup>th</sup> Int. Offshore and Polar Conf. (ISOPE'2001)*, Stavanger, Norway, 2001.
- (2) Sumi, Y., Finite element comparative study of ship structural details, *Proc. of the 13<sup>th</sup> Int. Conf. of Ship and Offshore Structures Congress, ISSC'97 - Volume 1*, Edited by T. Moan and S. Berge, Trondheim, Norway, 1997.
- (3) Tveiten, B. W. (1999), *Fatigue Assessment of Welded Aluminum Ship Details*, Dr. Ing. thesis, NTNU, Trondheim, Norway, 1999.
- (4) Tveiten, B. W. and Moan, T., *Journal of Marine Structures*, Vol. 13, No. 3, 2000, pp. 189-212.
- (5) IIW, *Recommendations for fatigue design of welded joints and components. ISO standard proposal*, Technical Report IIW-XIII-1539-96/XV-845-96, IIW, 1996.
- (6) Niemi, E., *On the determination of hot spot stresses in the vicinity of edge gussets*, Doc. IIW-XIII-1555-94, IIW, 1994.
- (7) Dong, P., A Robust Structural Stress Procedure for Characterizing Fatigue Behavior of Welded Joints, Reprinted From: *Fatigue and Failure of Spot Welds and Weld Joints (SP-1621)*, SAE 2001 Detroit, Michigan, 2001.

⊥

□



- (8) CEN, *Design of aluminum structures-Part 2: Structures susceptible to fatigue*, Eurocode 9, ENV 1999-2, CEN, Brussels, 1999.
- (9) Partanen, T., Torvi, T. and Niemi, E., *On size effects in fatigue of welded joints*, Doc. IIW-XIII-1535-1994, IIW, 1994.
- (10) Partanen, T. and Niemi, E., *Welding in the World*, Vol. 43, No. 1, 1999, pp. 16-22.
- (11) Maddox, S. J., Scale effect in fatigue of fillet welded aluminum alloys, *Proc. of 6<sup>th</sup> Int. Conf. on Aluminum Weldments*, AWS, 1995.
- (12) Niemi, E., *Structural Stress Approach to Fatigue Analysis of Welded Components*, Doc. IIW-XIII-1819-00, IIW, 2001.
- (13) Macdonald, K., Haagensen, P. J. and Sjøvik, O. P., Progress in fatigue assessment of welded hollow-section aluminum structures, *Proc. of the Int. Conf. of Aluminum Structures - INALCO'98*, United Kingdom, 1998.
- (14) Ye, N., Moan, T. and Tveiten, B. W., Fatigue Analysis of Aluminium Box-Stiffener Lap Joints by Nominal, Structural and Notch Stress Range Approaches, *Proc. of PRADS'2001*, Shanghai, China, 2001.
- (15) Ye, N., Moan, T. and Tveiten, B. W., Improving Fatigue Strength of Aluminium Cruciform Joints by Weld Toe Grinding, To appear, 2002.
- (16) Maddox, S. J., *Hot-spot fatigue data for welded steel and aluminium as a basis for design*, Doc. IIW-XIII-1900-01, IIW, 2001.

## FIGURES

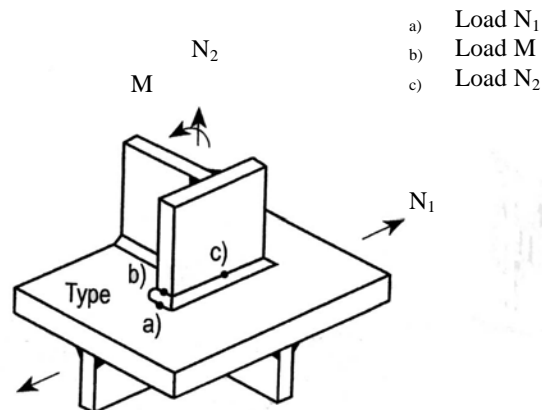


Figure 1 Types of weld toe failure seen in welded plate structures (Figure from Fricke [1]).

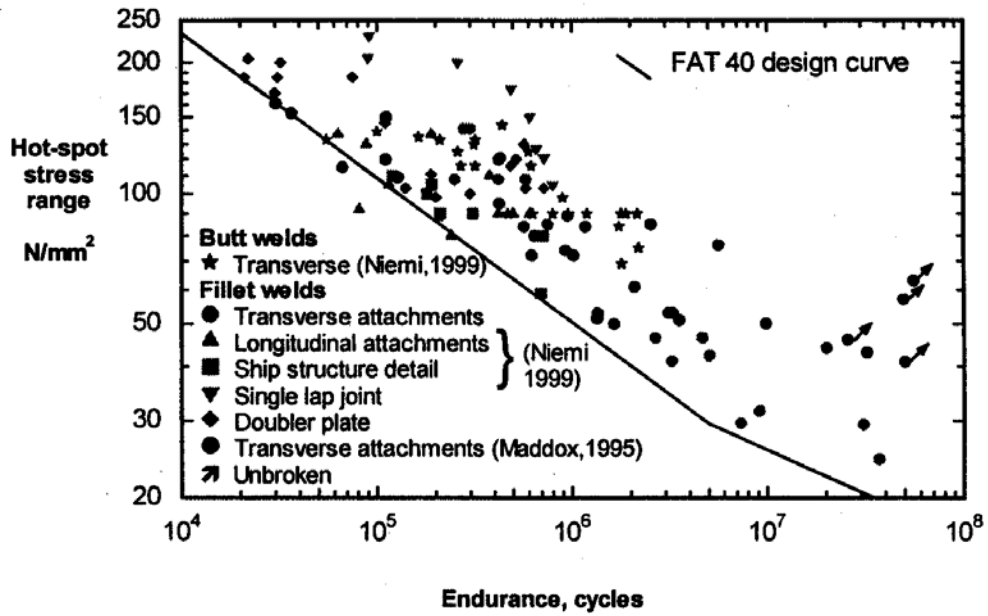


Figure 2 S-N data expressed in terms of IIW [5] structural stress range definition (Figure from Maddox [16]).

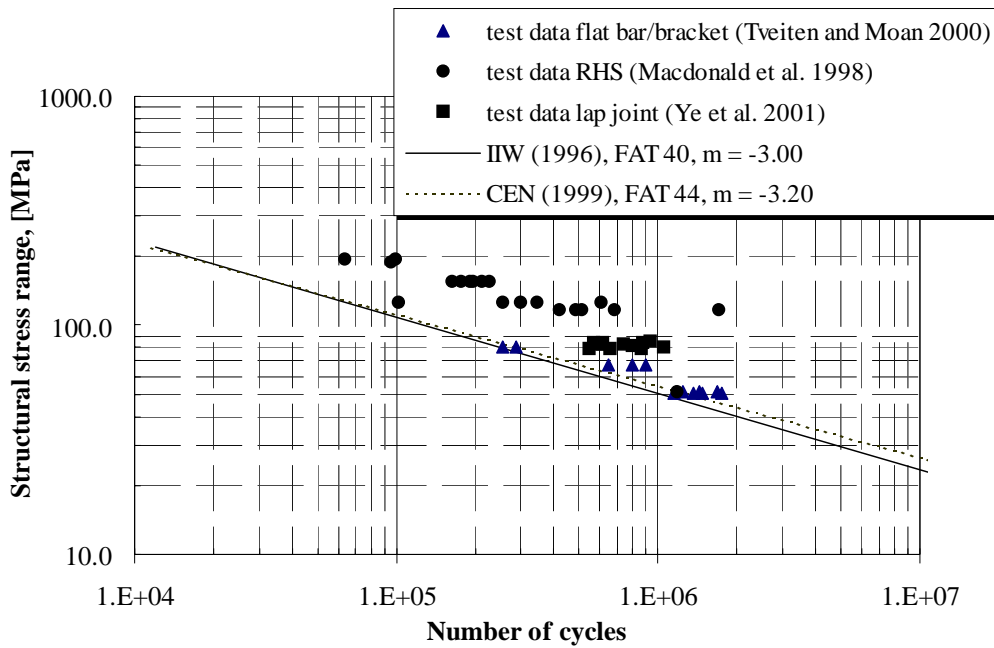


Figure 3 S-N data expressed in terms of the structural stress range definition suggested by Tveiten and Moan [4] and IIW [5].

**6**     *Appendix B: Materials certificates*





Hydro  
Aluminium  
Profiler

Hydro Aluminium Profiler as, Karmøy  
N-4265 Håvik, Norway  
Telefon : +47 52 85 45 00  
Telefax : +47 52 85 49 04  
Foretaksregisteret  
NO 942 613 466 MVA

TESTCERTIFICATE/PRÜFZEUGNIS

Customer/Kunde

HYDRO ALUMINIUM MARITIME AS K  
KARMØY  
4262 AVALDSNES  
NORGE

EN 10204 / 3.1.C

Material ALU-PROFIL		Profil HMA0169	Net. weight/Netto-Gewicht 909 KG
BILDEKK		Our Order no./Auftragsbestätigung Nr. 3/99451-01	
		Customer Order no./Kunden - Bestellnummer 61075/RS-HMA0169	
Material - Specification/Material - Spezifikation			
Alloy/Legierung NV-6082	Temper/Zustand T6	Heat Treatment/Aushärtung 5 HRS AT 185C	
Proof stress/ Streckgrenze Rp 0,2 (N/mm2) 260	Tensile strength/ Zugfestigkeit Rm (N/mm2) 310	Min. elongation/Bruchdehnung A pct. 10	Elongation gauge length/Bruchdehnung mezlänge 5,65√SO

Chemical Analysis/Chemische Zusammensetzung								
Al. rest	Si	Fe	Cu	Mn	Mg	Cr	Zn	Ti
min	0,7			0,4	0,6			
max	1,3	0,5	0,1	1,0	1,2	0,25	0,2	0,1

Test Results/Prüfe resultate							
Batch no./ Produktions Nr.	Test no./ Pruf Nr.	Rp 0,2 N/mm2	Rm N/mm	A pct.	Hardness HB Brinell-Härte	Other tests/ Andere Tests	Remarks/ Bemerkungen
5250	3342/98	291	322	12	102	1 KOLLI	T. TAKEN P.K.
		292	325	12	102		
Heat treatment/Aushärtung 5 HRS AT 185C							

Chemical Analysis/Chemische Zusammensetzung									
Cast no./Guss Nr.	Al. rest	Si	Fe	Cu	Mn	Mg	Cr	Zn	Ti
60750		0,98	0,18		0,55	0,66		0,01	

Certificate no./Prüfzeugnis Nr. 17729	Identification/Aussteller 3/99451-01	The material was tested at the final stage and it satisfied the above requirements./ Das Material wurde im Endzustand geprüft und erfüllt die oben erwähnten Anforderungen.
	HGS 7746 NV	
HGS 7746 <i>Jørn Halverson</i> Date/Datum 98.12.10	Identification placed/ Identifikation Ausgestellt END	Med hilsen/Mit freundlichen Grüßen Hydro Aluminium Profiler as Avd. Karmøy <i>Olaf A. Thønhøeg</i> Quality Manager/ Verantwortlicher f. die Qualitätsprüfung
Place - Karmøy/Ort - Karmøy		

COMMANDE CLIENT - Customer Order - Kundenbestellung		DESTINATAIRE - Consignee - Empfänger	COMMANDE PECHINEY RHENALU
A13582 0/8624008 NORSK LAKSEV		KVAERNER FJELLSTRAND N-5632 OMASTRAND NORVEGE	36515/051 AVIS D'EXPEDITION - Dispatch Note - Lieferschein
		NUMERO - Number - Nummer: 414420	18 Mar 1999

TOLE NV.5083 H116 DNV.SHIPS.PART.2  
ED.01.96  
DIM 2000 /5000 /12  
RECEPTION NORSKE VERITAS PV  
EN10204.3.2  
LIVRAISON SANS PROTEC.INT COLIS  
4000 KG NET

\*SANS PROTECTION INTERCALAIRE =  
RESERVES\*

12 UNITES

CAISSE Case Kiste	LOT CONTROLE Inspection lot Los	PRODUIT Product Produkt	PLATEAU Slab Walztafel	ETAT Temper Zustand	SENS Direction Richtung	ESSAIS DE TRACTION Tensile Tests Zugversuche			AUTRES ESSAIS Other tests Andere Proben		
						R	R 0,2	A %			
						Tensile Strength MPA	Yield Strength MPA	Elongation %			
516481	36515/051	12 PLATES	247589/04	H116	TL	342	236	20			
					TL	342	241	20			
					TL	343	244	19			
					TL	343	248	17			
					TL	347	254	20			

Norsk Stål as  
Bergen

COULEE - Castings Schmelze	COMPOSITION CHIMIQUE - Chemical Composition - Zusammensetzung											
	SI	FE	CU	MN	MG	CR	NI	ZN	TI	ZR	PB	B
247589	0,09	0,25	0,08	0,58	4,41	0,13	35*	0,13	0,02	34*	33*	6*

\* en ppm

We certify that subject to the exceptions and engineering departures above mentioned the present supply has been manufactured to the technical specifications of customer contract, order or sub-order, and that after completion of all inspections and tests, it complies in EVERY ASPECT with the particular specifications which are there attached with the drawings and all the relative standards and regulations in force.



LYO : 98234001

09 MARS 1999

A. THULIERE

*[Handwritten signature]*

ISO 9002



CERTIFICAT N° 1992/797a

DECISION DE **P.O.M. BARTHOMEUF**  
Conclusion of chief inspector  
Entscheidung des Leiters der Abteilung Kontrolle

**B. SCHAFFHAUSER**  
15/02/99 NM

OBSERVATIONS DE  
LA SURVEILLANCE  
Remarks of  
official inspector  
Bemerkungen von  
der Beaufsichtigung

This is to certify that above material is manufactured by an approved process and tested in accordance with DNV Rules. Certificate being issued according to the authorized DNV MSA n° R-1498 controled by regular audits.

# Kværner Fjellstrand a.s

## Welding Procedures, Fatigue Testing NTNU, test specimens type 1,2,3,4

### Welding general :

Welding method : Pulsed MIG  
Filler wire: Al-MIG wire, Ø 1.2mm. Type 5183; AlMg4,5Mn  
Manufacturer: Lincoln Electric

Welding equipment : OTC 12, TRA350; Daihen Corporation, Japan.  
OTC wire feeder, CMW 145

### Test specimen no 4:

#### Butt joint :

Welding parameters: **A) Root bead , (1) :**

Voltage: 23-24 V  
Current: 160-165 Amps,  
DC, negative earth(base material negative)  
Welding speed: 60 cm/min

**B) Back gauging by saw**

**C) Final beads (cap) (2) and (3) :**

Voltage: 24 V  
Current: 160-165 Amps,  
DC, negative earth(base material negative)  
Welding speed: 64 cm/min

#### Lapjoint :

Welding parameters: Fillet weld size : leg length 3 mm  
Voltage: 20-22 V  
Current: 140-145 Amps,  
DC, negative earth (base material negative)  
Welding speed: 55 cm/min

### Test specimen no 1,2 & 3:

#### Transverse frame, fillet weld :

Welding parameters: Fillet weld throath thickness 3 mm  
Voltage: 23-24 V  
Current: 170Amps,  
DC, negative earth(base material negative)  
Welding speed: 50 cm/min



INSPECTION CERTIFICATE OF MATERIALS

**COPY**

DNV certificate acc. to Classification Rules.  
 3.1C acc. to ISO 10474/EN 10204

Product	90 pcs rolled aluminium plate 6 mm x 2000 mm x 5000 mm Lot Nos.: 712667; 712668 and 712669	Total mass	14956 kg
Manufacturer	Alusuisse Swiss Aluminium Ltd, Chippis, Switzerland	Manufacturer's order No.	24632 Item 02
Purchaser	Kvaerner Fjellstrand A/S, Omastrand, Norway	Purchaser's order No.	23592 dtd 06.06.97

Destination/Supplementary information  
 For use in the construction of DNV Classed vessels

**MATERIAL SPECIFICATION**

Material standard and grade DNV Rules Pt. 2 Ch. 2 Sec. 9 NV-5083-H116	Any additional requirements
---	-----------------------------

**SPECIFIED MECHANICAL PROPERTIES**

TENSILE PROPERTIES					CHARPY V-NOTCH IMPACT PROPERTIES				
Specimen type/ dimensions	Yield point R <sub>eH</sub> or R <sub>p0,2</sub> N/mm <sup>2</sup>	Tensile strength R <sub>m</sub> N/mm <sup>2</sup>	Elongation A <sub>5</sub> %	Reduction of area Z %	Orien- tation L or T	Test temp. °C	Width of test piece mm	Energy, J, min.	
								Single	Average
Flat 12 x t transverse	min 215	min 305	min 10	---	---	---	---	---	---

Remarks Ref. Table A5 DNV Rules

**SPECIFIED CHEMICAL COMPOSITION**

Element	Si	Fe	Mn	Mg	Cr	Zn	Ti	Cu					
Specific value(s)	max 0,40	max 0,40	0,40 -	4,0 -	0,05 -	max 0,25	max 0,15	max 0,10					

Remarks Ref. Table A1 of DNV Rules

<p>Marking: soft stamped with: NV5083 H116 6.0 mm Lot No &amp; trademark</p> <p><i>NV</i></p> <p>The stamping is placed: plate surface/ tag</p>	<p>The materials are tested and inspected in the <b>H116 tempered</b> condition, and are found to be in accordance with the above specification. (For test results, see <i>see enclosed</i>)</p> <p>If applicable state drawing number and approval date n/a</p> <p>Chippis/Schwäbisch Hall Place                      1997-08-29 Date</p>	
---	--	--

It is agreed that save as provided below Det Norske Veritas, its subsidiaries, bodies, officers, directors, employees and agents shall have no liability for any loss, damage or expense allegedly caused directly or indirectly by their mistake or negligence, breach of warranty, or any other act, omission or error by them, including gross negligence or wilful misconduct by any such person with the exception of gross negligence or wilful misconduct by the governing bodies or senior executive officers of Det Norske Veritas. This applies regardless of whether the loss, damage or expense has affected anyone with whom Det Norske Veritas has a contract or a third party who has acted or relied on decisions made or information given by or on behalf of Det Norske Veritas. \* However, if any person uses the services of Det Norske Veritas or its subsidiaries or relies on any decision made or information given by or on behalf of them and in consequence suffers a loss, damage or expense proved to be due to their negligence, omission or default, then Det Norske Veritas will pay by way of compensation to such person a sum representing his proved loss. \* In the event Det Norske Veritas or its subsidiaries may be held liable in accordance with the sections above, the amount of compensation shall under no circumstances exceed the amount of the fee, if any, charged for that particular service, decision, advice or information. \* Under no circumstances whatsoever shall the individual or individuals who have personally caused the loss, damage or expense be held liable. \* In the event that any provision in this section shall be invalid under the law of any jurisdiction, the validity of the remaining provisions shall not in any way be affected.

1997



**TEST RESULTS**

**MECHANICAL PROPERTIES**

TENSILE TESTS						CHARPY V-NOTCH IMPACT TESTS							
Cast. No.	Test No.	Yield point R <sub>eH</sub> or R <sub>p0,2</sub> N/mm <sup>2</sup>	Tensile strength R <sub>m</sub> N/mm <sup>2</sup>	Elongation A <sub>5</sub> %	Reduction of area Z %	Orientation L or T	Width of test piece mm	Test temp °C	Energy, J, min.				
									1	2	3	Ave.	
1-7191-1291 Lot:-	712667	240,7	334,1	17,29									
	712667	242,1	335,7	16,67									
	712667	242,1	335,8	18,84									
1-71911291 Lot:-	712668	235,5	335,2	19,51									
	712668	234,4	334,3	18,16									
	712668	235,5	335,3	16,78									
1-7191-1291 Lot:-	712669	250,8	335,3	15,27									
	712669	251,9	339,0	14,92									
	712669	253,4	338,9	14,39									



Remarks HB range 99 to 105 measured on test specimens.

**CHEMICAL COMPOSITION**

Cast. No.	Si	Fe	Cu	Mn	Mg	Cr	Ni	Zn	Ti				
1-7191-1291	0,17	0,29	0,026	0,58	4,56	0,09	0,003	0,033	0,017				

Remarks Cast analyses as declared by Alusuisse in works certificate dated 29.08.97

Process: Rolled aluminium  
Heat treatment (state temperatures) H116

Non-destructive testing  
non specified or carried out

**ADDITIONAL INSPECTION**

Type and extent of inspection  
control of markings: satisfactory



Place.: Kværner Fjellstrand  
Ref.: PAAV  
Ord.No.: 990265

## DET NORSKE VERITAS

### WITNESSING OF WELDING PROCEDURES

This is to certify that the undersigned surveyor attended at Kværner Fjellstrand, Omastrand in order to witness welding procedures for test specimens intended for Fatigue Testing of Ship Details at NTNU.

The test specimens were welded according to

- Drawing no. HAS 1-1571 A "Test specimens no. 1,2 and 3"
- Drawing no. HAS 1-1572 A "Test specimens no. 4 Lap Joint"

The specimens were witnessed during manufacturing and welding parameters recorded. A total of 60 (4 x 15) specimens produced.

#### Test specimen no.1,2&3

**Transverse frame, fillet weld :**

Welding parameters: Fillet weld throat thickness 3 mm

Voltage: 23-24 V

Current: 170 A, DC, negative earth (base material negative)

Welding speed: 50 <sup>cm</sup>/min

#### Test specimen no.4

**Butt joint :**

Welding parameters: **A) Root bed, (1)**

Voltage: 23-24 V

Current: 160-165 A, DC, negative earth (base material negative)

Welding speed: 60 <sup>cm</sup>/min

**B) Back gauging by saw**

**C) Final beads (cap) (2) and (3)**

Voltage: 24 V

Current: 160-165 A, DC, negative earth (base material negative)

Welding speed: 64 <sup>cm</sup>/min

If any person suffers loss or damage which is proved to have been caused by any negligent act or omission of Det Norske Veritas, then Det Norske Veritas shall pay compensation to such person for his proved direct loss or damage. However, the compensation shall not exceed an amount equal to ten times the fee charged for the service in question, provided that the maximum compensation shall never exceed USD 2 million. In this provision "Det Norske Veritas" shall mean the Foundation Det Norske Veritas as well as all its subsidiaries, directors, officers, employees, agents and any other acting on behalf of Det Norske Veritas.

PAAV

Place.: Kværner Fjellstrand  
Ref.: PAAV  
Ord. Nr.: 990265

**Lap joint :**

Welding parameters: Fillet weld size : leg length 3 mm

Voltage: 20-22 V

Current: 140-145 A, DC, negative earth (base material negative)

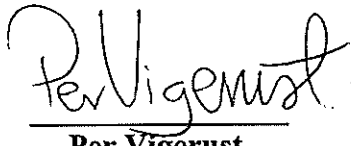
Welding speed: 55 <sup>cm</sup>/min

After completion of welding the specimens were visually inspected and found in order.  
Material certificates were presented and reviewed.

Place: Kværner Fjellstrand

Date: 99.03.31

Sign.:



Per Vigerust  
Surveyor

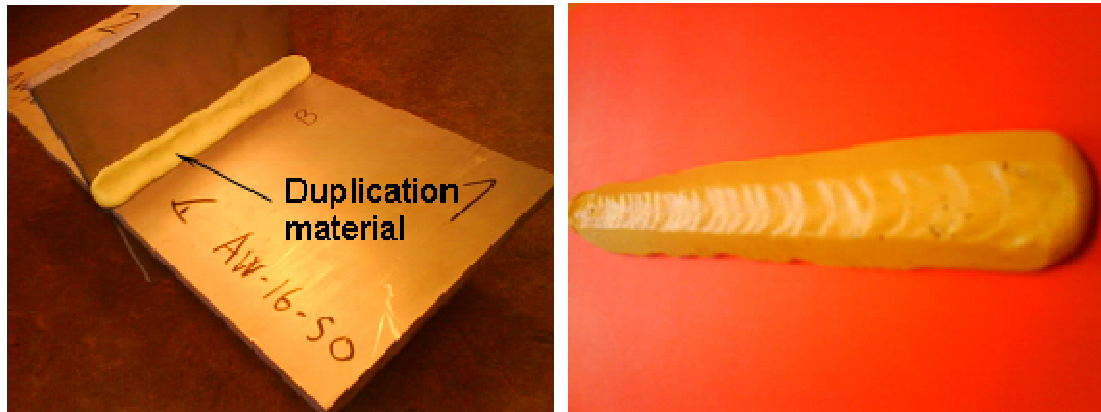




## **7**     *Appendix C: Measuring weld parameters*



The weld profiles are reproduced by means of imprints out of the real welds. A high consistency impression material OPTOSIL together with the corresponding activator OPTOSIL-XANTOPREN was used to duplicate the weld profile as a sample shown in Figure 7-1. The photo to the left shows how the duplicating material is fitted to the weld profile and the duplicated profile is shown in the photo to the right.



a) T-joint with duplication material

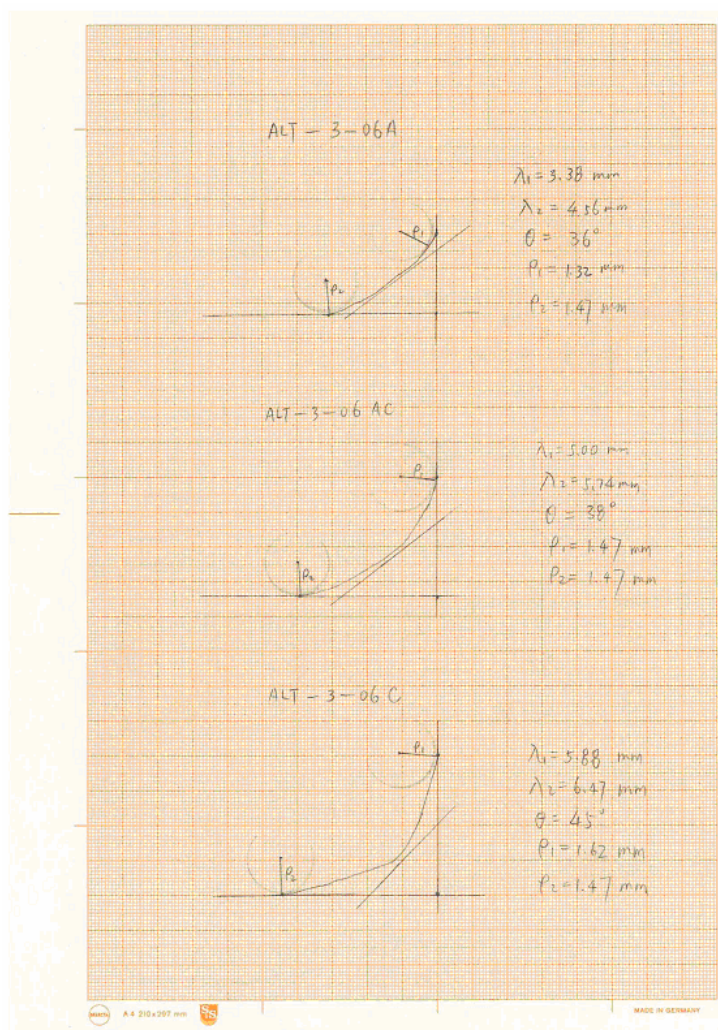
b) Duplicated weld profile

**Figure 7-1 Duplication of the weld profile**

The imprint was then be sliced into pieces as shown in Figure 7-2. Each piece is photographed using a microscope camera with a reasonable magnifying ratio. The photo to the right side shows a photo example.

The magnified weld profiles on photo paper was then reproduced by ink drawing utilizing transparent millimetre-block paper through which the out edge of the weld profile on the photo paper can be visible due to the transparency. Figure 7-3 shows an example by which the parameters of the weld are recorded. It should be noted here that the original samples to the left are for T-joint fillet weld profile while the magnified photo (to the right) represents the lap joint fillet weld profile. The readout values are then scaled back to the real values by dividing the magnifying ratio of the microscope.



**Figure 7-2 Magnified weld profile for measuring weld parameters****Figure 7-3 Measuring the weld parameter by transparent millimetre block paper**



**8**      *Appendix D: Photos in colour*



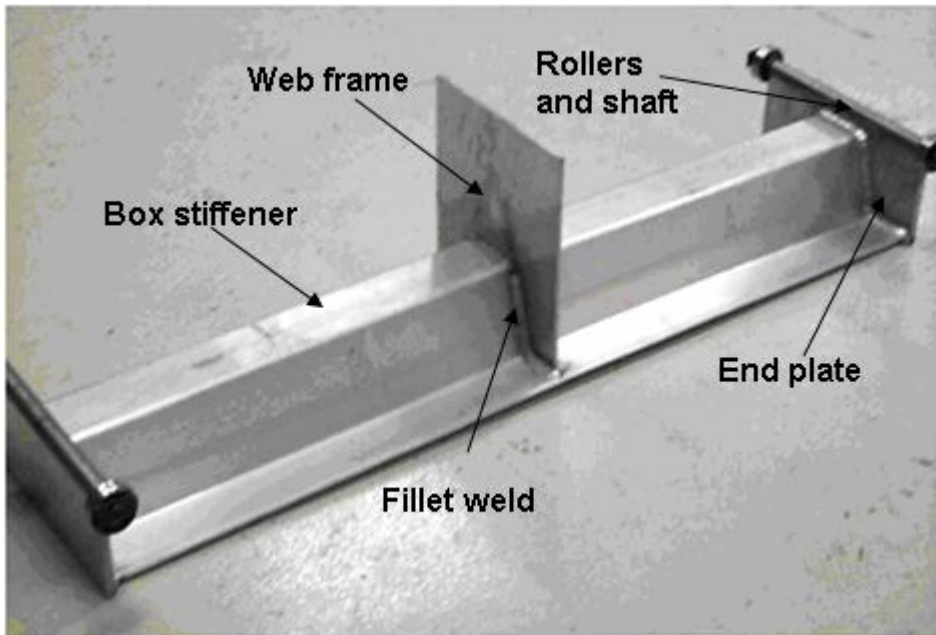


**Figure 8-1 Overview of the web frame/box stiffener connection**

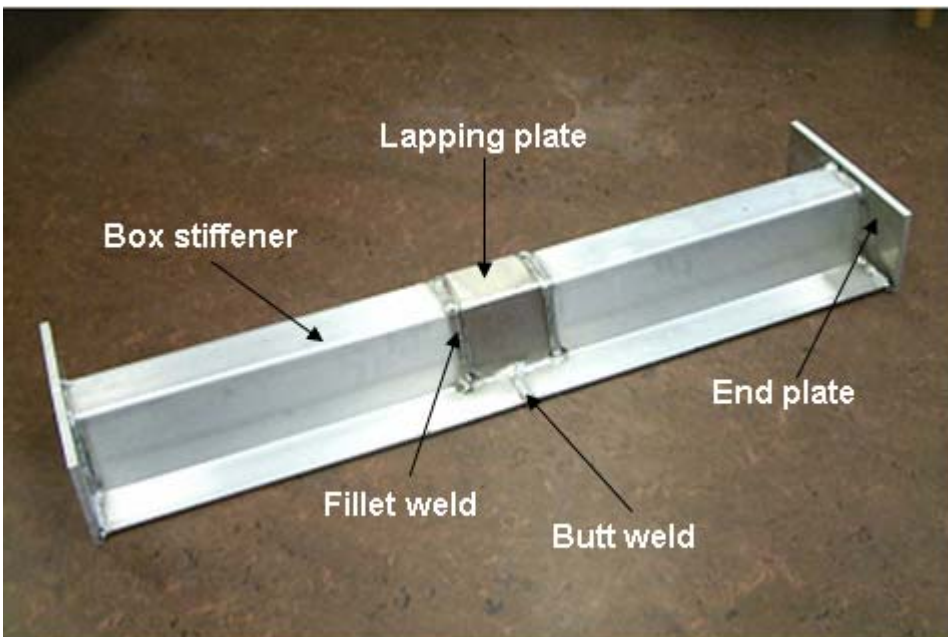


**Figure 8-2 Overall of the lap joint**

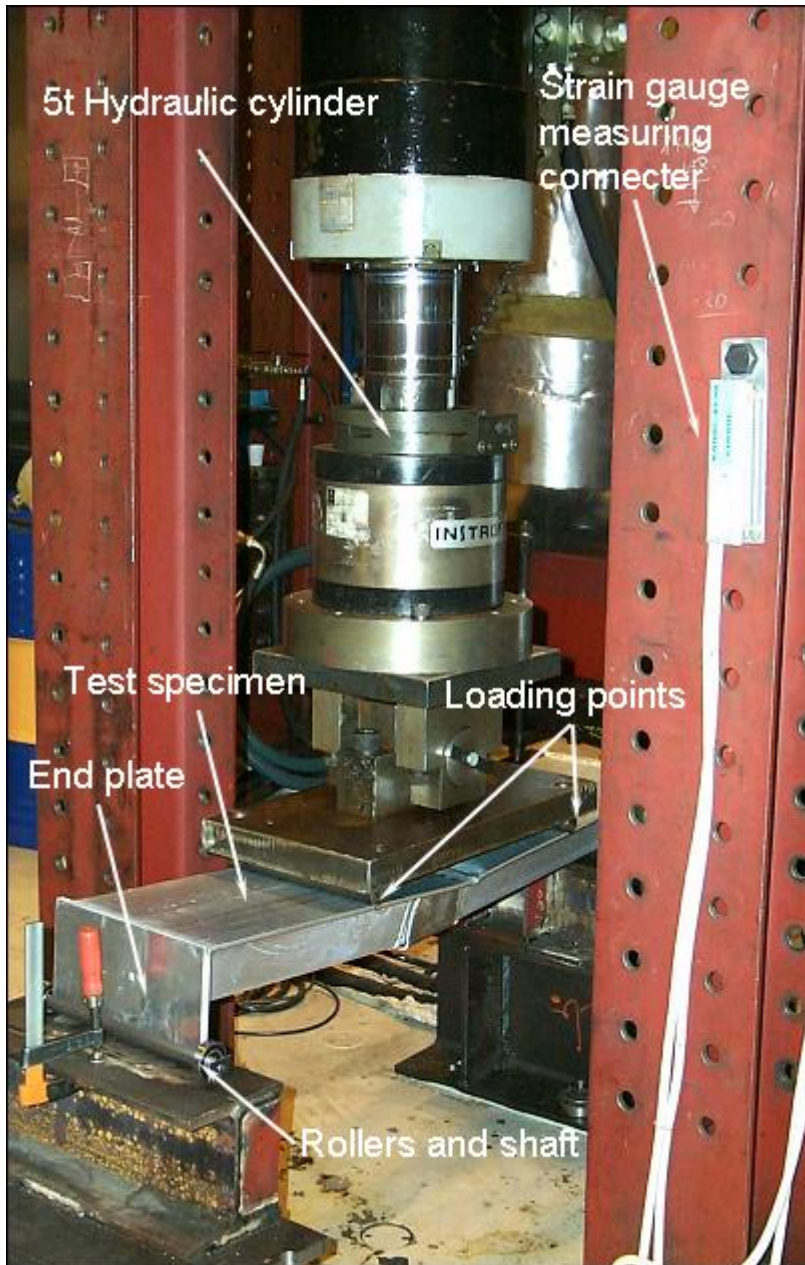


**Figure 8-3 Test set up for four-point bending load condition**



**Figure 8-4 Photograph of as-welded (to the left) and toe-ground specimens**



**R A P P O R T E R**  
**UTGIIT VED**  
**INSTITUTT FOR MARIN TEKNIKK**  
**(tidligere: FAKULTET FOR MARIN TEKNIKK)**  
**NORGES TEKNISK-NATURVITENSKAPELIGE UNIVERSITET**

UR-79-01 <u>Brigt Hatlestad</u> , MK:	The finite element method used in a fatigue evaluation of fixed offshore platforms. (Dr.Ing. Thesis)
UR-79-02 <u>Erik Pettersen</u> , MK:	Analysis and design of cellular structures. (Dr.Ing. Thesis)
UR-79-03 <u>Sverre Valsgård</u> , MK:	Finite difference and finite element methods applied to nonlinear analysis of plated structures. (Dr.Ing. Thesis)
UR-79-04 <u>Nils T. Nordsve</u> , MK:	Finite element collapse analysis of structural members considering imperfections and stresses due to fabrication. (Dr.Ing. Thesis)
UR-79-05 <u>Ivar J. Fylling</u> , MK:	Analysis of towline forces in ocean towing systems. (Dr.Ing. Thesis)
UR-80-06 <u>Nils Sandsmark</u> , MM:	Analysis of Stationary and Transient Heat Conduction by the Use of the Finite Element Method. (Dr.Ing. Thesis)
UR-80-09 <u>Sverre Haver</u> , MK:	Analysis of uncertainties related to the stochastic modelling of ocean waves. (Dr.Ing. Thesis)
UR-85-46 <u>Alf G. Engseth</u> , MK:	Finite element collapse analysis of tubular steel offshore structures. (Dr.Ing. Thesis)
UR-86-47 <u>Dengody Sheshappa</u> , MP:	A Computer Design Model for Optimizing Fishing Vessel Designs Based on Techno-Economic Analysis. (Dr.Ing. Thesis)
UR-86-48 <u>Vidar Aanesland</u> , MH:	A Theoretical and Numerical Study of Ship Wave Resistance. (Dr.Ing. Thesis)
UR-86-49 <u>Heinz-Joachim Wessel</u> , MK:	Fracture Mechanics Analysis of Crack Growth in Plate Girders. (Dr.Ing. Thesis)
UR-86-50 <u>Jon Taby</u> , MK:	Ultimate and Post-ultimate Strength of Dented Tubular Members. (Dr.Ing. Thesis)
UR-86-51 <u>Walter Lian</u> , MH:	A Numerical Study of Two-Dimensional Separated Flow Past Bluff Bodies at Moderate KC-Numbers. (Dr.Ing. Thesis)
UR-86-52 <u>Bjørn Sortland</u> , MH:	Force Measurements in Oscillating Flow on Ship Sections and Circular Cylinders in a U-Tube Water Tank. (Dr.Ing. Thesis)
UR-86-53 <u>Kurt Strand</u> , MM:	A System Dynamic Approach to One-dimensional Fluid Flow. (Dr.Ing. Thesis)
UR-86-54 <u>Arne Edvin Løken</u> , MH:	Three Dimensional Second Order Hydrodynamic Effects on Ocean Structures in Waves. (Dr.Ing. Thesis)
UR-86-55 <u>Sigurd Falch</u> , MH:	A Numerical Study of Slamming of Two-Dimensional Bodies. (Dr.Ing. Thesis)
UR-87-56 <u>Arne Braathen</u> , MH:	Application of a Vortex Tracking Method to the Prediction of Roll Damping of a Two-Dimension Floating Body. (Dr.Ing. Thesis)
UR-87-57 <u>Bernt Leira</u> , MR:	Gaussian Vector Processes for Reliability Analysis involving Wave-Induced Load Effects. (Dr.Ing. Thesis)
UR-87-58 <u>Magnus Småvik</u> , MM:	Thermal Load and Process Characteristics in a Two-Stroke Diesel Engine with Thermal Barriers (in Norwegian). (Dr.Ing. Thesis)
MTA-88-59 <u>Bernt Arild Bremdal</u> , MP:	An Investigation of Marine Installation Processes - A Knowledge - Based Planning Approach. (Dr.Ing. Thesis)
MTA-88-60 <u>Xu Jun</u> , MK:	Non-linear Dynamic Analysis of Space-framed Offshore Structures. (Dr.Ing. Thesis)
MTA-89-61 <u>Gang Miao</u> , MH:	Hydrodynamic Forces and Dynamic Responses of Circular Cylinders in Wave

	Zones. (Dr.Ing. Thesis)
MTA-89-62 <u>Martin Greenhow</u> , MH:	Linear and Non-Linear Studies of Waves and Floating Bodies. Part I and Part II. (Dr.Techn. Thesis)
MTA-89-63 <u>Chang Li</u> , MH:	Force Coefficients of Spheres and Cubes in Oscillatory Flow with and without Current. (Dr.Ing. Thesis)
MTA-89-64 <u>Hu Ying</u> , MP:	A Study of Marketing and Design in Development of Marine Transport Systems. (Dr.Ing. Thesis)
MTA-89-65 <u>Arild Jæger</u> , MH:	Seakeeping, Dynamic Stability and Performance of a Wedge Shaped Planing Hull. (Dr.Ing. Thesis)
MTA-89-66 <u>Chan Siu Hung</u> , MM:	The dynamic characteristics of tilting-pad bearings.
MTA-89-67 <u>Kim Wikstrøm</u> , MP:	Analysis av projekteringen for ett offshore projekt. (Licenciat-avhandling)
MTA-89-68 <u>Jiao Guoyang</u> , MR:	Reliability Analysis of Crack Growth under Random Loading, considering Model Updating. (Dr.Ing. Thesis)
MTA-89-69 <u>Arnt Olufsen</u> , MK:	Uncertainty and Reliability Analysis of Fixed Offshore Structures. (Dr.Ing. Thesis)
MTA-89-70 <u>Wu Yu-Lin</u> , MR:	System Reliability Analyses of Offshore Structures using improved Truss and Beam Models. (Dr.Ing. Thesis)
MTA-90-71 <u>Jan Roger Hoff</u> , MH:	Three-dimensional Green function of a vessel with forward speed in waves. (Dr.Ing. Thesis)
MTA-90-72 <u>Rong Zhao</u> , MH:	Slow-Drift Motions of a Moored Two-Dimensional Body in Irregular Waves. (Dr.Ing. Thesis)
MTA-90-73 <u>Atle Minsaas</u> , MP:	Economical Risk Analysis. (Dr.Ing. Thesis)
MTA-90-74 <u>Knut-Aril Farnes</u> , MK:	Long-term Statistics of Response in Non-linear Marine Structures. (Dr.Ing. Thesis)
MTA-90-75 <u>Torbjørn Sotberg</u> , MK:	Application of Reliability Methods for Safety Assessment of Submarine Pipelines. (Dr.Ing. Thesis)
MTA-90-76 <u>Zeuthen, Steffen</u> , MP:	SEAMAID. A computational model of the design process in a constraint-based logic programming environment. An example from the offshore domain. (Dr.Ing. Thesis)
MTA-91-77 <u>Haagensen, Sven</u> , MM:	Fuel Dependant Cyclic Variability in a Spark Ignition Engine - An Optical Approach. (Dr.Ing. Thesis)
MTA-91-78 <u>Løland, Geir</u> , MH:	Current forces on and flow through fish farms. (Dr.Ing. Thesis)
MTA-91-79 <u>Hoen, Christopher</u> , MK:	System Identification of Structures Excited by Stochastic Load Processes. (Dr.Ing. Thesis)
MTA-91-80 <u>Haugen, Stein</u> , MK:	Probabilistic Evaluation of Frequency of Collision between Ships and Offshore Platforms. (Dr.Ing. Thesis)
MTA-91-81 <u>Sødahl, Nils</u> , MK:	Methods for Design and Analysis of Flexible Risers. (Dr.Ing. Thesis)
MTA-91-82 <u>Ormberg, Harald</u> , MK:	Non-linear Response Analysis of Floating Fish Farm Systems. (Dr.Ing. Thesis)
MTA-91-83 <u>Marley, Mark J.</u> , MK:	Time Variant Reliability under Fatigue Degradation. (Dr.Ing. Thesis)
MTA-91-84 <u>Krokstad, Jørgen R.</u> , MH:	Second-order Loads in Multidirectional Seas. (Dr.Ing. Thesis)
MTA-91-85 <u>Molteberg, Gunnar A.</u> , MM:	The Application of System Identification Techniques to Performance Monitoring of Four Stroke Turbocharged Diesel Engines. (Dr.Ing. Thesis)
MTA-92-86 <u>Mørch, Hans Jørgen Bjelke</u> , MH:	Aspects of Hydrofoil Design: with Emphasis on Hydrofoil Interaction in Calm Water. (Dr.Ing. Thesis)



MTA-92-87 <u>Chan Siu Hung</u> , MM:	Nonlinear Analysis of Rotordynamic Instabilities in High-speed Turbomachinery. (Dr.Ing. Thesis)
MTA-92-88 <u>Bessason, Bjarni</u> , MK:	Assessment of Earthquake Loading and Response of Seismically Isolated Bridges. (Dr.Ing. Thesis)
MTA-92-89 <u>Langli, Geir</u> , MP:	Improving Operational Safety through exploitation of Design Knowledge - an investigation of offshore platform safety. (Dr.Ing. Thesis)
MTA-92-90 <u>Sævik, Svein</u> , MK:	On Stresses and Fatigue in Flexible Pipes. (Dr.Ing. Thesis)
MTA-92-91 <u>Ask, Tor Ø.</u> , MM:	Ignition and Flame Growth in Lean Gas-Air Mixtures. An Experimental Study with a Schlieren System. (Dr.Ing. Thesis)
MTA-86-92 <u>Hessen, Gunnar</u> , MK:	Fracture Mechanics Analysis of Stiffened Tubular Members. (Dr.Ing. Thesis)
MTA-93-93 <u>Steinebach, Christian</u> , MM:	Knowledge Based Systems for Diagnosis of Rotating Machinery. (Dr.Ing. Thesis)
MTA-93-94 <u>Dalane, Jan Inge</u> , MK:	System Reliability in Design and Maintenance of Fixed Offshore Structures. (Dr.Ing. Thesis)
MTA-93-95 <u>Steen, Sverre</u> , MH:	Cobblestone Effect on SES. (Dr.Ing. Thesis)
MTA-93-96 <u>Karunakaran, Daniel</u> , MK:	Nonlinear Dynamic Response and Reliability Analysis of Drag-dominated Offshore Platforms. (Dr.Ing. Thesis)
MTA-93-97 <u>Hagen, Arnulf</u> , MP:	The Framework of a Design Process Language. (Dr.Ing. Thesis)
MTA-93-98 <u>Nordrik, Rune</u> , MM:	Investigation of Spark Ignition and Autoignition in Methane and Air Using Computational Fluid Dynamics and Chemical Reaction Kinetics. A Numerical Study of Ignition Processes in Internal Combustion Engines. (Dr.Ing. Thesis)
MTA-94-99 <u>Passano, Elizabeth</u> , MK:	Efficient Analysis of Nonlinear Slender Marine Structures. (Dr.Ing. Thesis)
MTA-94-100 <u>Kvålsvold, Jan</u> , MH:	Hydroelastic Modelling of Wetdeck Slamming on Multihull Vessels. (Dr.Ing. Thesis)
MTA-94-102 <u>Bech, Sidsel M.</u> , MK:	Experimental and Numerical Determination of Stiffness and Strength of GRP/PVC Sandwich Structures. (Dr.Ing. Thesis)
MTA-95-103 <u>Paulsen, Hallvard</u> , MM:	A Study of Transient Jet and Spray using a Schlieren Method and Digital Image Processing. (Dr.Ing. Thesis)
MTA-95-104 <u>Hovde, Geir Olav</u> , MK:	Fatigue and Overload Reliability of Offshore Structural Systems, Considering the Effect of Inspection and Repair. (Dr.Ing. Thesis)
MTA-95-105 <u>Wang, Xiaozhi</u> , MK:	Reliability Analysis of Production Ships with Emphasis on Load Combination and Ultimate Strength. (Dr.Ing. Thesis)
MTA-95-106 <u>Ulstein, Tore</u> , MH:	Nonlinear Effects of a Flexible Stern Seal Bag on Cobblestone Oscillations of an SES. (Dr.Ing. Thesis)
MTA-95-107 <u>Solaas, Frøydis</u> , MH:	Analytical and Numerical Studies of Sloshing in Tanks. (Dr.Ing. Thesis)
MTA-95-108 <u>Hellan, øyvind</u> , MK:	Nonlinear Pushover and Cyclic Analyses in Ultimate Limit State Design and Reassessment of Tubular Steel Offshore Structures. (Dr.Ing. Thesis)
MTA-95-109 <u>Hermundstad, Ole A.</u> , MK:	Theoretical and Experimental Hydroelastic Analysis of High Speed Vessels. (Dr.Ing. Thesis)
MTA-96-110 <u>Bratland, Anne K.</u> , MH:	Wave-Current Interaction Effects on Large-Volume Bodies in Water of Finite Depth. (Dr.Ing. Thesis)
MTA-96-111 <u>Herfjord, Kjell</u> , MH:	A Study of Two-dimensional Separated Flow by a Combination of the Finite Element Method and Navier-Stokes Equations. (Dr.Ing. Thesis)
MTA-96-112 <u>Æsøy, Vilmar</u> , MM:	Hot Surface Assisted Compression Ignition in a Direct Injection Natural Gas Engine. (Dr.Ing. Thesis)

MTA-96-113 <u>Eknes, Monika L.</u> , MK:	Escalation Scenarios Initiated by Gas Explosions on Offshore Installations. (Dr.Ing. Thesis)
MTA-96-114 <u>Erikstad, Stein O.</u> , MP:	A Decision Support Model for Preliminary Ship Design. (Dr.Ing. Thesis)
MTA-96-115 <u>Pedersen, Egil</u> , MH:	A Nautical Study of Towed Marine Seismic Streamer Cable Configurations. (Dr.Ing. Thesis)
MTA-97-116 <u>Moksnes, Paul O.</u> , MM:	Modelling Two-Phase Thermo-Fluid Systems Using Bond Graphs. (Dr.Ing. Thesis)
MTA-97-117 <u>Halse, Karl H.</u> , MK:	On Vortex Shedding and Prediction of Vortex-Induced Vibrations of Circular Cylinders. (Dr.Ing. Thesis)
MTA-97-118 <u>Igland, Ragnar T.</u> , MK:	Reliability Analysis of Pipelines during Laying, considering Ultimate Strength under Combined Loads. (Dr.Ing. Thesis)
MTA-97-119 <u>Pedersen, Hans-P.</u> , MP:	Levendefiskteknologi for fiskefartøy. (Dr.Ing. Thesis)
MTA-98-120 <u>Vikestad, Kyrre</u> , MK:	Multi-Frequency Response of a Cylinder Subjected to Vortex Shedding and Support Motions. (Dr.Ing. Thesis)
MTA-98-121 <u>Azadi, Mohammad R. E.</u> , MK:	Analysis of Static and Dynamic Pile-Soil-Jacket Behaviour. (Dr.Ing. Thesis)
MTA-98-122 <u>Ulltang, Terje</u> , MP:	A Communication Model for Product Information. (Dr.Ing. Thesis)
MTA-98-123 <u>Torbergsen, Erik</u> , MM:	Impeller/Diffuser Interaction Forces in Centrifugal Pumps. (Dr.Ing. Thesis)
MTA-98-124 <u>Hansen, Edmond</u> , MH:	A Discrete Element Model to Study Marginal Ice Zone Dynamics and the Behaviour of Vessels Moored in Broken Ice. (Dr.Ing. Thesis)
MTA-98-125 <u>Videiro, Paulo M.</u> , MK:	Reliability Based Design of Marine Structures. (Dr.Ing. Thesis)
MTA-99-126 <u>Mainçon, Philippe</u> , MK:	Fatigue Reliability of Long Welds Application to Titanium Risers. (Dr.Ing. Thesis)
MTA-99-127 <u>Haugen, Elin M.</u> , MH:	Hydroelastic Analysis of Slamming on Stiffened Plates with Application to Catamaran Wetdecks. (Dr.Ing. Thesis)
MTA-99-128 <u>Langhelle, Nina K.</u> , MK:	Experimental Validation and Calibration of Nonlinear Finite Element Models for Use in Design of Aluminium Structures Exposed to Fire. (Dr.Ing. Thesis)
MTA-99-129 <u>Berstad, Are J.</u> , MK:	Calculation of Fatigue Damage in Ship Structures. (Dr.Ing. Thesis)
MTA-99-130 <u>Andersen, Trond M.</u> , MM:	Short Term Maintenance Planning. (Dr.Ing. Thesis)
MTA-99-131 <u>Tveiten, Bård Wathne</u> , MK:	Fatigue Assessment of Welded Aluminium Ship Details. (Dr.Ing. Thesis)
MTA-99-132 <u>Søreide, Fredrik</u> , MP:	Applications of underwater technology in deep water archaeology. Principles and practice. (Dr.Ing. Thesis)
MTA-99-133 <u>Tønnessen, Rune</u> , MH:	A Finite Element Method Applied to Unsteady Viscous Flow Around 2D Blunt Bodies With Sharp Corners. (Dr.Ing. Thesis)
MTA-99-134 <u>Elvekrok, Dag R.</u> , MP:	Engineering Integration in Field Development Projects in the Norwegian Oil and Gas Industry. The Supplier Management of Norne. (Dr.Ing. Thesis)
MTA-99-135 <u>Fagerholt, Kjetil</u> , MP:	Optimeringsbaserte Metoder for Ruteplanlegging innen skipsfart. (Dr.Ing. Thesis)
MTA-99-136 <u>Bysveen, Marie</u> , MM:	Visualization in Two Directions on a Dynamic Combustion Rig for Studies of Fuel Quality. (Dr.Ing. Thesis)
MTA-2000-137 <u>Storteig, Eskild</u> , MM:	Dynamic characteristics and leakage performance of liquid annular seals in centrifugal pumps. (Dr.Ing. Thesis)
MTA-2000-138 <u>Sagli, Gro</u> , MK:	Model uncertainty and simplified estimates of long term extremes of hull girder loads in ships. (Dr.Ing. Thesis)

MTA-2000-139 <u>Tronstad, Harald</u> , MK:	Nonlinear analysis and design of cable net structures like fishing gear based on the finite element method. (Dr.Ing. Thesis)
MTA-2000-140 <u>Kroneberg, André</u> , MP:	Innovation in shipping by using scenarios. (Dr.Ing. Thesis)
MTA-2000-141 <u>Haslum, Herbjørn Alf</u> , MH:	Simplified methods applied to nonlinear motion of spar platforms. (Dr.Ing. Thesis)
MTA-2001-142 <u>Samdal, Ole Johan</u> , MM:	Modelling of Degradation Mechanisms and Stressor Interaction on Static Mechanical Equipment Residual Lifetime. (Dr.Ing. Thesis)
MTA-2001-143 <u>Baarholm, Rolf Jarle</u> , MH:	Theoretical and experimental studies of wave impact underneath decks of offshore platforms. (Dr.Ing. Thesis)
MTA-2001-144 <u>Wang, Lihua</u> , MK:	Probabilistic Analysis of Nonlinear Wave-induced Loads on Ships. (Dr.Ing. Thesis)
MTA-2001-145 <u>Kristensen, Odd H. Holt</u> , MK:	Ultimate Capacity of Aluminium Plates under Multiple Loads, Considering HAZ Properties. (Dr.Ing. Thesis)
MTA-2001-146 <u>Greco, Marilena</u> , MH:	A Two-Dimensional Study of Green-Water Loading. (Dr.Ing. Thesis)
MTA-2001-147 <u>Heggelund, Svein E.</u> , MK:	Calculation of Global Design Loads and Load Effects in Large High Speed Catamarans. (Dr.Ing. Thesis)
MTA-2001-148 <u>Babalola, Olusegun T.</u> , MK:	Fatigue Strength of Titanium Risers - Defect Sensitivity. (Dr.Ing. Thesis)
MTA-2001-149 <u>Mohammed, Abuu K.</u> , MK:	Nonlinear Shell Finite Elements for Ultimate Strength and Collapse Analysis of Ship Structures. (Dr.Ing. Thesis)
MTA-2002-150 <u>Holmedal, Lars E.</u> , MH:	Wave-current interactions in the vicinity of the sea bed. (Dr.Ing. Thesis)
MTA-2002-151 <u>Rognebakke, Olav F.</u> , MH:	Sloshing in rectangular tanks and interaction with ship motions. (Dr.Ing. Thesis)
MTA-2002-152 <u>Lader, Pål Furset</u> , MH:	Geometry and Kinematics of Breaking Waves. (Dr.Ing. Thesis)
MTA-2002-153 <u>Yang, Qinzhen</u> , MH:	Wash and wave resistance of ships in finite water depth. (Dr.Ing. Thesis)
MTA-2002-154 <u>Melhus, Øyvind</u> , MM:	Utilization of VOC in Diesel Engines. Ignition and combustion of VOC released by crude oil tankers. (Dr.Ing. Thesis)
MTA-2002-155 <u>Ronæss, Marit</u> , MH:	Wave Induced Motions of Two Ships Advancing on Parallel Course. (Dr.Ing. Thesis)
MTA-2002-156 <u>Økland, Ole D.</u> , MK:	Numerical and experimental investigation of whipping in twin hull vessels exposed to severe wet deck slamming. (Dr.Ing. Thesis)
MTA-2002-157 <u>Ge, Chunhua</u> , MK:	Global Hydroelastic Response of Catamarans due to Wet Deck Slamming. (Dr.Ing. Thesis)
MTA-2002-158 <u>Byklum, Eirik</u> , MK:	Nonlinear Shell Finite Elements for Ultimate Strength and Collapse Analysis of Ship Structures. (Dr.Ing. Thesis)
IMT-2003-1 <u>Chen, Haibo</u> , MK:	Probabilistic Evaluation of FPSO-Tanker Collision in Tandem Offloading Operation. (Dr.Ing. Thesis)
IMT-2003-2 <u>Skaugset, Kjetil Bjørn</u> , MK:	On the Suppression of Vortex Induced Vibrations of Circular Cylinders by Radial Water Jets. (Dr.Ing. Thesis)
IMT-2003-3 <u>Chezian, Muthu</u>	Three-Dimensional Analysis of Slamming. (Dr.Ing. Thesis)
IMT-2003-4 <u>Buhaug, Øyvind</u>	Deposit Formation on Cylinder Liner Surfaces in Medium Speed Engines. (Dr.Ing. Thesis)
IMT-2003-5 <u>Tregde, Vidar</u>	Aspects of Ship Design: Optimization of Aft Hull with Inverse Geometry Design. (Dr.Ing. Thesis)

IMT-2003-6 Wist, Hanne Therese	Statistical Properties of Successive Ocean Wave Parameters. (Dr.Ing. Thesis)
IMT-2004-7 Ransau, Samuel	Numerical Methods for Flows with Evolving Interfaces. (Dr.Ing. Thesis)
IMT-2004-8 Soma, Torkel	Blue-Chip or Sub-Standard. A data interrogation approach of identity safety characteristics of shipping organization. (Dr.Ing. Thesis)
IMT-2004-9 Ersdal, Svein	An experimental study of hydrodynamic forces on cylinders and cables in near axial flow. (Dr.Ing. Thesis)
IMT-2005-10 Brodtkorb, Per Andreas	The Probability of Occurrence of Dangerous Wave Situations at Sea. (Dr.Ing. Thesis)
IMT-2005-11 Yttervik, Rune	Ocean current variability in relation to offshore engineering. (Dr.Ing. Thesis)
IMT-2005-12 Fredheim, Arne	Current Forces on Net-Structures. (Dr.Ing. Thesis)
IMT-2005-13 Heggernes, Kjetil	Flow around marine structures. (Dr.Ing. Thesis)
IMT-2005-14 Fouques, Sebastien	Lagrangian Modelling of Ocean Surface Waves and Synthetic Aperture Radar Wave Measurements. (Dr.Ing. Thesis)
IMT-2006-15 Holm, Håvard	Numerical calculation of viscous free surface flow around marine structures. (Dr.Ing. Thesis)
IMT-2006-16 Bjørheim, Lars G.	Failure Assessment of Long Through Thickness Fatigue Cracks in Ship Hulls. (Dr.Ing. Thesis)
IMT-2006-17 Hansson, Lisbeth	Safety Management for Prevention of Occupational Accidents. (Dr.Ing. Thesis)
IMT-2006-18 Zhu, Xinying	Application of the CIP Method to Strongly Nonlinear Wave-Body Interaction Problems. (Dr.Ing. Thesis)
IMT-2006-19 Reite, Karl Johan	Modelling and Control of Trawl Systems. (Dr.Ing. Thesis)
IMT-2006-20 Smogeli, Øyvind Notland	Control of Marine Propellers. From Normal to Extreme Conditions. (Dr.Ing. Thesis)
IMT-2007-21 Storhaug, Gaute	Experimental Investigation of Wave Induced Vibrations and Their Effect on the Fatigue Loading of Ships. (Dr.Ing. Thesis)
IMT-2007-22 Sun, Hui	A Boundary Element Method Applied to Strongly Nonlinear Wave-Body Interaction Problems. (PhD Thesis, CeSOS)
IMT-2007-23 Rustad, Anne Marthine	Modelling and Control of Top Tensioned Risers. (PhD Thesis, CeSOS)
IMT-2007-24 Johansen, Vegar	Modelling flexible slender system for real-time simulations and control applications.
IMT-2007-25 Wroldsen, Anders Sunde	Modelling and control of tensegrity structures. (PhD Thesis, CeSOS)
IMT-2007-26 Aronsen, Kristoffer Høyve	An experimental investigation of in-line and combined in-line and cross flow vortex induced vibrations. (Dr.avhandling, IMT)
IMT-2007-27 Zhen, Gao	Stochastic response analysis of mooring systems with emphasis on frequency-domain analysis of fatigue due to wide-band processes. (PhD-thesis CeSOS).
IMT-2007-28 Thorstensen, Tom Anders	Lifetime Profit Modelling of Ageing Systems Utilizing Information about Technical Condition. (Dr.ing. thesis, IMT)
IMT-2007-29 Ye, Naiquan	Fatigue Assessment of Aluminium Welded Box-stiffener Joints in Ships (Dr.ing. thesis, IMT)